Activation of the innate immune system by endoplasmic reticulum stress and proteasome inhibition

Inaugural-Dissertation

zur Erlangung des Doktorgrades

der Hohen Medizinischen Fakultät

der Rheinischen Friedrich-Wilhelms-Universität

Bonn

Fabian Ullrich

aus Dinslaken

2023

Angefertigt mit der Genehmigung

der Medizinischen Fakultät der Universität Bonn

1. Gutachterin: Prof. Dr. med. Eva Bartok
2. Gutachter: Prof. Dr. rer. nat. Ulrich Schweizer

Tag der Mündlichen Prüfung: 22. August 2023

Aus dem Institut für klinische Chemie und klinische Pharmakologie

Direktor: Prof. Dr. med. Gunther Hartmann

This work is dedicated to my parents

and to everyone who ever had to wait for me

while I was just quickly finishing something in the lab.

LIST OF ABBREVIATIONS **9**

1. INTRODUCTION **14**

1.1. Mechanisms and functions of immunity **14**
1.1.1. Pattern recognition as a basic principle of innate immunity 14
1.1.2. Coordination of innate and adaptive immune responses 15
1.1.3. Immunorecognition of nucleic acids 16
1.1.3.1. Mechanisms of RNA sensing 17
1.1.3.2. Mechanisms of DNA sensing 19
1.1.3.3. Innate sensing of mitochondrial DNA 22
1.1.4. Inflammasomes 23
1.1.5. Aberrant activation of innate immune signaling pathways 25

1.2. Endoplasmic reticulum stress and its implications in immunity **27**
1.2.1. Mechanisms and functions of the Unfolded Protein Response 27
1.2.2. Interaction of innate immunity and endoplasmic reticulum stress pathways 31

1.3. The proteasome and its therapeutic manipulation **33**
1.3.1. Protein degradation by the ubiquitin-proteasome system 33
1.3.2. Proteasome inhibition and its therapeutic use 35
1.3.3. Proteasome inhibition and immunity 36

1.4. Aim of the study **38**

2. MATERIALS AND METHODS **40**

2.1. Materials **40**

2.2. Methods **46**
2.2.1. Cell culture methods 46
2.2.1.1. Cell culture conditions 46
2.2.1.2. Differentiation of THP-1 cells 46
2.2.1.3. Generation of ρ0 THP-1 cells 46

2.2.1.4. Generation of ASC-GFP$^+$ THP-1 cells 47
2.2.1.5. Generation of knockout cell lines via CRISPR/Cas9 47
2.2.1.6. Differentiation of BlaER1 cells 47
2.2.1.7. Isolation of peripheral blood mononuclear cells 48
2.2.1.8. Isolation of primary human monocytes 48
2.2.1.9. Isolation of primary human fibroblasts 48
2.2.1.10. Differentiation of primary human macrophages 48
2.2.1.11. Cell stimulation and transfection 49
2.2.1.12. Inflammasome priming 49
2.2.2. Readout Assays 49
2.2.2.1. Enzyme-linked immunosorbent assay 49
2.2.2.2. RNA isolation, cDNA synthesis, and quantitative real-time polymerase chain reaction 50
2.2.2.3. Quantification of cell viability 50
2.2.2.4. Light microscopy 51
2.2.2.5. ASC speck quantification 51
2.2.2.6. Stochastic optical reconstruction microscopy 51
2.2.3 Figure design and statistical analysis 51

3. RESULTS 53

3.1. Activation of antiviral innate immune pathways by ER stress 53
3.1.1. Pharmacological induction of ER stress and an innate immune response by Tunicamycin and Thapsigargin 53
3.1.2. cGAS and STING are required for type-I IFN induction following treatment with ER stressors 59
3.1.3. The ATF6 branch of the UPR mediates the type-I IFN response to ER stress 62
3.1.4. CXCL-10 secretion following ER stress is driven by mitochondrial DNA 63

3.2 Activation of the inflammasome by proteasome inhibitors 66
3.2.1. Treatment with proteasome inhibitors induces secretion of IL-1β, but not CXCL-10 66

3.2.2. IL-1β secretion occurs at proteasome inhibitor concentrations necessary for cytotoxic activity 68
3.2.3. Hallmarks of inflammasome activation can be detected in cells treated with proteasome inhibitors 70
3.2.4. The BTZ-induced IL-1β response is independent of NLRP3 in PBMC 74

4. DISCUSSION 78

4.1. ER stress-mediated activation of innate immunity 78
4.1.1. ER stressors lead to cGAS/STING-dependent type-I IFN secretion in the presence of mitochondrial DNA 78
4.1.2. cGAS/STING-dependent recognition of mtDNA provides a mechanistic explanation for ER stress-mediated activation of innate immunity 79
4.1.3. Type-I IFN secretion following ER stress may counteract viral evasion of immune recognition and enable DNA-dependent immune sensing of RNA viruses 81
4.1.4. Signaling of nucleic acid receptors and the unfolded protein response converges in programmed cell death 83

4.2. Inflammasome activation by proteasome inhibitors 84
4.2.1. Proteasome inhibition induces hallmarks of inflammasome activation 84
4.2.2. NLRP3-dependent and independent IL-1β release in multiple myeloma and bortezomib treatment occur via different stimuli 85
4.2.3. Potential adverse effects of bortezomib treatment on the multiple myeloma microenvironment 87

5. SYNOPSIS 90

6. LIST OF FIGURES 92

7. LIST OF TABLES 93

8. BIBLIOGRAPHY 94

9. ACKNOWLEDGEMENTS **119**

List of abbreviations

ABC	Activated B-cell-like
AGS	Aicardi-Goutières syndrome
AIM2	Absent in Melanoma 2
ASC	Apoptosis-associated, speck-like protein containing a CARD
ATF4	Activating transcription factor 4
ATF6	Activating transcription factor 6
ATF6f	ATF6 cytosolic fragment
ATP	Adenosine triphosphate
BiP	Binding immunoglobulin protein
BTZ	Bortezomib
bZIP	Basic Leucine zipper
CANDLE	Chronic atypical neutrophilic dermatosis with lipodystrophy and elevated temperature
CARD	Caspase activation and recruitment domain
Cas9	CRISPR-associated 9
CDN	Cyclic dinucleotide
cGAMP	Cyclic guanosine-monophosphate-adenosine-monophosphate
cGAS	Cyclic guanylate-adenylate synthase
CHOP	C/EBP homologous protein
CP	Core particle
CpG	Cytosine-phosphate-guanine
CRISPR	Clustered Regularly Interspersed Short Palindromic Repeats
CXCL10	C-X-C motif chemokine ligand 10
DAMP	Damage-associated molecular pattern
DC	Dendritic cell
DENV	Dengue virus
DLBCL	Diffuse large B cell lymphoma
DMEM	Dulbecco's Modified Eagle Medium
DMSO	Dimethyl sulfoxide
DM2	Myotonic dystrophy type 2 (dystrophia myotonica 2)

DNA	Deoxyribonucleic Acid
dNTP	Dinucleotide triphosphate
ds	Double-stranded
EDTA	Ethylenediaminetetraacetic acid
EC_{50}	Half maximal effective concentration
ELISA	Enzyme-linked immunosorbent assay
eIF2α	eukaryotic initiation factor 2α
ER	Endoplasmic reticulum
ERAD	ER-associated degradation
FCS	Fetal Calf Serum
GADD34	Growth arrest and DNA damage-inducible protein 34
GFP	Green fluorescent protein
GSDMD	Gasdermin D
HEK	Human embryonic kidney
HIV-1	Human Immunodeficiency virus 1
hr	Human recombinant
HSV-1	Herpes simplex virus 1
HT-DNA	Herring testes DNA
IAV	Influenza A viruses
IC_{50}	Half maximal inhibitory concentration
IFN	Interferon
IFNAR	Interferon α receptor
IFIT1	Interferon-induced protein with tetratricopeptide repeats 1
IKKε	Inhibitor of NF-κB signaling kinase ε
IL	Interleukin
IRE1	Inositol-requiring enzyme 1
IRF	Interferon regulatory factor
ISG	Interferon-stimulated genes
ISG15	IFN-stimulated gene protein 15
ISGF3	Interferon-stimulated gene factor 3
IVT4	In vitro transcript 4
kDa	Kilodalton

KSHV	Kaposi's sarcoma-associated herpesvirus
LGP2	Laboratory of genetics and physiology 2
LPS	Lipopolysaccharide
MACS	Magnetic cell separation
MAVS	Mitochondrial antiviral signaling protein
M-CSF	Monocyte colony-stimulating Factor
MDA5	Melanoma differentiation associated protein 5
MHC	Major histocompatibility complex
MM	Multiple myeloma
mRNA	Messenger RNA
mtDNA	Mitochondrial Deoxyribonucleic Acid
MYD88	Myeloid differentiation primary response 88
NA	Nucleic acid
NF-κB	Nuclear factor κ light chain enhancer of activated B cells
NLR	NOD-like Receptor
NLRC4	NLR family CARD containing protein 4
NLRP	NLR family pyrin domain containing
NS1	Nonstructural protein 1
PAMP	Pathogen-associated molecular patterns
PBMCs	Peripheral blood mononuclear cells
PBS	Phosphate-buffered saline
PERK	dsRNA-activated protein kinase-like ER kinase
PKR	Protein Kinase R
PMA	Phorbol-12-myristate-13-acetate
PolyI:C	Polyinosinic:polycytidylic acid
PP1	Protein phosphatase 1
PRAAS	Proteasome-associated autoinflammatory syndromes
PRR	Pattern Recognition Receptor
RIDD	Regulated IRE1-dependent decay
RIG-I	Retinoic acid-inducible gene I
RLR	RIG-I-like Receptor
ROS	Reactive oxygen species

RP	Regulatory particle
RPMI	Roswell Park Memorial Institute
RSAD2	Radical SAM domain-containing 2
RT	Reverse Transcriptase
SAVI	STING-associated vasculopathy with onset in infancy
SD	Standard deviation
SEM	Standard error of the mean
SERCA	Sarcoplasmic/endoplasmic reticulum calcium ATPase
ss	Single-stranded
STAT	Signal transducer and activator of transcription
STING	Stimulator of Interferon Genes
STORM	Stochastic optical reconstruction microscopy
S1P	Site-1 protease
S2P	Site-2 protease
TASL	TLR adaptor interacting with SLC15A4 on the lysosome
TBK1	TANK-binding kinase 1
TFAM	Transcription factor A, mitochondrial
TLR	Toll-like Receptor
TME	Tumor microenvironment
TN	Tunicamycin
TNF	Tumor necrosis factor
TOMM20	Mitochondrial import receptor subunit TOM20 homolog
TPG	Thapsigargin
TREX1	Three prime repair exonuclease 1
TRIF	TIR-domain containing adapter inducing IFNβ
TRIM25	Tripartite motif containing protein 25
TYK2	Tyrosine kinase 2
UPR	Unfolded protein response
WT	Wild type
XBP1	X-Box-binding protein 1
$XBP1_s$	Spliced X-Box-binding protein 1
ZNF9	Zinc finger protein 9

β2M	β_2-microglobulin

1. Introduction

1.1. Mechanisms and functions of immunity

Every living being exists in constant interaction with its environment. Thus, the ability to recognize potential pathogens and other threats to cellular integrity and to counteract them an appropriate manner is essential to survival. The cellular and molecular mechanisms which recognize such threats and protect organisms from disease are known as the immune system.

In jawed vertebrates, two complementary forms of immune defense have developed: (i) the innate immune system, which is found in diverse lifeforms, including plants, fungi and invertebrates and allows for rapid detection of threats through barrier functions and conserved, germline-encoded "pattern recognition receptors" (PRRs), and (ii) the adaptive immune system, which first developed in jawed vertebrates and utilizes clonal selection to generate highly specialized receptors. Adaptive immune cells undergo further refinement upon recognition of a specific antigen. This adaptive immune system provides a more effective immune response to repeated antigen challenge but requires days to weeks to be established (Medzhitov, 2008; Medzhitov & Janeway, 2000; Murphy & Weaver, 2018)

Although effector mechanisms in innate and adaptive immune responses are quite distinct, both systems contribute to the establishment of an inflammatory response to potentially harmful stimuli (Medzhitov, 2008). Rapidly initiating, non-specific innate immune responses act as a "first line of defense" against potential pathogens and activate the more specific adaptive immune response, which then is able to confer immunological memory.

1.1.1. Pattern recognition as a basic principle of innate immunity

Recognition of molecular patterns is a central mechanism of innate immunity in all known organisms (Janeway, 1989). Metazoans utilize a diverse repertoire of PRRs to initiate inflammatory signaling upon recognition of intrinsic and extrinsic danger signals. Broadly, their ligands can be divided into two groups: damage-associated molecular

patterns (DAMPs) and pathogen-associated molecular patterns (PAMPs). DAMPs are endogenous molecules released as danger signals from cells undergoing stress, injury, or immunogenic cell death, and their detection leads to sterile inflammation. In contrast, PAMPs are microbial and viral structures detected by PRRs (Newton & Dixit, 2012). Both DAMPs and PAMPs serve as PRR ligands and induce an immune response characterized by the release of inflammatory cytokines (Newton & Dixit, 2012).

PRRs can be subdivided in different groups based on their structure and their subcellular localization. Membrane-bound PRRs such as Toll-like Receptors (TLRs) are found on the cell surface as well as in endosomes. Cytosolic receptors include NOD-like Receptors (NLRs), Retinoic Acid-Inducible Gene I (RIG-I)-like receptors (RLRs), Absent in melanoma 2 (AIM2)-like receptors, and the DNA sensor cyclic GMP-AMP synthase (cGAS) (Lamkanfi & Dixit, 2014).

1.1.2. Coordination of innate and adaptive immune responses

The innate immune system is highly effective in detecting and overcoming harmful events, yet its ability to establish immunological memory is limited to epigenetic mechanisms (Netea et al., 2016). Thus, in mammals, the adaptive immune system is the primary source of immune memory due to its ability to generate cells equipped with receptors specific to unique antigens through somatic recombination (Iwasaki & Medzhitov, 2015). These cells possess the ability to differentiate into subsets with highly selective tasks. Adaptive immunity can be divided into humoral immunity, which is principally mediated by antibodies produced by B cells, and cellular immunity, which mainly results from cytotoxic and regulatory function of T cells (Murphy & Weaver, 2018). Innate and adaptive immune responses have to be closely coordinated in order to mount effective pathogen defense and thus form a complex immune hierarchy (Iwasaki & Medzhitov, 2015; Medzhitov, 2008).

Initially, secretion of cytokines and chemokines, such as members of the Interleukin (IL) family and type-I Interferons (IFN), upon PRR activation in both immune and non-immune cells, activates T lymphocytes and recruits them to sites of potential harm. Once activated, $CD8^+$ T lymphocytes can elicit their cytotoxic functions directly, whereas $CD4^+$ T lymphocytes attract innate immune cells such as monocytes/macrophages and

neutrophilic granulocytes via secretion of IFN γ, IL-12, and IL-22 and mediate regulatory functions in adaptive immunity (Luckheeram et al., 2012). A subset of $CD4^+$ T cells, T-follicular helper cells, interacts with humoral immunity by secretion of IFN γ in order to initiate antibody production by activated B cells (Luckheeram et al., 2012). Memory T and B cells as well as circulating antibodies contribute to the formation of immunological memory that enables a faster response to reoccurring threats (Iwasaki & Medzhitov, 2015).

1.1.3. Immunorecognition of nucleic acids

Ribonucleic Acid (RNA) and Deoxyribonucleic Acid (DNA) are essential carriers of biological information for every organism. However, detection of non-self RNA and DNA is essential to determining the presence of microbes within cells (Bartok & Hartmann, 2020). Thus, during evolution, innate immune sensing of nucleic acids (NA) developed as a sort of *Faustian bargain*, enabling detection of exogenous genetic material at the cost of potential autoreactivity.

Defense mechanisms against non-self NA are present even in unicellular organisms. Prokaryotes and invertebrates dispose of adaptive immune mechanisms which detect foreign NA based on their sequence. Prominent examples include Clustered Regularly Interspersed Short Palindromic Repeats (CRISPR)-based mechanisms in prokaryotes and RNA interference in eukaryotes (Siomi & Siomi, 2009; Terns & Terns, 2011). However, vertebrates principally make use of germline-encoded PRRs that detect exogenous or altered NA based on their molecular features (Bartok & Hartmann, 2020). Of note, recent studies have established ancient evolutionary origins, as part of the phage defense system in bacteria, for several vertebrate NA sensors (Margolis et al., 2017).

In vertebrates, NA sensing initiates several innate immune effector mechanisms (i) NA restriction factors directly limit replication of intracellular pathogens such as viruses in a cell-intrinsic manner (Yan & Chen, 2012), (ii) The initiation of a multicellular immune response occurs through secretion of cytokines and chemokines, most prominently type-I IFNs such as IFNα and IFNβ, which are of critical importance in antiviral defense (Stetson & Medzhitov, 2006b). Type-I IFN release as a consequence of NA sensing

pathways appears logical as the presence of foreign genetic material is a hallmark of viral infection (Hartmann, 2017). Type-I IFNs employ autocrine and paracrine defense mechanisms to limit pathogen spread. Moreover, they have a central role in orchestrating the antiviral response of professional immune cells, including promoting antigen presentation and cross-presentation and recruiting and activating lymphocytes (Stetson & Medzhitov, 2006b). Interestingly, type-I IFNs have also been shown to initiate negative feedback loops in order to prevent excess inflammatory signaling (Ivashkiv & Donlin, 2014).

Signaling downstream of the heterodimeric transmembrane IFNα receptor (IFNAR) is essential to the antimicrobial activity of type-I IFN. Binding of type-I IFNs to the IFNAR activates Janus Kinase 1 (JAK1) and Tyrosine Kinase 2 (TYK2), which in turn phosphorylate signal transducer and activator of transcription (STAT) 1 and STAT2 (Ivashkiv & Donlin, 2014). Once phosphorylated, these transcription factors dimerize and, upon translocation to the nucleus, form a multimolecular complex called IFN-stimulated gene factor 3 (ISGF3) with IFN regulatory factor (IRF9). ISGF3 binds to specific response elements across the genome and thus induces transcription of IFN-stimulated genes (ISGs) (Ivashkiv & Donlin, 2014). Over 350 ISGs with highly diversified antiviral activities have been identified to date. However, the degree to which their roles in antiviral defense have been characterized varies considerably (Schoggins et al., 2011). In general, it should be noted that ISG responses depend on context and cell type, and their regulation is complex owing to their potentially devastating effects on the host organism (Ivashkiv & Donlin, 2014).

1.1.3.1. Mechanisms of RNA sensing

Exogenous RNA may be present in the cytosol during infection with viruses or intracellular bacteria as well as in the endosome following the efferocytosis of infected cells. However, both compartments physiologically contain host RNA, rendering immunorecognition of RNA particularly challenging (Bartok & Hartmann, 2020).

In the endosome of human cells, RNA recognition occurs through membrane-bound TLRs, namely TLR3, TLR7 and TLR8. TLR3 is a double-stranded (ds) RNA sensor that can be located either at the cell surface or in endosomes of non-immune cells. It signals

via TIR-domain containing adapter inducing IFNβ (TRIF) and induces secretion of type-I IFNs as well as inflammatory signaling via Nuclear factor κ light chain enhancer of activated B cells (NF-κB) (Bartok & Hartmann, 2020). TLR7 and TLR8 are products of a gene duplicate on the X chromosome. In contrast to TLR3, TLR7 and TLR8 sense degradation products of single-stranded (ss) RNA and are selectively expressed on immune cells. Both signal via Myeloid differentiation primary response 88 (MYD88) and TLR adaptor interacting with SLC15A4 on the lysosome (TASL) to induce IRF5-dependent IFNβ secretion (Heinz et al., 2020). Furthermore, cytokine secretion is distinct between TLR7 and TLR8, as is their expression pattern (Bartok & Hartmann, 2020; Ostendorf et al., 2020)

RNA sensing also occurs independently of membrane-bound TLRs by cytosolic PRRs. RIG-I and Melanoma differentiation associated protein 5 (MDA5), together with the putative RNA restriction factor Laboratory of genetics and physiology 2 (LGP2), form the RLR family and induce a type-I IFN-dependent immune response via Mitochondrial antiviral signaling protein (MAVS). Downstream of RLR activation, MAVS forms “prion-like” protein stretches, is phosphorylated at its c-terminus by the kinases TANK-binding kinase 1 (TBK1) and Inhibitor of NF-κB signaling kinase ε (IKKε), and subsequently binds to IRF3 to induce type-I IFN transcription (Hou et al., 2011; S. Liu et al., 2015).

The molecular requirements for recognition of RNA by RIG-I have been characterized extensively. Initially, 5’-triphosphate RNA was identified as the minimal RIG-I ligand (Hornung et al., 2006). However, further investigation revealed that RIG-I actually recognizes short, blunt-ending dsRNA and methylation of the 5’-terminal nucleotide is crucial to prevent self-recognition (Schlee et al., 2009; Schuberth-Wagner et al., 2015). A minimal MDA5 ligand has not yet been conclusively identified; however, experimental evidence demonstrates that MDA5 is activated by long dsRNA of high molecular weight (Hartmann, 2017).

It is worth noting that RLRs are expressed almost ubiquitously in nucleated cells, emphasizing their importance in viral defense. All three known RLRs bind dsRNA in the cytosol, which is a hallmark of virus infection (Bartok & Hartmann, 2020). Due to their broad expression and their relatively well-characterized signaling mechanisms, RLRs are subject to extensive study as potential targets for therapeutic manipulation of innate immunity (Hartmann, 2017).

1.1.3.2. Mechanisms of DNA sensing

DNA, the central carrier of genetic information in cellular organisms, is found both in the host and most pathogens. Thus, it can act both as a DAMP and a PAMP. Analogous to RNA detection, DNA recognition by the innate immune system primarily occurs in the endolysosomal and the cytosolic compartment (Hartmann, 2017).

To date, only one endosomal DNA sensor, TLR9, has been identified (Hemmi et al., 2000). In contrast to the RNA sensor TLR3, TLR9 signaling from the cell surface appears to be nonphysiological, as TLR9 surface translocation in an experimental setting results in a strong autoinflammatory phenotype (Mouchess et al., 2011). TLR9 preferentially recognizes ssDNA oligonucleotides containing a high number of unmethylated cytosine-phosphate-guanine (CpG) motifs which are more frequent in viral and prokaryotic than in eukaryotic DNA. Endosomal CpG-DNA sensing by TLR9 activates innate immunity via the adaptor molecules MYD88 and TASL (Heinz et al., 2020).

An IFN-mediated immune response to cytosolic DNA was first described in an infection model of intracellular bacteria species (Stetson & Medzhitov, 2006a). Several years later, cyclic guanylate-adenylate synthase (cGAS) was identified as the sequence-independent, direct cytosolic DNA sensor inducing a type-I IFN response (L. Sun et al., 2013). Initially thought to be a cytosolic protein, it has recently been demonstrated that cGAS is predominantly localized in the nucleus where its autoactivation is inhibited by continuous sequestration and maintenance of an inactive state through binding to cytosolic proteins (Michalski et al., 2020; Pathare et al., 2020).

For DNA recognition, homodimeric cGAS directly binds to dsDNA, inducing a conformational switch to enable synthesis of a unique second messenger, cyclic guanosine-monophosphate-adenosine-monophosphate (cGAMP), containing a non-canonical 2’-5’-linkage that confers resistance to RNase-mediated degradation (Civril et al., 2013; Gao et al., 2013a; Jiaxi Wu et al., 2013). Length-dependent dsDNA recognition by cGAS leads to the formation of ladder-like cGAS-DNA-structures (Andreeva et al., 2017). As structural hallmarks of DNA are highly similar between organisms, it has been proposed that cytosolic mislocalization of DNA would be sufficient for induction of cGAS-dependent immunity. Cytosolic DNA is usually rapidly

degraded by Three prime repair exonuclease 1 (TREX1) and is only detected in the case of overwhelming abundance or TREX1 misfunction. Consequently, genetic ablation of TREX1 and structural resistance of DNA to TREX1-mediated degradation have been demonstrated to induce a DNA-dependent type-I IFN response (Ablasser et al., 2014; Gehrke et al., 2013). Fine-tuning of DNA recognition and downstream signaling of cGAS appears to be a delicate process that remains under continuous investigation.

2'-3'-cGAMP synthesized by activated cGAS binds to Stimulator of IFN genes (STING), an endoplasmic reticulum (ER)-resident signaling protein. Prior to the identification of cGAS, STING had been described to be a sensor for cyclic dinucleotides (CDNs) employed as second messengers in bacteria (Burdette et al., 2011). However, the discovery of 2'3'-cGAMP as an endogenous CDN has revealed its primary function in vertebrate immunity as a signaling protein downstream of cGAS. CDN binding of STING leads to conformational changes, formation of STING homodimers, and phosphorylation at the C-terminus by a TBK1/IKKε complex, a mechanism shared with MAVS and TRIF. STING subsequently forms multimeric clusters at the Golgi apparatus and then binds to IRF3 which is in turn phosphorylated itself. pIRF3, as described previously, acts as a transcription factor for type-I IFNs (Liu et al., 2015). In addition to type-I IFN secretion, STING signaling leads to the release of other proinflammatory cytokines such as tumor necrosis factor (TNF). Interestingly, cytokine secretion downstream of STING activation is differentially regulated. Whereas IRF3 phosphorylation and IFN secretion is highly dependent on TBK1 kinase activity, NF-κB-dependent TNF secretion following STING activation is mediated redundantly by TBK1 and IKKε and involves other IKK family kinases (Balka et al., 2020).

Outside of its role in mediating inflammatory cytokine secretion, STING executes a variety of IFN-independent functions such as induction of autophagy, i.e. cellular "self-digestion". It has been proposed that IFN-independent functions of STING evolutionarily predate its role in mediating IFN secretion (Gui et al., 2019).

In an analogy to RLRs, the cGAS-STING pathway has emerged as an attractive therapeutic target in recent years, and small molecule inhibitors enabling manipulation of both cGAS and STING have been developed (Haag et al., 2018; Lama et al., 2019).

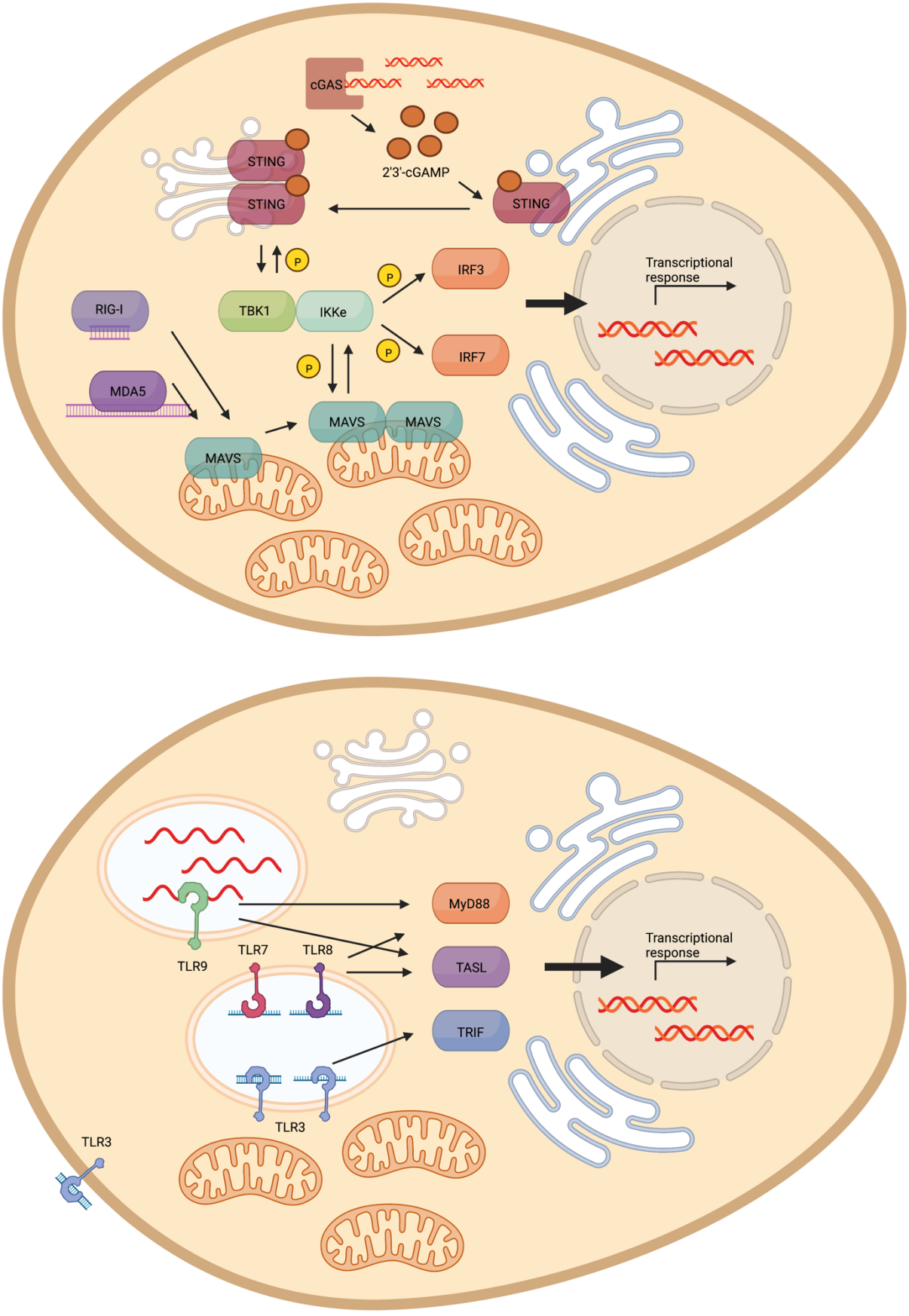
cGAS
2'3'-cGAMP
STING
STING
STING
P
P
IRF3
TBK1
IKKe
RIG-I
P
IRF7
MDA5
MAVS
MAVS
MAVS
Transcriptional response
MyD88
TLR7
TLR8
TLR9
TASL
TRIF
TLR3
TLR3
Transcriptional response

Figure 1: Overview of intracellular nucleic acid recognition
Upper panel: Selected cytosolic NA receptors and schematic signaling pathways. RIG-I and MDA5 recognize cytosolic RNA and induce a transcriptional response via the mitochondrial protein MAVS. The cytosolic DNA receptor cGAS activates STING via the second messenger 2‘3‘-cGAMP. Both MAVS and STING recruit the TBK1/IKKε kinase complex which phosphorylates IRF3 and IRF7 to induce a transcriptional response.
Lower panel: Endosomal NA receptors. TLR9 recognizes endosomal ssDNA based on CpG methylation motifs. TLR7 and TLR8 are structurally similar receptors that recognize ssRNA in the endosome. TLR3 may recognize ssRNA and dsRNA in the endosome and on the cell surface. TLR7, TLR8, and TLR9 signal via MyD88 and TASL while TLR3 signals via TRIF. Adapted from Bartok & Hartmann, 2020.

1.1.3.3. Innate sensing of mitochondrial DNA

Mitochondria, in contrast to other cell organelles, contain their own genetic information encoded in mitochondrial DNA (mtDNA). mtDNA has a length of about 17,000 base pairs and contains 37 genes that mostly play roles in oxidative phosphorylation or encode proteins that are involved in mitochondrial scaffolding. It is structurally distinct from nuclear DNA, as it is circular and not organized in histones. Physiologically, mtDNA is bound to transcription factor A, mitochondrial (TFAM), that serves as a structural scaffold and as an initiating transcription factor at the same time (West & Shadel, 2017).
Under homeostatic conditions, mtDNA is confined to the mitochondrial matrix, yet several cellular processes such as infection and aging lead to mtDNA leakage into the cytosol. (West & Shadel, 2017) Circular mtDNA is naturally resistant to degradation by TREX1 whose nuclease activity only acts on free 3’ ends of DNA strains (Gehrke et al., 2013). Thus, cytosolic mtDNA is prone to recognition by cGAS and subsequent induction of a type-I IFN response (West, 2017).
cGAS-dependent mtDNA recognition in the cytosol has been described in several contexts. In gram-negative bacterial sepsis, intracellular lipopolysaccharide (LPS) leads to formation of Gasdermin D (GSDMD) pores in the mitochondrial membrane. Cytosolic mtDNA leaking through these pores confers cGAS-mediated endothelial inflammation and injury (Huang et al., 2020). Contrastingly, TFAM deficiency as well as HSV-1 infection lead to mitochondrial stress and subsequent mtDNA cytosolic translocation, which potentiates antiviral innate immune responses and improves viral clearance (West et al., 2015). However, other viruses such as Dengue virus (DENV) have developed

mechanisms to impair cGAS responses to mtDNA by expressing proteases that degrade the cellular DNA sensing machinery (Aguirre et al., 2017).

mtDNA-mediated IFN responses also play a role in sterile inflammation. In type 2 myotonic dystrophy, translation of RNA repeats leads to cytosolic accumulation of protein complexes which induce mitochondrial stress, leading to mtDNA release into the cytosol and autoinflammation mediated by type-I IFNs (Günther et al., 2022). The underlying mechanisms of this response have been investigated in the present study (See section 4.1).

1.1.4. Inflammasomes

NF-κB and IFN-mediated immunity is largely regulated on the transcriptional level and relies on *de novo* translation of effector molecules. Contrastingly, inflammasomes, multiprotein complexes containing a sensor protein and the protease caspase 1, allow for rapid induction of an immune response independent of transcriptional control via caspase 1-mediated proteolytic maturation of the inactive precursor form of IL-1β (Broz & Dixit, 2016; Thornberry et al., 1992). In most cases, inflammasomes also contain an additional adaptor protein, Apoptosis-associated, speck-like protein containing a CARD (ASC) (Broz & Dixit, 2016). To date, over half a dozen *bona fide* inflammasome-forming sensor proteins have been identified, with NLR family pyrin domain containing (NLRP) 1, NLRP3, NLR family Caspase activation and recruitment domain (CARD) containing protein 4 (NLRC4), and AIM2 arguably being the best-characterized members of this family. Different inflammasome receptor proteins can be activated by various DAMPs and PAMPs. However, for some, no molecular ligand has been conclusively identified to date (Lamkanfi & Dixit, 2014).

Lysosomal rupture and reactive oxygen species (ROS) were initially proposed to be the crucial signals for NLRP3 inflammasome assembly. However, it has now been established that potassium efflux is the common denominator of NLRP3-activating events (Muñoz-Planillo et al., 2013; Xu et al., 2020). Interestingly, NLRP3 is also activated downstream of cGAS-mediated DNA recognition in human myeloid cells (Gaidt et al., 2017). Nonetheless, the exact mechanism of potassium level measurement by NLRP3 remains elusive (Broz & Dixit, 2016).

NLRP1 is activated by bacterial toxins in a complex process termed functional degradation and has been reported to serve as a sensor for intracellular dsRNA (Bauernfried et al., 2020; Sandstrom et al., 2019). NLRC4 is activated directly by the bacterial structural protein Flagellin (Broz & Dixit, 2016). AIM2, in contrast, has been described to be an important sensor of intracellular infection as it mediates inflammasome assembly upon recognition of cytosolic dsDNA (Hornung et al., 2009).

The mode of inflammasome activation is context-dependent as it may require a previous priming step in certain cells types. Transcriptional upregulation of inflammasome components occurs as a result of NF-κB dependent signaling following recognition of inflammatory cues by PRRs. The activation of inflammasome proteins curtail the conversion of the inactive protease procaspase 1 into its active form caspase 1 to enable downstream immune signaling. While certain inflammasomes, such as NLRC4, are thought to directly interact with caspase 1, others, such as NLRP3 and AIM2, have been demonstrated to form a functional inflammasome with ASC (Lamkanfi & Dixit, 2014). ASC serves as an adaptor protein and, in a striking analogy to other immune adaptor proteins such as MAVS, aggregates into multimeric, “prionoid” fibrils for signaling. Cells harboring mutations that abrogate its ability to polymerize demonstrate defective inflammasome signaling. In contrast to apoptotic cell death that is immunologically “silent” and mediated by other members of the caspases family, cell death following inflammasome activation activates the host immune system via release of DAMPs (Broz & Dixit, 2016).

Inflammasome-associated cell death is termed pyroptosis, and it is characterized by GSDMD membrane pore formation (Shi et al., 2015). Morphologically, pyroptosis manifests as atypical chromatin condensation and cell swelling. It is generally associated with activation of inflammatory caspases and usually, if not always, inflammasome formation. Pyroptosis may also serve as means of creating pore-induced intracellular traps, i.e. dead macrophages, containing intracellular bacteria (Galluzzi et al., 2018). NLRP3 activation downstream of GSDMD pore formation mediated by caspase-4/5-dependent recognition of intracellular LPS has been termed “non-canonical” inflammasome activation (Kayagaki et al., 2011).

The involvement of inflammasomes in human disease has sparked considerable interest in the pharmacological manipulation of inflammasome activation. This has led to the

development of a specific inhibitor of NLRP3, and other methods of inflammasome inhibition and activation for therapeutic purposes are currently being developed (Coll et al., 2015). Activation of NLRP3, and possibly other inflammasome proteins, may be beneficial in the context of immunotherapy approaches (Ghiringhelli et al., 2009).

1.1.5. Aberrant activation of innate immune signaling pathways

Immune effector mechanisms are carefully regulated to limit potential autoimmune damage while maximizing immune control. Lack of negative feedback regulation of the immune response leads to immunopathology and, as a consequence, to the development of autoimmune disease (Iwasaki & Medzhitov, 2015).

Autoimmune disease is a major health burden with a relatively high prevalence of up to 10% of the general population. Due to its significant morbidity and its frequent occurrence at a relatively young age, it heavily affects a significant fraction of the population at peak reproductive age (Cooper et al., 2009; Rosenblum et al., 2015). While most autoimmune diseases are characterized by the pathophysiological involvement of adaptive immunity, a subset of conditions, characterized by autoinflammation driven by sterile innate immune activation, has been termed *autoinflammatory* diseases. As immune responses are the net result of all activated adaptive and immune mechanisms, it should be stated that effector pathways of adaptive immunity may also have a role in autoinflammatory disease pathophysiology, and vice versa. The genetic and phenotypic spectrum of autoinflammatory disease is constantly expanding, and various pathways involved in innate immune signaling have found to be relevant for pathogenesis. (Lee-Kirsch, 2017).

Autoinflammatory diseases present with clinical signs of inflammation such as redness, swelling, pain, fever, and loss of function in various body parts and organs (de Jesus et al., 2015; Gabay & Kushner, 1999). These disorders can potentially affect all organ systems and result from a plethora of causative mutations, many of which lead to aberrant activation of TNF or inflammasome signaling. Disease presentation may be chronic or in periodic flares (Goldbach-Mansky et al., 2006; Kuemmerle-Deschner, 2015; McDermott et al., 1999).

A variety of mutations in genes encoding for proteins involved in NA metabolism and sensing confer a clinically distinct type of autoinflammatory disease, the type-I interferonopathies. Its prototype, Aicardi-Goutières syndrome (AGS), was described in 1984 by the eponymous French pediatricians (Aicardi & Goutières, 1984). AGS, as well as other type-I interferonopathies, phenotypically resembles intrauterine viral infection. It manifests in neonates as leukoencephalopathy with basal ganglia calcification, characterized by neurological symptoms including dystonia and recurring seizures, and fever episodes (Lee-Kirsch, 2017). AGS is mostly caused by mutations in genes involved in RNA recognition. However, mutations in other pathways are described for AGS as well as for other type-I interferonopathies such as STING-associated vasculopathy with onset in infancy (SAVI) (Y. Liu et al., 2014). Different type-I interferonopathies are phenotypically distinct, although there is considerable symptom overlap owing to the shared pathomechanism.

Chronic atypical neutrophilic dermatosis with lipodystrophy and elevated temperature (CANDLE), a distinct type of type-I interferonopathy, has been connected to inactivating mutations in different proteasome subunits, leading to insufficient degradation and thus accumulation of waste protein (Brehm et al., 2015). CANDLE has been proposed to be a result of ER stress-mediated autoinflammation. However, more recent results propose intracellular accumulation of IL-24 due to defective proteolytic degradation, leading to activation of protein kinase R (PKR), as the underlying pathomechanism (Davidson et al., 2022; Ebstein et al., 2019).

Development of specific inhibitors has enabled targeted treatment of autoinflammatory diseases based on the underlying inflammatory pathway. In the case of type-I interferonopathies, abrogation of IFNAR-dependent downstream signaling through pharmacologic targeting of the JAK/STAT pathway has proven effective (Kothur et al., 2018). Additional therapies, e.g. inhibition of reverse transcriptase (RT) in order to limit reverse transcription of endogenous retroelements and thus erroneous recognition of self-NA ligands, may be considered for affected patients (Rice et al., 2018).

Nonetheless, a deeper understanding of the underlying pathological mechanisms in autoinflammatory disease is urgently needed. On the one hand, intensified research may lead to improved treatment options for patients affected by Mendelian autoinflammatory disease (and potentially non-Mendelian conditions where

autoinflammation plays a pathophysiological role). On the other hand, discoveries concerning autoinflammatory disease pathology may deepen our understanding of general innate immune mechanisms and hold potential for the development of antimicrobial agents and immunotherapies.

1.2. Endoplasmic reticulum stress and its implications in immunity

Disturbances in protein turnover are a prototypical stress signal that alerts the innate immune system. Synthesis and processing at the ER are pivotal cellular functions for secreted proteins, which amount to approximately 30% of the average eukaryotic cell's proteome. In addition to its functions in protein biosynthesis, the ER also serves as a storage space and major regulator of intracellular calcium. Disturbances in ER integrity, leading to ER stress, may result from exogenous sources such as hypoxia, nutrient deprivation, and low pH, or from cell-intrinsic triggers, such as accumulation of misfolded proteins in the case of cell differentiation or metabolic dysregulation as well as calcium level perturbations (Bettigole & Glimcher, 2015).
In order to cope with ER stress, eukaryotic cells have developed versatile mechanisms to reduce protein load and maintain proteostasis, collectively termed the Unfolded Protein Response (UPR). While permanent ER stress and chronic activation of UPR pathways is a constant phenomenon in specialized secretory cells such as B cells, its occurrence in other cell types is a molecular hallmark of disease (Hetz, 2012).

1.2.1. Mechanisms and functions of the Unfolded Protein Response

The main objective of UPR mechanisms is the reduction of the amount of protein at the ER, which during ER stress exceeds the ER's capacity for coordinated processing. To this end, the UPR employs various mechanisms to control and limit protein processing, including increased transcription of chaperones and genes involved in protein degradation as well as blocking protein translation. Thus, protein processing capacity at the ER increases while protein folding load is reduced simultaneously. However, if disturbances to ER integrity cannot be resolved, the UPR then initiates cell death (Hetz, 2012).

The UPR consists of three signaling pathways, or branches, employed in parallel. Each branch of the UPR is characterized by a distinct transmembrane ER-resident signaling protein as its “master switch” (Walter & Ron, 2011).

In the first and phylogenetically oldest UPR branch, this role is fulfilled by inositol-requiring enzyme 1 (IRE1), present in the two isoforms IRE1α and IRE1β in mammalian cells. IRE1 is a bifunctional kinase/endonuclease that is activated by indirect sensing of unfolded proteins in proximity to the ER. Mechanistically, IRE1 has been found to bind to the chaperone protein Binding immunoglobulin protein (BiP) in its inactive form, repressing autoactivation. In the case of increased protein folding load, BiP is recruited to contribute to protein folding, and its dissolution from IRE1 leads to lateral IRE1 oligomerization in the ER membrane enabling endonuclease activity. IRE1 then excises an intron from the transcription factor X-Box-binding protein 1 (XBP1) messenger RNA (mRNA) which is subsequently translated into the active transcription factor $XBP1_s$ ($_s$ indicating spliced) (Yoshida et al., 2001). $XBP1_s$ mediates transcriptional upregulation of chaperones, proteins involved in lipid synthesis for ER expansion, and genes essential for ER-associated degradation (ERAD) (Walter & Ron, 2011). During ERAD, misfolded proteins are retained in the ER and then translocated to the cytosol in order to be made available for subsequent proteasomal degradation (Hetz, 2012). In addition to its transcriptional effects mediated by $XBP1_s$, IRE1 regulates direct cleavage of selective mRNAs encoding ER-associated proteins, possibly via its endonuclease activity, in a process termed regulated IRE1-dependent decay (RIDD). Thus, the IRE1 branch of the UPR aims to alleviate ER stress by concomitantly increasing protein processing capacity and decreasing protein folding load (Walter & Ron, 2011).

The second enzymatic master regulator of the UPR, dsRNA-activated protein kinase-like ER kinase (PERK), mainly contributes to resolving ER stress by establishing a translational block. Upon sensing ER stress, PERK oligomerizes in the ER membrane where it is autophosphorylated and, in turn, phosphorylates and thus inhibits eukaryotic initiation factor 2α (eIF2α). As eIF2α is crucially required for the initiation of protein biosynthesis in mammals, translation is ubiquitously inhibited with the exception of certain mRNAs containing short open reading frames in their 5’ untranslated regions (Walter & Ron, 2011). One of these mRNAs encodes activating transcription factor 4 (ATF4), which drives expression of, i. a., C/EBP homologous protein (CHOP) and

growth arrest and DNA damage-inducible protein 34 (GADD34). While CHOP is a transcription factor for several apoptosis-related proteins and thus a driver of cell death, GADD34 acts as a negative regulator of the PERK pathway. It encodes a subunit of protein phosphatase 1 (PP1), which is able to dephosphorylate eIF2α (Walter & Ron, 2011). This mechanism can be targeted by the small molecule inhibitor Guanabenz to protect cells from ER stress through maintenance of phospho-eIF2α levels, reducing transcriptional activity (Tsaytler et al., 2011).

The third signaling branch of the UPR counteracts ER stress via the effects of activating transcription factor 6 (ATF6) (Haze et al., 1999). ATF6 represents a family of basic Leucine zipper (bZIP) transcription factors with at least seven members in humans, with ATF6A and ATF6b being most broadly expressed (Thuerauf et al., 2007; K. Yamamoto et al., 2007). During ER stress, ER-resident ATF6 translocates to the Golgi apparatus for proteolytic processing by site-1 protease (S1P) at the luminal domain and by site-2 protease at the transmembrane domain, releasing an N-terminal cytosolic fragment (ATF6f). ATF6f subsequently mediates transcriptional upregulation of ERAD components, XBP1, and chaperones such as BiP (Hetz, 2012). Additionally, ATF6 has been shown to contribute to the maintenance of ER function during different cellular states in a unique mechanism that is non-redundant with IRE1 and PERK function, thus enabling survival of cells undergoing chronic ER stress (Wu et al., 2007).

Altogether, all three UPR pathways license increased protein folding capacity at the ER through distinct transcriptional programs. Additionally, IRE1 and PERK reduce protein folding load, employing translation blocking and mRNA degradation, respectively (Walter & Ron, 2011).

Regulation of UPR pathways remains incompletely understood. While IRE1 is the unique response pathway to ER stress in lower eukaryotes such as yeast, the mammalian UPR demonstrates considerable redundancy. Among the UPR effectors, XBP1 seems to be of special importance in “physiological” ER stress, such as in secretory cells. Furthermore, the existence of various ATF6 family members and IRE1 paralogs in mammals with differential expression patterns hints at a high degree of tissue tropism in the mammalian UPR branches that remains to be fully elucidated (Walter & Ron, 2011).

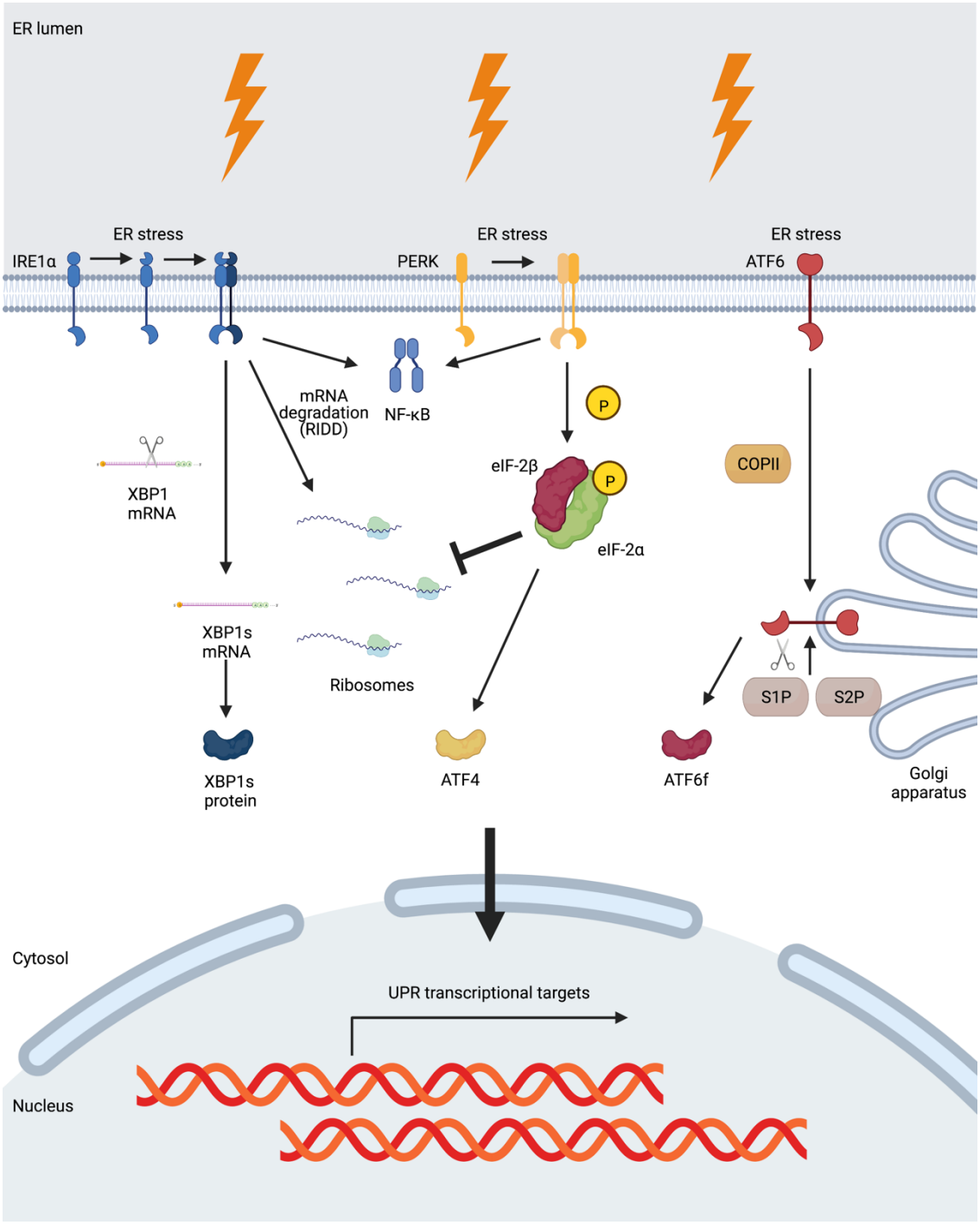

Figure 2: Schematic overview of the unfolded protein response
The three main UPR branches are depicted here. In case of ER stress, IRE1α is activated and dimerizes in the ER membrane. IRE1α homodimers possess a nuclease activity that allows for splicing of XBP1 mRNA, leading to translation of the XBP1s transcription factor. Furthermore, IRE1α degrades mRNAs in a process termed regulated IRE1-dependent decay (RIDD).
PERK dimerizes upon ER stress, and PERK homodimers phosphorylate eIF2α to induce a global translation block via inhibition of translation initiation. peIF2α activates the

transcription factor ATF4. Both PERK and IRE1α homodimers exhibit NF-kB activating activity.
The third UPR sensor, ATF6, translocates from the ER membrane to the Golgi apparatus during ER stress, where it is processed by Site-1 and Site-2 proteases (S1P and S2P). A cytosolic fragment, ATF6f, is generated.
XBP1s, ATF4 and ATF6f act as transcription factors mediating the transcriptional activity of the UPR.

1.2.2. Interaction of innate immunity and endoplasmic reticulum stress pathways

Cellular stress is a prototypical activating signal for the immune system. Consequently, interactions between ER stress, the UPR, cellular physiology, and immunity are numerous. Nonetheless, they remain incompletely understood.
Interestingly, physiological functions of the UPR seem to be indispensable even for early development, illustrated by the fact that XBP1 deficiency in mice leads to early embryonic lethality due to insufficient organogenesis (Bettigole & Glimcher, 2015). Furthermore, XBP1 plays an important role in plasma cell differentiation (Reimold et al., 2001). XBP1 is also critically involved in the development of Paneth cells that control inflammation in the intestinal epithelium as well as in dendritic cell maturation (Bettigole & Glimcher, 2015). The PERK-eIF2α branch of the UPR has been shown to play a critical role in the maintenance of the hematopoietic stem cell pool (van Galen et al., 2014).
Furthermore, direct roles for ER stress and the UPR in immune responses have been described. On the one hand, UPR activation may occur downstream of PRR activation. This effect has been described in macrophages, where ligation of TLR4 as well as TLR2 induces ER stress-independent activation of the IRE1-XBP1 branch of the UPR, mediating production of pro-inflammatory cytokines at the expense of canonical UPR gene targets (Martinon et al., 2010). On the other hand, ER stress is a potential activator of innate immune responses. Enhancement of PRR signaling in cells pre-treated with ER stressors has been described extensively. To this end, various studies make use of the ER stress-inducing small molecules Tunicamycin (TN) and Thapsigargin (TPG) for pharmacological induction of the UPR (Liu et al., 2012; Menu et al., 2012; Smith et al., 2008). TN induces ER stress via inhibition of N-linked glycosylation, which is a prerequisite for lysosomal degradation of waste protein. TPG acts as an inhibitor of

sarcoplasmic/endoplasmic reticulum calcium ATPase (SERCA), thus curtailing ER stress via perturbation of cellular calcium homeostasis. Both TN- and TPG-induced ER stress have been found to amplify type-I IFN responses to known PRR ligands such as the synthetic RNA receptor ligand polyinosinic:polycytidylic acid (polyI:C) and the TLR4 ligand LPS (Liu et al., 2012; Smith et al., 2008). One study observed that the enhancement of type-I IFN signaling was absent in XBP-1 knockdown cells. However, this study used HEK293T cells that only inaccurately reflect the physiological immune response to NA (Smith et al., 2008; L. Sun et al., 2013). A later study by the same group further characterized the interaction between ER stress and type-I IFN secretion. Here, the authors again observed increased type-I IFN secretion following PRR stimulation after pre-treatment with ER stressors. Signaling amplification could be abrogated by inhibiting S1P processing of ATF6, indicating a dependency on the ATF6 UPR branch. STING-TBK1 colocalization as well as IRF3 nuclear translocation and phosphorylation occurred following treatment with ER stressors alone, whereas IFN transcript numbers were not markedly increased in this condition (Liu et al., 2012). Interestingly, TLR4 activation has also been shown to induce activation of the IRE1-XBP1 UPR branch, whereas XBP1 activation was required for optimal TLR responses and a lack of XBP1 activation was associated with increased susceptibility to bacterial infection (Martinon et al., 2010). These results indicate a reciprocal relationship between PRR activation and the UPR. Although ER stress-mediated IFN signaling appears to be a useful addition to innate immunity's repertoire of defense mechanisms, its mechanism and regulation remain incompletely understood (Smith, 2014).

In addition to its role in IFN-mediated inflammation, ER stress has been implicated in innate immunity by its ability to induce inflammasome activation. Initial studies described UPR-independent inflammasome assembly following TN and TPG treatment *in vitro* (Menu et al., 2012). Continued research has revealed a more sophisticated mechanism by which ER stress supposedly induces inflammasome-dependent inflammation. Specifically, ER stress, provoked by bacterial infection with *Brucella abortus* strain RB51, mediated IRE1- and NLRP3-mediated cleavage of Caspase 2 and subsequent release of mitochondrial contents which, in turn, induced canonical NLRP3 inflammasome assembly (Bronner et al., 2015).

Although various mechanisms of ER stress-mediated activation and regulation of inflammation have been identified, continued efforts are required to further elucidate underlying pathways and their therapeutic potential.

1.3. The proteasome and its therapeutic manipulation

1.3.1. Protein degradation by the ubiquitin-proteasome system

Constant protein turnover in all living cells raises the need for an efficient protein degradation machinery. The lysosome, the first cellular organelle of this purpose to be discovered, possesses impressive protein degradation capacity. However, it mainly degrades proteins of extracellular origin and exhibits relatively little substrate specificity (Glickman & Ciechanover, 2002). Obviously, a more complex and tunable cellular degradation apparatus is required for the efficient, cell-intrinsic regulation of proteostasis (Glickman & Ciechanover, 2002). This machinery is found in the eukaryotic proteasome, a macromolecular complex dedicated to intracellular protein disposal. The fully assembled proteasome complex, also termed 26S proteasome, is composed of a 20S core particle (CP) with catalytic activity, and a 19S regulatory particle (RP). Both CP and RP contain multiple subunits, 14 for of the CP and at least 19 for the RP (Murata et al., 2009).

The individual subunits of the CP build up the quaternary structure of a proteolytic chamber. In its center, proteasome subunits β1, β2, and β5 contain the proteasome's active sites and mediate three mechanistically distinct types of protease activity, namely caspase-like, trypsin-like, and chymotrypsin-like activity. Each active site has the ability to cleave peptide bonds in order to sequester amino acid chains, yet their mechanisms of action vary. Trypsin-like active sites cut polypeptides preferably after basic residues, whereas chymotrypsin-like active sites exhibit their activity mainly after hydrophobic amino acid residues. The third group of active sites with caspase-like activity cleaves peptide bonds preferentially after aspartic acid residues (Kisselev & Goldberg, 2001). Aside from waste protein removal, the proteasome's proteolytic activity liberates amino acids that may serve as substrates for *de novo* protein synthesis (Glickman & Ciechanover, 2002).

In addition to amino acid salvage, products of proteasomal degradation include antigenic peptides that are destined for presentation on the cell surface by major histocompatibility complex (MHC) class I molecules (Goldberg & Rock, 1992). Next to the constitutively active proteasome subunits β1, β2, and β5, IFN-γ-inducible subunits β1i, β2i, and β5i contribute to the assembly of an analogous yet distinct protein complex termed the *immunoproteasome*. The immunoproteasome is characterized by an increased output of peptides ready for MHC-I-mediated presentation (Heinemeyer et al., 2004).

Whereas the 20S CP executes protein cleavage, the 19S RP regulates access to the proteolytic chamber in an adenosine triphosphate (ATP)-dependent manner. Furthermore, the RP selects proteasome substrates by recognizing proteins with polyubiquitin chains (Murata et al., 2009).

Ubiquitin is a polypeptide composed of 76 amino acids that serves as a molecular marker destining other proteins for proteasomal degradation. The process of protein ubiquitination is a multistep cascade involving several classes of enzymes. At first, E1 enzymes activate ubiquitin in an ATP-dependent manner. Secondly, activated ubiquitin is transferred to an E2-conjugating enzyme serving as a molecular carrier to the substrate, where the ubiquitin is bound by an E3 ubiquitin ligase. This reaction may occur in repetitive cycles, leading to the generation of a polyubiquitin chain covalently attached to a target protein. This target protein is subsequently degraded by the 26S proteasome. Ubiquitin molecules liberated during the degradation process can be reused afterwards (Glickman & Ciechanover, 2002). A broad variety of E3 ubiquitin ligases exists in eukaryotic cells with each enzyme recognizing distinct degradation signals on target proteins (Kisselev & Goldberg, 2001).

Interestingly, aside from their involvement in marking proteins for proteasomal degradation, E3 ubiquitin ligases fulfil other biological roles. For instance, they are essential for RIG-I activation, as RIG-I-mediated antiviral IFN signaling critically depends on ubiquitination of its N-terminal CARD domain by E3 family member tripartite motif containing protein 25 (TRIM25) (Gack et al., 2007).

1.3.2. Proteasome inhibition and its therapeutic use

The importance of the ubiquitin-proteasome system for intracellular protein turnover has sparked considerable interest in its pharmacological inhibition. Structurally, currently used proteasome inhibitors are short peptides with a C-terminal pharmacophore that is able to form a covalent adduct with one or more catalytic residues of proteasome subunits, thus reversibly or irreversibly inhibiting its proteolytic activities. Different chemical classes of proteasome inhibitors exist, and the majority of them are, to some extent, specific to the proteasome's chymotrypsin-like activity which appears to be rate-limiting in proteasomal protein degradation. As a consequence, inhibition of chymotrypsin-like catalytic residues has the greatest effect on proteolytic capacity reduction compared to the inhibition of other active sites. Furthermore, the hydrophobicity of Chymotrypsin-like activity inhibitors makes them highly cell-permeable and thus attractive for *in vitro* and *in vivo* use (Kisselev & Goldberg, 2001). Proteasome inhibitors were initially developed as research tools, and one of the first of many discoveries they enabled was the observation that proteasomal degradation is responsible for the generation of MHC class I-associated peptides that are presented as fragments of intracellular proteins on the cell surface (Rock et al., 1994).

However, in addition of their obvious utility in basic research, the discovery of their potent anti-inflammatory and anti-tumor proportions make proteasome inhibitors attractive candidates for clinical application (Kisselev & Goldberg, 2001).

Malignant cells, more than other cell types, are dependent on proteasomal degradation due to their increased load of misfolded or damaged protein as a consequence of their rapid proliferation. The abundance of waste proteins in tumor cells leading to cell death through activation of the UPR explains the particular toxicity of proteasome inhibitors in malignant cells (Teicher & Tomaszewski, 2015).

Both *in vitro* and *in vivo* studies demonstrated an impressive antiproliferative effect of proteasome inhibitors on multiple myeloma (MM) cells. MM is a neoplasm of plasma cells that accumulate at multiple site of the bone marrow and produce large quantities of non-functional immunoglobulins. Clinically, MM is predominantly characterized by myeloma-defining events, namely hypercalcemia, renal failure, anemia, and bone

lesions. In the United States, MM accounts for approximately 1% of all cancers, and consistently causes about 13,000 deaths per year (Rajkumar, 2020).

Bortezomib (BTZ) was the first proteasome inhibitor to enter clinical trials. It is a dipeptide boronic acid that acts as a reversible inhibitor of the proteasome's chymotrypsin-like catalytic sites. BTZ has demonstrated remarkable success in MM first line therapy as well as in relapsed or treatment-refractory disease and is used routinely in the clinic (Rajkumar, 2020; Richardson et al., 2003; San Miguel et al., 2008). Despite its ability to induce long-lasting remission, BTZ treatment is not curative in MM, and relapse is virtually inevitable. As a consequence, other proteasome inhibitors with the ability to overcome mechanisms of BTZ resistance, such as carfilzomib and ixazomib, have been developed and approved (Teicher & Tomaszewski, 2015). However, no trial including BTZ or one of these novel agents has revealed the option to definitively cure MM patients of disease. Therefore, continued efforts to investigate mechanisms of proteasome inhibition and their biological consequences are urgently required. Hopefully, results of these studies will pave the way to optimize MM treatment.

Of note, BTZ has been investigated as a therapeutic option in other hematologic cancers such as diffuse large B cell lymphoma (DLBCL). Interestingly, BTZ was efficient only in the activated B-cell-like (ABC) subtype of DLBCL, whose proliferation is largely dependent on inflammatory signaling mediated by NF-κB (Dunleavy et al., 2009). Efforts to therapeutically benefit from BTZ's anti-inflammatory properties for non-malignant diseases have been less successful, as the drug has failed to show efficacy in graft-versus-host disease prophylaxis following allogenic stem cell transplantation (Koreth et al., 2012).

1.3.3. Proteasome inhibition and immunity

Treatment with proteasome inhibitors such as BTZ does not only exhibit an effect on target cells, but also has systemic consequences to the host. Here, potential effects on immune signaling and functions are of particular interest as they may influence the interaction of the immune system with MM cells and/or contribute to common side effects of proteasome inhibitor treatment.

Lymphopenia is a common phenomenon in patients treated with BTZ and is reported to occur in up to 58% of all cases (Pellom et al., 2015). It is mainly attributed to a reduction of absolute T cell numbers caused by lymphocyte apoptosis; however, existing T cells also exert their function less efficiently due to impairment of cytokine production. As a consequence, insufficient CD4-T cell responses may result in Herpesvirus reactivation during BTZ treatment (Pellom et al., 2015).

In B lymphocytes, diminished antibody production following treatment with proteasome inhibitors has been demonstrated, probably mediated by their antiproliferative and proapoptotic effects and subsequent B cell lymphopenia. Similar proapoptotic mechanisms can be observed in innate immune cells such as DCs and natural killer cells (Pellom et al., 2015).

On the mechanistic level, the anti-inflammatory effects of BTZ and cognate proteasome inhibitors has classically been attributed to their ability to inhibit proteasomal degradation of endogenous NF-κB antagonists. However, experimental evidence suggests that BTZ treatment may have opposing effects, as it enhances constitutive NF-κB pathway activation in MM cells (Hideshima et al., 2009). Although the exact effect of BTZ on NF-κB signaling remains controversial, its interference with this important inflammatory pathway may account for its efficacy in NF-κB-driven cancers such as MM and ABC-DLBCL.

In alignment with the observation that proteasome inhibitors may also have pro-inflammatory effects, several studies have suggested that BTZ-mediated IL-1β signaling could influence the drug's role in the MM microenvironment.

It has been proposed that BTZ-mediated inflammatory polarization of host macrophages reduces the efficacy of proteasome inhibitor treatment, accelerating MM cell proliferation and disease progression in *in vivo* models (Beyar-Katz et al., 2016). Further investigation of this phenomenon has revealed that BTZ-exposed proinflammatory macrophages may promote the enrichment of tumor-initiating cells, a cell type that fuels MM cell proliferation and accounts for MM aggressiveness. Consequently, high IL-1β levels were associated with disease progression and death in MM patients included in the study (Beyar-Katz et al., 2019).

However, contrasting experimental data suggests a protective role for BTZ-mediated IL-1β production. In one study, treatment with TLR agonists prior to BTZ exposure led to

increased tumor cell death and increased survival in a leukemia mouse model. This effect was dependent on increased IL-1β cytokine levels following combination treatment with proteasome inhibitors and TLR agonists. IL-1β production only occurred when TLR agonists were administered before proteasome inhibitors, suggesting that a priming step would be necessary for BTZ-mediated cytokine secretion (Tang et al., 2018).

Altogether, these studies propose an important effect of cytokine secretion following proteasome inhibitor treatment; nonetheless, they differ considerably in their conclusions. Thus, further studies are required to determine whether proteasome inhibitor-mediated activation of innate immunity is detrimental or beneficial for this drug class's action on its target cells.

Pharmacological manipulation aside, genetic perturbations in proteasome assembly and activity are also known to activate the immune system. As mentioned before, mutations in different proteasome subunits confer type-I IFN-dependent autoinflammation and cause CANDLE and related disorders collectively termed proteasome-associated autoinflammatory syndromes (PRAAS). Causative mutations have been demonstrated to reduce proteolytic turnover of the proteasome, affecting the different types of catalytic proteasome activity to a varying degree. The effect of proteasome malfunction on type-I IFN secretion could be recapitulated by treating cells from healthy human donors with proteasome inhibitors (Brehm et al., 2015).

1.4. Aim of the study

Constant protein turnover is essential to every living cell in order to maintain homeostasis and exert its destined functions. Perturbations affecting the disposal of waste protein are prototypical stress signals.

Accumulation of intracellular proteins, leading to ER stress and subsequent activation of the UPR, has been described as a trigger for type-I IFN-mediated innate immune activation; however, no underlying mechanism has been conclusively identified. Analogously, an innate immune response occurs downstream of pharmacological inhibition and genetic impairment of proteasomal catalytic activity that has not been thoroughly characterized. Mutations underlying PRAAS have been identified to induce type-I IFN signaling, whereas proteasome inhibition has been shown to initiate secretion

of pro-inflammatory IL-1β in previous studies. However, both observations currently lack a convincing explanation at the mechanistic level.

Thus, my study set out to determine the cellular pathways underlying immune activation by distinct perturbations in protein turnover, in order to identify mechanisms relevant to human physiology and pathology.

2. Materials and methods

2.1. Materials

Table 1: Devices

Cell Counter	TC20™ Automated Cell Counter	Bio-Rad Laboratories, Feldkirchen, DE
Centrifuges	Centrifuge 5430 R Centrifuge 5810 R	Eppendorf, Hamburg, DE
CO_2 Incubator	MCO-170AICUVH	PHCbi, Oisterwijk, NL
Electrical Pipette	Xplorer™ 5-100 µl Electrical Pipette Xplorer™ 12-channel 50-1200 µl Electrical Pipette	Eppendorf, Hamburg, DE
Electroporation System	Neon™ Transfection System	ThermoFisher Scientific, Waltham, MA, USA
ELISA Reader	CyTation™ 3	BioTek, Winooski, VT, USA
Freezing Container	Mister Frosty™	ThermoFisher Scientific, Waltham, MA, USA
Light microscope	DMi8 automated	Leica, Wetzlar, DE
Microscope for STORM imaging	SR GSD	Leica, Wetzlar, DE
PCR Cycler	FlexCycler^2	Analytik Jena, Jena, DE
Pipettes	Rainin™ Pipet-Lite L-2 XLS+ Rainin™ Pipet-Lite L-20 XLS+ Rainin™ Pipet-Lite L-200 XLS+ Rainin™ Pipet-Lite L-1000 XLS+ Rainin™ Pipet-Lite Multi L12-50 XLS+ Rainin™ Pipet-Lite Multi L12-200 XLS+	Mettler-Toledo, Giessen, DE
Refrigerators	LKexv 3600 Mediline LKexv 1800 Mediline	Liebherr, Ochsenhausen, DE
Refrigerators for Sample Storage	MDF-DU502VHW-PE MDF-C2156VANW	PHCbi, Oisterwijk, NL
RT-PCR Cycler	QuantStudio™ 3 QuantStudio™ 5	Applied Biosystems, Waltham, MA, USA
Serological Pipette Operator	Rainin™ Pipet-X	Mettler-Toledo, Giessen, DE
Spectrophotometer	NanoDrop™ 8000	ThermoFisher Scientific, Waltham, MA, USA

Sterile Working Bench	Scanlaf Mars	Labogene, Allerød, DK
Thermomixer	ThermoMixer™ F 1.5 ThermoMixer™ F 2	Eppendorf, Hamburg, DE
Vortex mixer	VortexGenie™ 2	Scientific Industries, Bohemia, NY, USA

Table 2: Software

Data analysis and processing	Excel for Mac, Version 16.30	Microsoft, St. Redmond, WA, USA
Data analysis and visualization	Prism for macOS, Version 9.0.0	GraphPad Software, La Jolla, CA, USA
guideRNA design	CRISPR design tool	Feng Zhang laboratory, Massachussets Institute of Technology, Cambridge, MA, USA, crispr.mit.edu
Figure design	BioRender App	BioRender, Toronto, CN
Image analysis	FIJI (ImageJ), Version 2.1.0	Open source, public domain software on https://fiji.sc
Plasmid analysis	A Plasmid Editor (ApE)	M. Wayne Davis, University of Utah, Salt Lake City, UT, USA
Primer design	NCBI Primer-BLAST tool	National Library of Medicine, Bethesda, MD, USA, https://www.ncbi.nlm.nih.gov/tools/primer-blast/

Table 3: Consumables

Eppendorf™ Reaction Tubes (0.5, 1.5, 2.0 ml)	Eppendorf, Hamburg, DE
Falcon™ Centrifuge Tubes (15 ml, 50 ml)	Corning, Corning, NY, USA
PCR Strips and Cap Strips (8 wells)	Eppendorf, Hamburg, DE
Deep-well 384 Well Plate	Biotix, San Diego, CA, USA
384-well-plates for quantitative PCR	BIOplastics, Landgraaf, NL
96-well-plates for ELISA	Greiner Bio-One, Kremsmünster, AT
Supernatant Plates (96 wells, polystyrene)	Greiner Bio-One, Kremsmünster, AT
Pipette Tips (20 µl, 250 µl, 1000 µl, 1200 µl, each with and without filter)	Mettler-Toledo, Giessen, DE
Serological Pipettes (5 ml, 10 ml, 25 ml)	Corning, Corning, NY, USA
Cover slides for microscopy, 1.5mm thickness	Carl Roth GmbH, Karlsruhe, DE

Table 4: Cell Culture Plasticware

Tissue Culture Plates (6, 12, 24, 48, and 96 wells)	Faust Lab Science, Klettgau, DE
Tissue Culture Dishes (100 x 20 mm)	Sarstedt AG & Co. KG, Nümbrecht, DE
Tissue Culture Flasks (Sizes T25, T75, T175)	Sarstedt AG & Co. KG, Nümbrecht, DE

Table 5: Cell Culture Reagents

Roswell Park Memorial Institute (RPMI) medium	ThermoFisher Scientific, Waltham, MA, USA
Dulbecco's Modified Eagle Medium (DMEM)	ThermoFisher Scientific, Waltham, MA, USA
Opti-MEM™ Medium	ThermoFisher Scientific, Waltham, MA, USA
Fetal Calf Serum	ThermoFisher Scientific, Waltham, MA, USA
100x Penicillin/Streptomycin	ThermoFisher Scientific, Waltham, MA, USA
100x Antibiotic/Antimycotic	ThermoFisher Scientific, Waltham, MA, USA
100x Non-Essential Amino Acids (NEAA)	ThermoFisher Scientific, Waltham, MA, USA
100x Sodium Pyruvate	ThermoFisher Scientific, Waltham, MA, USA
Trypsin-EDTA (0.05%, 0.25%)	ThermoFisher Scientific, Waltham, MA, USA
Ampuwa™ Water for Injection	Fresenius Kabi, Bad Homburg, DE
0.9% Sodium Chloride	Fresenius Kabi, Bad Homburg, DE
Ficoll-Paque Plus Reagent™	VWR, Darmstadt, DE
Red Blood Cell Lysis Buffer	ThermoFisher Scientific, Waltham, MA, USA
Invitrogen™ Lipofectamine™ 2000 Transfection Reagent	ThermoFisher Scientific, Waltham, MA, USA
Human recombinant (hr) IL-3	PeproTech, Cranbury, NJ, USA
hrM-CSF	PeproTech, Cranbury, NJ, USA
β-Estradiol	Sigma Aldrich, St. Louis, MI, USA

Table 6: Reagents for molecular biology experiments

5xEvaGREEN qPCR master mix	BioBudget, Krefeld, DE
RNEasy™ Mini RNA Isolation Kit	Qiagen, Venlo, NL
DNAse I and DNAse I Buffer	ThermoFisher Scientific, Waltham, MA, USA
Ethylenediaminetetraacetic acid (EDTA)	ThermoFisher Scientific, Waltham, MA, USA
Gibson Assembly™ Master Mix	New England Biolabs, Ipswich, MA, USA
RiboLock™ RNAse Inhibitor	ThermoFisher Scientific, Waltham, MA, USA
RevertAid™ Reverse Transcriptase and RevertAid™ Buffer	ThermoFisher Scientific, Waltham, MA, USA
Deoxynucleotide Triphosphate Mix	ThermoFisher Scientific, Waltham, MA, USA
Oligo(dT) Primers and Random Hexamers for cDNA synthesis	Integrated DNA Technologies, Coralville, IA, USA

Table 7: Materials for magnetic cell separation

CD14 MicroBeads, human	Miltenyi, Bergisch Gladbach, DE
MACS MS Columns	Miltenyi, Bergisch Gladbach, DE
MiniMACS Separator	Miltenyi, Bergisch Gladbach, DE

Table 8: Chemicals

Bortezomib	Cayman Chemicals, Ann Arbor, MI, USA

Dimethyl sulfoxide (DMSO)	Carl Roth, Karlsruhe, DE
Ethanol, purity >99.5%	Carl Roth, Karlsruhe, DE
Epoxomicin	Selleck Chemicals, Houston, TX, USA
Formaldehyde 37%	Sigma Aldrich, St. Louis, MI, USA
Hoechst 33258 DNA Dye	Sigma Aldrich, St. Louis, MI, USA
MCC-950	Sigma Aldrich, St. Louis, MI, USA
Nigericin	InvivoGen, San Diego, CA, USA
Pam3CSK4	Sigma Aldrich, St. Louis, MI, USA
Phorbol-12-myristate-13-acetate	InvivoGen, San Diego, CA, USA
Thapsigargin	Cayman Chemicals, Ann Arbor, MI, USA
Triton™ X 100	Carl Roth, Karlsruhe, DE
Tunicamycin	Cayman Chemicals, Ann Arbor, MI, USA

Table 9: Nucleic Acids

Herring testes DNA	Sigma Aldrich, St. Louis, MI, USA
In Vitro Transcript 4 (IVT4)	Hartmann Lab, University of Bonn
pBlue Plasmid	Addgene, Watertown, MA, USA
pLex-MCS-ASC-GFP Plasmid	Addgene, Watertown, MA, USA
EF1a-Cas9-U6-sgRNA expression plasmid	Thomas Zillinger, Bonn, DE

Table 10: Commercial Kits

CellTiterBLue™ Cell Viability Assay	Promega, Walldorf, DE
Human IL-1ß ELISA Kit	BD Biosciences, Franklin Lakes, NJ, USA
Human CXCL-10 ELISA Kit	BD Biosciences, Franklin Lakes, NJ, USA

Table 11: Antibodies used for imaging

TOMM20 rabbit monoclonal antibody	Cell Signaling Technology Europe B.V., Frankfurt am Main, DE
Anti-DNA Antibody, clone AC-30-10, mouse monoclonal antibody	Sigma Aldrich, St. Louis, MI, USA
Goat anti-Rabbit IgG Secondary Antibody, Alexa Fluor 488	ThermoFisher Scientific, Waltham, MA, USA
Goat anti Mouse IgG1 Secondary Antibody, Alexa Fluor 555	ThermoFisher Scientific, Waltham, MA, USA

Table 12: Primer Sequences for RT-PCR

ACTB	forward	TAGCACCATGAAGATCAAGAT
	reverse	CCGATCCACACAGAGTACTT
B2M	forward	CACTGAAAAAGATGAGTATGCC
	reverse	AACATTCCCTGACAATCCC
IFIT1	forward	GTGCTTGAAGTGGACCCTGA
	reverse	CCTGCCTTAGGGGAAGCAAA
CXCL-10	forward	GGCAATCAAGGAGTACCTCTCT
	reverse	CCTGGCGTCGTGATTAGTGAT

IFNB1	forward	ACGCCGCATTGACCATCTAT
	reverse	GTCTCATTCCAGCCAGTGCT
MT-ND1	forward	ACGCCATAAAACTCTTCACCAAAG
	reverse	GGGTTCATAGTAGAAGAGCGATGG
RSAD2	forward	CCTGTCCGCTGGAAAGTGTT
	reverse	GACACTTCTTTGTGGCGCTC
XBP1	forward	GCAGCACTCAGACTACGTGCAC
	reverse	GCTGGCAGGCTCTGGGGAAG
XBP1s	forward	TGCTGAGTCCGCAGCAGGTG
	reverse	GCTGGCAGGCTCTGGGGAAG
All primer sequences are listed in 5'-3' direction		

Table 13: guideRNA sequences for CRISPR-mediated generation of knockout cell lines

Cell line	Gene	guideRNA sequence
THP-1	CGAS	GGCCGCCCGTCCGCGCAACT
	STING	CTAGCCCCCAAAGGGTCACC
	IRF3	GCACGCGCTTCCGCATCCCT
	RIG-I	GGGTCTTCCGGATATAATCC
	MAVS	GTCCTGCTCCTGATGCCCGC
	CASP1	gRNA sequence not available
	NLRP3	ATTGAAGTCGATCATTAGCG
	ATF6A	TGAAAGAGTCCCGGGCTAAA
	ATF6B	GACGCAGCTCTTCCGTTGCC
	ERN1	GTGGAAGTACCCGTTCCCCA
	EIF2AK3	TCGTCTGGTTCCGGACCCCG
HT-29	CGAS	AGTTGCGCGGACGGGCGGCC
	STING	CTAGCCCCCAAAGGGTCACC

Table 14: Genomic sequences of target loci in genetically edited cell lines

Cell line	Gene	Clones	Genomic sequence (first and second allele)
THP-1	CGAS	1	GCCCCAGT[+T]TGCGCGGAC
			homozygous
		2	CCCCAGT[-bp]GCGCGGAC
			AGGCCG[+GCGGGTCTCGACCCCCGTTCGCCTAGG]GCGCCCC
	STING	1	CAAAGGGTC[+A]ACCAGGCAGGCA
			CAAAGGGTC[+T]ACCAGGCAGGCA
		2	CAAAGGGTC[+C]ACCAGGCAGGCA
			CAAAGGGTC[+G]ACCAGGCAGGCA
	IRF3	1	CCGTGCTTCCAAGG[-1bp]ATGCGGAAGCGC
			homozygous
	RIG-I	1	CCGGAT[-5bp]CCTGGAAG
			GATATA.TCCTGGA
	MAVS	1	CCAGCG[-23bp]CTGGG
			homozygous

	NLRP3	1	TAGCCACGC.AATGAT	
			TGGATC[-17bp]GACTTCA	
		2	TAGCCACGC[+T]TAATGAT	
			TGGATC[-17bp]GACTTCA	
		3	ACGCT.AATGATC	
			homozygous	
	CASP1	1	Loss of CASP1 expression validated via Western Blot	
		2	Loss of CASP1 expression validated via Western Blot	
	ERN1	1	CCTTGG[-bp]GAACGG	
			homozygous	
		2	CCTTGG[-bp]GAACGG	
			CCTTGG[-7bp]GTACTT	
	EIF2AK3	1	CCTCGG[-1bp]GTCCGG	
			CCTCGG[+G]GGTCCG	
		2	CCTCGG[+G]GGTCCG	
			homozygous	
	ATF6A ATF6B	1	ATF6A	CCTTTT[+A]AGCCCG
				CCTTTTA[-11bp]TTTCAC
			ATF6B	CCGGGC[-1bp]ACGGAA
				CCGGGC[+G]AACGGA
		2	ATF6A	TGGGGG[-46bp]ACTCTT
				CACCTT[-2bp]AGCCCG
			ATF6B	TCCGGG[-5bp]GAAGAG
				CCGGGC[-2bp]CGGAAG
				CCGGGC[-1bp]ACGGAA
HT-29	CGAS	1	Loss of cGAS expression validated via Western Blot	
		2	Loss of cGAS expression validated via Western Blot	
	STING	1	Loss of STING expression validated via Western Blot	
		2	Loss of STING expression validated via Western Blot	

2.2. Methods

2.2.1. Cell culture methods

2.2.1.1. Cell culture conditions

Primary cells and cell lines were kept in an incubator at 37°C and an atmospheric CO_2 concentration of 5%. All cell culture experiments were conducted under sterile conditions at working benches with laminar air flow. HEK293T cells, HT29 cells, and primary human fibroblasts were cultivated in Dulbecco's modified Eagle medium (DMEM) with 10% fetal calf serum (FCS), 1% non-essential amino acids (NEAA), 1% sodium pyruvate, 100 I.U./ml penicillin and 100 µg/ml streptomycin. THP-1 cells, BlaER1 cells, myeloma cell lines (KMS-11, KMS-11/BTZ, RPMI8226), and primary human peripheral blood mononuclear cells (PBMC) were cultivated in Roswell Park Memorial Institute 1640 (RPMI1640) medium with the same supplements. Cell lines were screened for mycoplasma contamination regularly.

2.2.1.2. Differentiation of THP-1 cells

THP-1 acute monocytic leukemia cells were differentiated using phorbol-12-myristate-13-acetate (PMA). Cells were incubated with PMA at a concentration of 300 ng/ml for 3 hours, washed three times with phosphate-buffered saline (PBS), and subsequently plated at a concentration of 5 x 10^5 cells/ml in RPMI1640 medium. Stimulations were performed the following day after a medium exchange.

2.2.1.3. Generation of ρ0 THP-1 cells

ρ0 THP-1 cells that are devoid of mtDNA were generated by long-term incubation of wild type (WT) THP-1 cells with 50 ng/ml of Ethidium Bromide (EtBr). After four and eight weeks, total DNA was extracted from the cells and copy numbers of mtDNA and nuclear DNA were assessed via qPCR and compared to WT cells. B2M and MT-ND1 were used as reference genes for nuclear DNA and mtDNA (Widdrington et al., 2017).

2.2.1.4. Generation of ASC-GFP$^+$ THP-1 cells

ASC-GFP$^+$ THP-1 cells, overexpressing ASC with an N-terminal green fluorescent protein (GFP), were generated using a retroviral vector generated with a pLex-MCS-ASC-GFP plasmid (de Almeida et al., 2015). Cells stably expressing the ASC-GFP construct were selected by fluorescence-assisted cell sorting (FACS) at the University of Bonn Flow Cytometry Core Facility.

2.2.1.5. Generation of knockout cell lines via CRISPR/Cas9

For generation of knockout cell-lines, gRNAs targeting the respective gene of interest were selected with the CRISPR design tool (crispr.mit.edu). THP-1 and HT29 WT cells were transiently electroporated with EF1alpha-Cas9-2A-EGFP/U6-guideRNA expression plasmids targeting cGAS, STING, IRF3, NLRP3, CASP1, ATF6A, ATF6B, ERN1, or EIF2AK3. Electroporation settings were 1250 V, 1 pulse of 50 ms duration. Cells were sorted for EGFP expression after 18 hours by the University of Bonn Flow Cytometry Core Facility and seeded as single-cell colonies via limiting dilution. After expansion, clones with frameshift mutations in the respective gene locus were identified by Sanger sequencing. Cell lines discussed in this study were generated by Prof. Dr. Eva Bartok, Dr. Thomas Zillinger (THP-1), and Katarzyna Andryka-Cegielski (HT29) with my assistance.

2.2.1.6. Differentiation of BlaER1 cells

BlaER1 cells are a human transgenic lymphoma cell line that can transdifferentiated into monocyte-like cells (Rapino et al., 2013). BlaER1 cells were differentiated by incubation with 10 ng/ml hrM-CSF, 10 ng/ml hrIL-3, and 100 nM β-estradiol in RPMI medium for 6-7 days at a density of 3 x 10^5 – 5 x 10^5 cells/ml for 6 days. After 6 days, the RPMI medium was replaced and cells were left to recover at least 2 hours prior to stimulation.

2.2.1.7. Isolation of peripheral blood mononuclear cells

PBMC were isolated either from buffy coats obtained from healthy blood donors at the University of Bonn blood donation center, or from EDTA blood obtained from healthy volunteers. Written consent was obtained from each donor. A Ficoll gradient was used to isolate PBMC from whole blood samples. Erythrocyte lysis was performed during the isolation process.

2.2.1.8. Isolation of primary human monocytes

$CD14^+$ human monocytes were isolated from PBMC generated as described in section 2.2.1.7. During PBMC isolation designated for monocyte isolation, no erythrocyte lysis was performed. Magnetic cell separation (MACS) with anti-CD14 antibody beads was employed according to the manufacturer's instructions (Miltenyi et al., 1990). $CD14^+$ monocytes were further differentiated into macrophages as described in section 2.2.1.10.

2.2.1.9. Isolation of primary human fibroblasts

Fibroblasts were generated from resected adenoids from otherwise healthy donors undergoing adenotomy at either University Hospital Bonn or Waldkrankenhaus Bonn. Written consent was obtained from all donors, as approved by the ethics committee of the University Hospital Bonn (application number: 031/18). Briefly, adenoids were digested with 0.25% trypsin-EDTA and subsequently incubated in DMEM with the aforementioned supplements. Adherent fibroblasts were cultivated further in DMEM for experiments.

2.2.1.10. Differentiation of primary human macrophages

Primary human macrophages were differentiated from $CD14^+$ human monocytes generated as described above (see 2.2.1.8). Briefly, monocytes were seeded at a density of $1x10^6$ cells/ml in RPMI1640 with the aforementioned supplements and 10

ng/ml of recombinant M-CSF in a 10 cm cell culture dish. A medium exchange was performed after three days. At day six, cells were detached from the cell culture dish using 10 mM ethylenediamidetetraacetic acid (EDTA) and re-seeded at a density of $1x10^6$ cells/ml in RPMI1640 cell culture medium for stimulation.

2.2.1.11. Cell stimulation and transfection

Stimulation experiments were performed using the reagent concentration and exposure time stated in the figure legend for each experiment. Unless indicated otherwise, Lipofectamine™ 2000 was used as transfection reagent. 0.25 µl of Lipofectamine™ 2000 was used for each well in a 96 well cell culture plate. Transfection reagent and nucleotides were dissolved in equal amounts of OptiMEM cell culture medium and incubated for 20 minutes. Afterwards, medium with Lipofectamine™ 2000 or nucleotides were mixed in a 1:1 ratio and incubated for another 20 minutes prior to stimulation.

2.2.1.12. Inflammasome priming

Inflammasome priming in primary human cells and BlaER1 cells was performed by exposure to TLR2 agonist Pam3CSK4 at a concentration of 2 µg/ml for four hours, followed by stimulation. In THP-1 cells, inflammasome priming was performed using PMA differentiation as described in section 2.2.1.2.

2.2.2. Readout Assays

2.2.2.1. Enzyme-linked immunosorbent assay

Concentrations of proteins secreted from cells into the cell culture supernatant were assessed using enzyme-linked immunosorbent assay (ELISA). Briefly, ELISA is an enzyme immunoassay for protein quantification using protein-specific antibodies. ELISA was performed with complete kits for specific proteins according to the manufacturer's instructions in 96-well cell culture plates. Marker concentration was assessed on a cell

imaging reader and absolute protein concentrations were calculated using a recombinant protein standard curve on every plate.

2.2.2.2. RNA isolation, cDNA synthesis, and quantitative real-time polymerase chain reaction

RNA was isolated from whole cell lysate using the Qiagen RNEasy™ kit according to the manufacturer's instructions. On-column DNase I digestion was performed during the isolation process. RNA concentration was measured using a spectrophotometer. After isolation, RNA was stored at -20°C for short-term and at -80°C for long-term storage.
cDNA synthesis was performed by combining 10 µl of RNA (diluted to an equal concentration of NA for each sample in an experiment), 1 µl of reverse transcriptase, 4 µl of 5x reverse transcriptase buffer, 2 µl of dinucleotide triphosphates (dNTP), 0.5 µl of RNAse inhibitor, 0.25 µl of Oligo(dT), 0.25 µl of randomly generated DNA hexamers, and 2 µl of de-ionized water in a reaction tube and incubating the reaction at 55 °C for one hour. cDNA was diluted 1:5 before quantitative PCR (qPCR).
qPCR was performed on a QuantStudio™ cycler using a SYBR Green I-based approach with primers designed using the NCBI primer blast tool or adapted from the literature (van Schadewijk et al., 2012; Widdrington et al., 2017). Experimental results are displayed either as $2^{-\Delta ct}$ or as $2^{-\Delta\Delta ct}$, specified in the figure legend for each figure. All calculations were performed in Microsoft Excel™.

2.2.2.3. Quantification of cell viability

Cellular metabolic activity was assessed as a surrogate parameter for cell viability by using the CellTiterBlue™ assay kit according to the manufacturer's instructions. 20 µl of reagent was used per 100 µl of medium in a 96-well plate. Reactions were incubated for 4 hours at 37°C degrees temperature. Fluorescence was assessed on a cell imaging reader and relative metabolic activity was normalized to an untreated control condition.

2.2.2.4. Light microscopy

For microscopy experiments, ASC-GFP$^+$ THP-1 cells were differentiated as described above and plated in 24-well plates. After stimulation, cells were counterstained with Hoechst 33258 DNA dye for 30 minutes and subsequently washed five times with PBS. Afterwards, microscopy was performed on a Leica Dmi8 light microscope. Magnification is indicated by a scale bar in each microscopy picture.

2.2.2.5. ASC speck quantification

After acquisition of images as described in section 2.2.2.4. ASC specks and nuclei were counted automatically using FIJI. Size limits were 3-infinite µM for nuclei in the DAPI channel, and 3-12 µM for ASC specks in the GFP channel.

2.2.2.6. Stochastic optical reconstruction microscopy

Stochastic optical reconstruction microscopy (STORM) allows for high resolution imaging below the optical diffraction limit. Briefly, series of images are generated where, in each picture, only a fraction of fluorophores are emitting a signal generated through laser excitation (Rust et al., 2006). For STORM, human primary fibroblasts were plated at a density of 3 x 10^5 cells/ml. After treatment with ER stressors or controls, cells were fixed with formaldehyde and permeabilized with triton X. Subsequently, cells were incubated with an anti-DNA mouse monoclonal antibody and an anti-TOMM20 rabbit monoclonal antibody for visualization mtDNA and Mitochondrial import receptor subunit TOM20 homolog (TOMM20). Secondary staining was performed using anti-mouse and anti-rabbit antibodies, respectively. Subsequently, cells were imaged on a STORM microscope in series of 15,000 images. Image processing was performed using FIJI.

2.2.3 Figure design and statistical analysis

Figures were designed using GraphPad Prism 9 or Microsoft PowerPoint software. Overview figures were generated using BioRender. Statistical analysis was performed

using GraphPad Prism 9. Quantitative data were analyzed for normality using the Shapiro-Wilk test, and further statistical analysis was performed as indicated according to the results. Statistical methods used for each figure are specified in the figure legends. Results with a p value <0.05 were considered statistically significant. Quantitative data are shown as mean ± standard error of the mean (SEM) or mean + standard deviation (SD).

3. Results

3.1. Activation of antiviral innate immune pathways by ER stress

3.1.1. Pharmacological induction of ER stress and an innate immune response by Tunicamycin and Thapsigargin

TN and TPG are widely employed as tools to investigate mechanisms and consequences of ER stress *in vitro* and *in vivo*. As mentioned in section 1.2.2, TN is a small molecule inhibitor of N-linked glycosylation which perturbs folding of ER-nascent proteins and subsequently activates the UPR (Smith et al., 2008). In contrast, TPG induces ER stress via inhibition of Sarcoplasmic/Endoplasmic Reticulum Calcium ATPase (SERCA), the key enzyme regulating ER calcium storage capacity (Liu et al., 2012).

To validate the ability of TN and TPG to induce the ER stress in primary cells at doses that have been widely used in immunological studies, XBP1 mRNA splicing was assessed via relative quantification of XBP1 and $XBP1_s$ transcript levels in primary human fibroblasts using qPCR (Liu et al., 2012; Smith et al., 2008). Under homeostatic conditions, alternative splicing of XBP1 occurs at a very low frequency but substantially increases during ER stress, resulting in the translation of the ER master regulator $XBP1_s$ (Hetz, 2012). As expected, treatment with both small molecules increased XBP1 splicing and reversed the ratio of XBP1 and $XBP1_s$ mRNA in comparison to the control treatment (Figure 3).

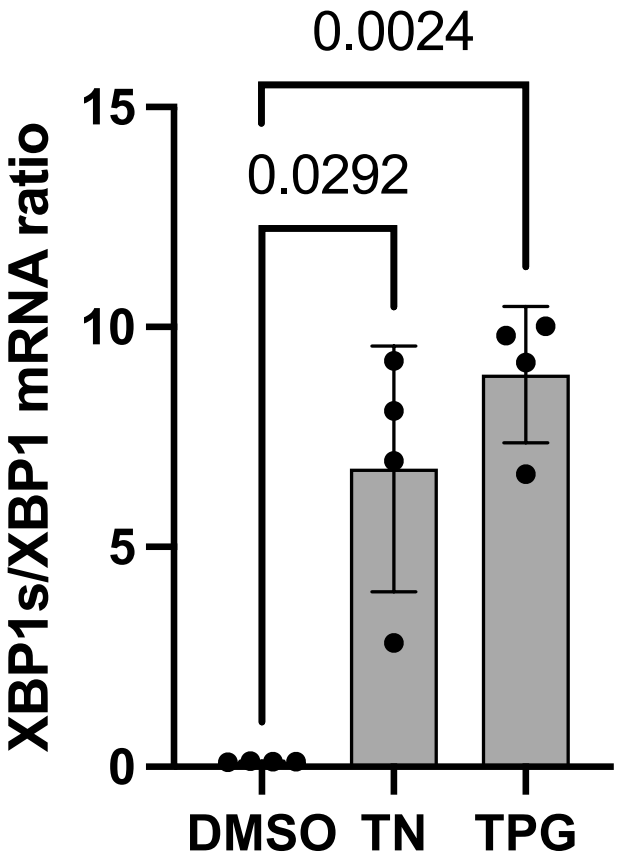

Figure 3: Assessment of XBP1 splicing after Tunicamycin and Thapsigargin treatment in fibroblasts
Primary human fibroblasts were treated with Tunicamycin (TN, 10 µg/ml) or Thapsigargin (TPG, 1 µM) or a DMSO solvent control (0.1%) for 4 hours. Whole cell RNA was extracted and abundance of XBP1 and XBP1s mRNA was assessed via qPCR. Bars depict mean ± SEM of n=4 human donors. Each data point represents an individual donor. Significance was determined by one-way ANOVA with Dunnett's multiple comparisons test.

Other authors have established a connection between ER stress and innate immunity. However, these studies focused on stress-mediated enhancement of PRR activation and subsequent type-I IFN signaling (Liu et al., 2012; Martinon et al., 2010; Smith et al., 2008; Zeng et al., 2010). Moreover, one study described ER stress-induced IRF3 phosphorylation and STING:TBK1 colocalization in the absence of another PRR ligand; but no mechanism underlying this observation could be determined (Liu et al., 2012). To investigate a potential antiviral response downstream of ER stress, we treated primary human immune and non-immune cells with TPG and TN and measured IFNB1 mRNA. After 4 hours of TPG treatment, IFNB transcript numbers were increased as compared

to the untreated control in human primary fibroblasts (Figure 4A) as well as in human primary macrophages (Figure 4B). TN treatment also led to increased IFNB1 mRNA levels, but, in contrast to TPG, the threshold for statistical significance was not reached. mRNA levels of Interferon-induced protein with tetratricopeptide repeats 1 (IFIT1), radical SAM domain-containing 2 (RSAD2), and C-X-C motif chemokine ligand 10 (CXCL-10) were also quantified, since as ISGs they can be used as surrogate markers of IFN activity (Rodero et al., 2017). In particular, CXCL-10 is linked to type-I IFN induction by its properties as an ISG, but can also be induced directly by IRF3 and NF-κB without the need for prior type-I IFN secretion and may thus serve as a surrogate assay for the activation of IRF3-dependent pathways in an experimental setting (Brownell et al., 2014). However, while an increase was observed in some donors, neither IFIT1 nor RSAD2 mRNA levels were increased significantly overall in TN- or TPG-treated fibroblasts (Figure 4B and 4C). Furthermore, CXCL-10 transcription was not observed in macrophages, although it could be induced by a plasmid DNA control (Figure 4E). It is unclear why type-I IFN induction did not lead to increased CXCL10 expression in this model since ISG induction occurs already occurs at very low levels of IFNAR activation (Schneider et al., 2014).

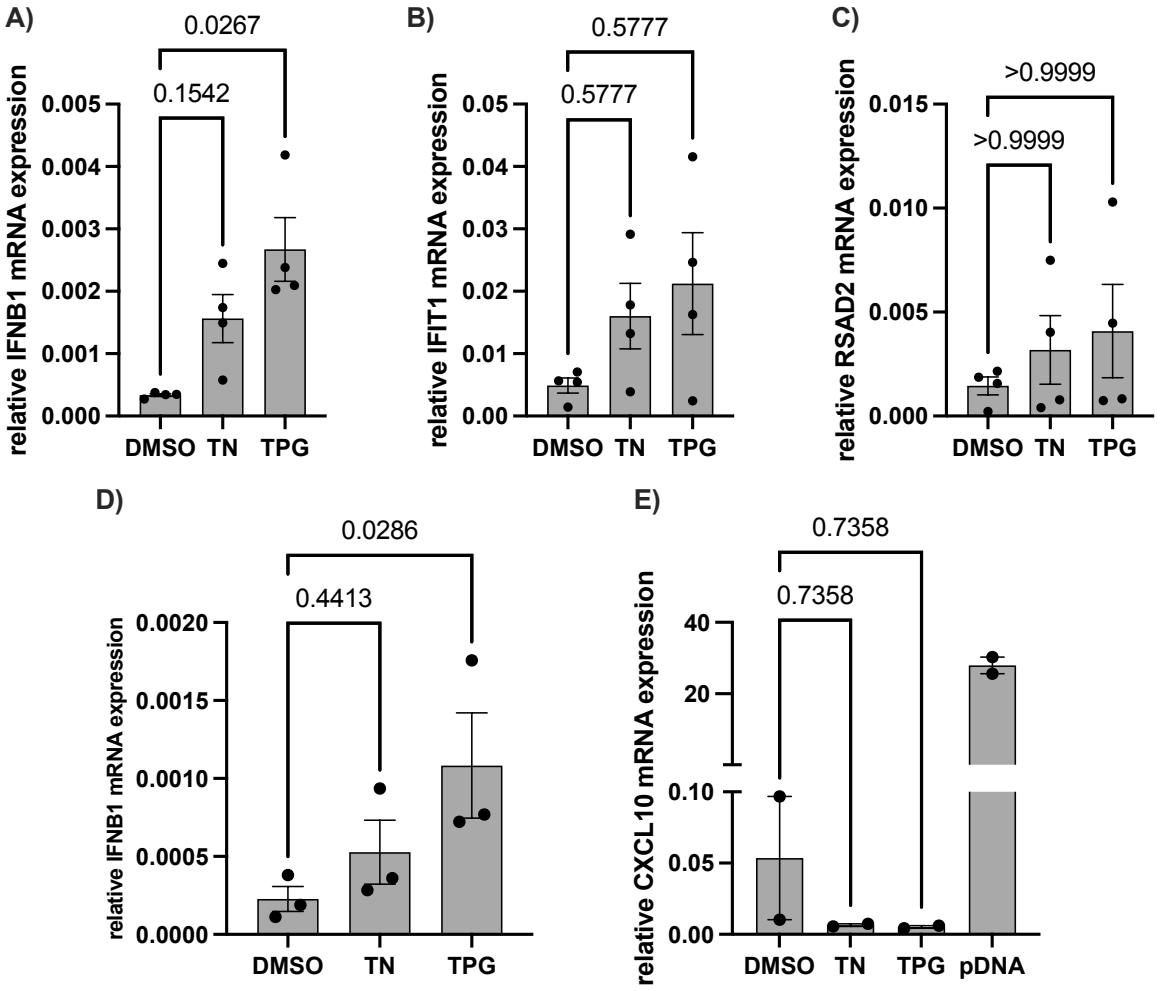

Figure 4: IFNB1 and ISG expression following treatment of primary human cells with ER stressors
Primary human fibroblasts (A-C) and macrophages (D-E) were treated with Tunicamycin (TN, 10 µg/ml), Thapsigargin (TPG, 1 µM), plasmid DNA (pDNA, 400 ng/ml, panel E), or a DMSO solvent control (0.1%) for 4 hours. Whole cell RNA was extracted and IFNB1 (A, D), IFIT1 (B), RSAD2 (C), and CXCL-10 (E) mRNA expression were assessed additionally. Bars depict mean ± SEM, n=4 donors for fibroblasts (A-C) n=3 (D) or n=2 (E) human donors for macrophages. Each data point represents an individual donor. Significance was determined by Friedman test with Dunn's multiple comparisons test.

Theoretically, protein levels could diverge from mRNA measurements, especially during ER stress given that the UPR can alter the post-transcriptional fate of gene products (Reich et al., 2020). To investigate type-I IFN signaling at the protein level, CXCL-10 secretion was assessed via ELISA.

Analogous to the modest levels of IFNB1 mRNA and ISG transcripts observed in primary human cells, no significant CXCL-10 secretion could be observed in human

macrophages (Figure 5A) and fibroblasts (Figure 5B) following exposure to small molecule ER stressors. Nonetheless, CXCL-10 induction was observed in fibroblasts of individual donors (Figure 5B), raising the possibility of inter-individual differences in the cellular response to ER stress. However, no statistically significant relation was determined between individual IFNB1 transcription and CXCL-10 secretion ($r=0.8$, $p=0.33$ for TN treatment, $r=-0.4$, $p=0.75$ for TPG treatment, Spearman's correlation).
Additionally, no CXCL-10 secretion could be measured in the human embryonic kidney (HEK) cell line HEK293T (Figure 5C). However, treatment with TN and TPG led to a marked increase in supernatant CXCL-10 levels in the human monocytic cell line THP-1 (Figure 5D), which originates from acute monocytic leukemia cells in a pediatric patient and is a widely-used tool to study immune responses to NA (Auwerx, 1991; Gao et al., 2013b).

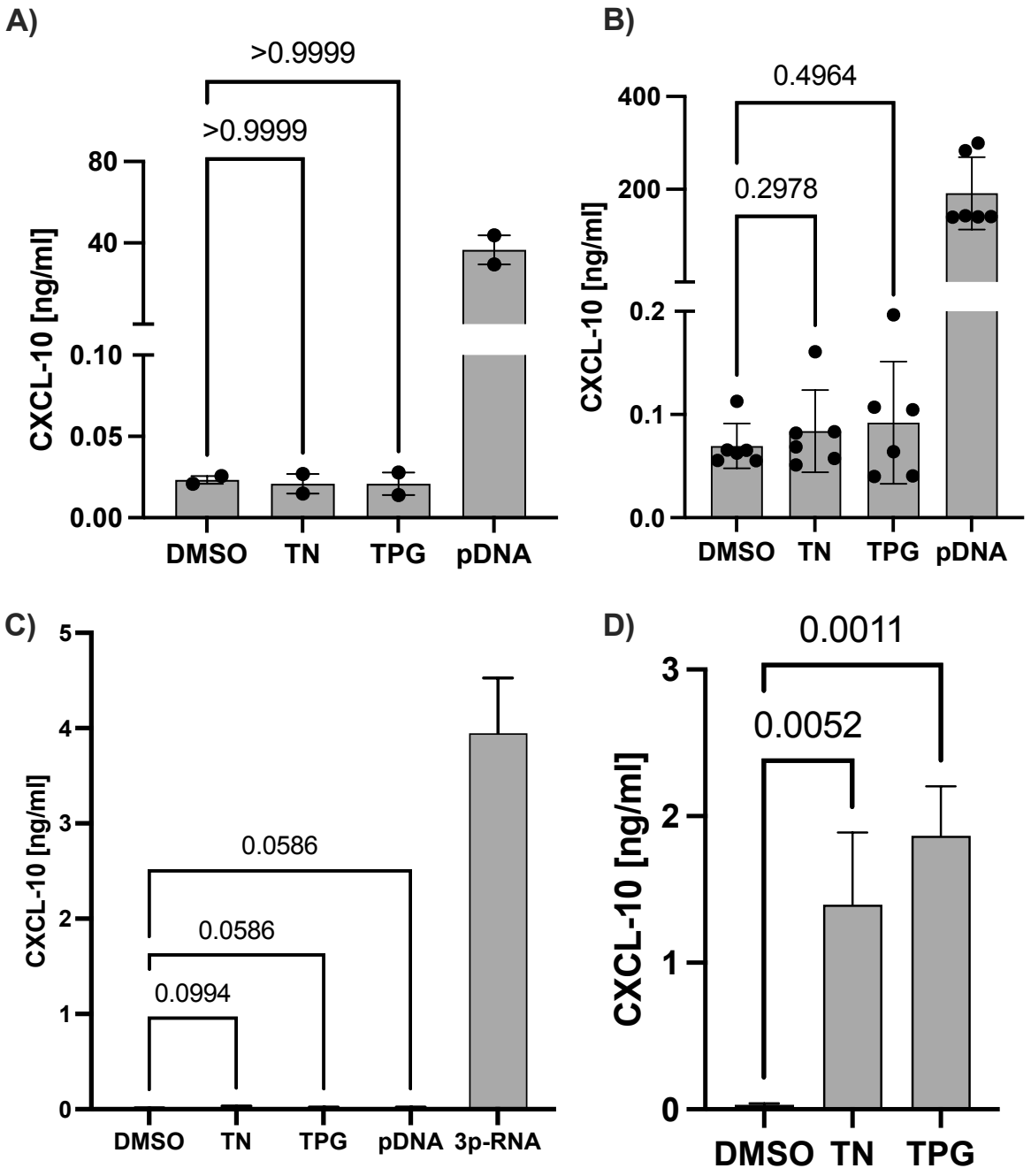

Figure 5: ER stressors induce CXCL-10 secretion as a surrogate for the type-I IFN response in THP-1 cells, but not in HEK293T cells or primary human cells
(A) Primary human macrophages were treated with Tunicamycin (TN, 20 µg/ml), Thapsigargin (TPG, 1 µM), plasmid DNA (pDNA, 400 ng/ml), or a DMSO control (0,1%). (B) Primary human fibroblasts were treated with TN (20 µg/ml), TPG (1 µM), pDNA (400 ng/ml) or a DMSO control (0.1%). (C) HEK293T cells were treated with TN (10 µg/ml), TPG (1 µM), pDNA (400 ng/ml), 5'-triphosphate dsRNA (3p-RNA, 100 ng/ml), or a DMSO control (0.1%). (D) THP-1 cells were treated with TN (10 µg/ml), TPG (1 µM), or a DMSO control (0.1%).

Supernatants were collected after 24 hours and cytokine secretion was assessed via ELISA. Bars depict mean ± SEM of 2 (A) or 6 donors (B) with each data point representing an individual donor, or mean + SD of triplicates (C, D). Significance was determined by Friedman test with Dunn's multiple comparisons test (A, B) or one-way ANOVA with Dunnett's multiple comparisons test (C+D).

3.1.2. cGAS and STING are required for type-I IFN induction following treatment with ER stressors

While a CXCL-10 response to cytosolic RNA in the form of RIG-I ligands can be observed both in HEK293T cells and in THP-1 cells, only THP-1 cells secrete CXCL-10 in response to cytosolic DNA, as HEK293T cells only express very low levels of cGAS insufficient for a measurable type-I IFN response (Sun et al., 2013). Considering this striking difference in the response to NA stimuli, it could be hypothesized that IFN secretion following treatment with ER stressors might be dependent on the cGAS/STING pathway. Thus, CXCL-10 secretion following chemical induction of ER stress in THP-1 cells deficient in cGAS, STING, or IRF3 (provided by Dr. Thomas Zillinger) was measured. Indeed, CXCL-10 secretion was abrogated in cell lines deficient in cGAS, STING and IRF3 (Figure 6A). However, in RIG-I$^{-/-}$ or MAVS$^{-/-}$ THP-1 cell lines (provided by Dr. Thomas Zillinger), CXCL-10 secretion upon TN exposure was preserved (Figure 6B), indicating that the CXCL-10 response to ER stress is a consequence of cGAS/STING but not RIG-I/MAVS or MDA5/MAVS signaling by the innate immune system.

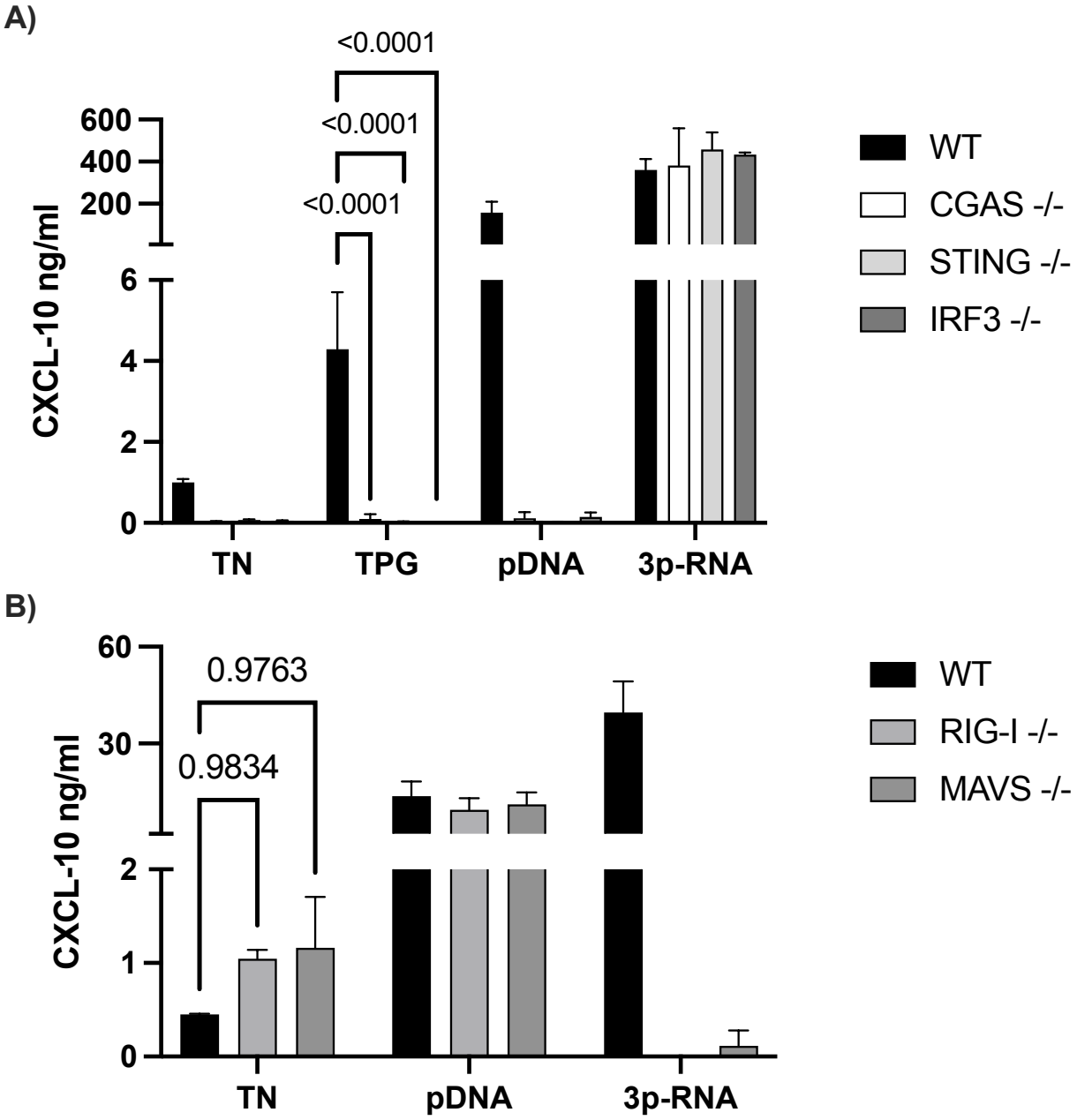

Figure 6: ER stress-induced CXCL-10 secretion is abrogated in THP-1 cells deficient in DNA, but not in RNA sensing

(A) WT, CGAS -/-, STING -/-, and IRF3 -/- THP-1 cells were treated with Tunicamycin (TN, 10 µg/ml) or Thapsigargin (TPG, 1 µM), or transfected with plasmid DNA (pDNA, 400 ng/ml) or 5'-triphosphate dsRNA (3p-RNA, 100 ng/ml). (B) WT, RIG-I -/- and MAVS -/- THP-1 cells were treated with TN or transfected with pDNA or 3p-RNA.

Supernatants were collected after 24 hours and cytokine secretion was assessed via ELISA. Bars are mean + SD of triplicates (A) or duplicates (B), representative of three (A) or two (B) experiments. For panel (A), two genotypically distinct CGAS -/- and STING -/- THP-1 cell lines were analyzed, one representative cell line per gene is shown. Significance was determined using two-way ANOVA with Šidák's correction for multiple comparisons.

It was then investigated whether a cGAS/STING dependent, ER stress-mediated type-I IFN response would also occur in non-immune cells. For this purpose, HT29, an epithelial cell line derived from human colon adenocarcinoma cells, was used (cell lines provided by Katarzyna Andryka-Cegielski). TN and TPG lead to the release of CXCL10 from these cells (Figure 7). Moreover, in line with the findings in THP-1 cells (Figure 6A), I observed cGAS/STING-dependent CXCL-10 secretion in response to transfected DNA as well as following treatment with TN and TPG, while the CXCL-10 response to RNA stimuli was unaffected in $cGAS^{-/-}$ and $STING^{-/-}$ HT29 cells.

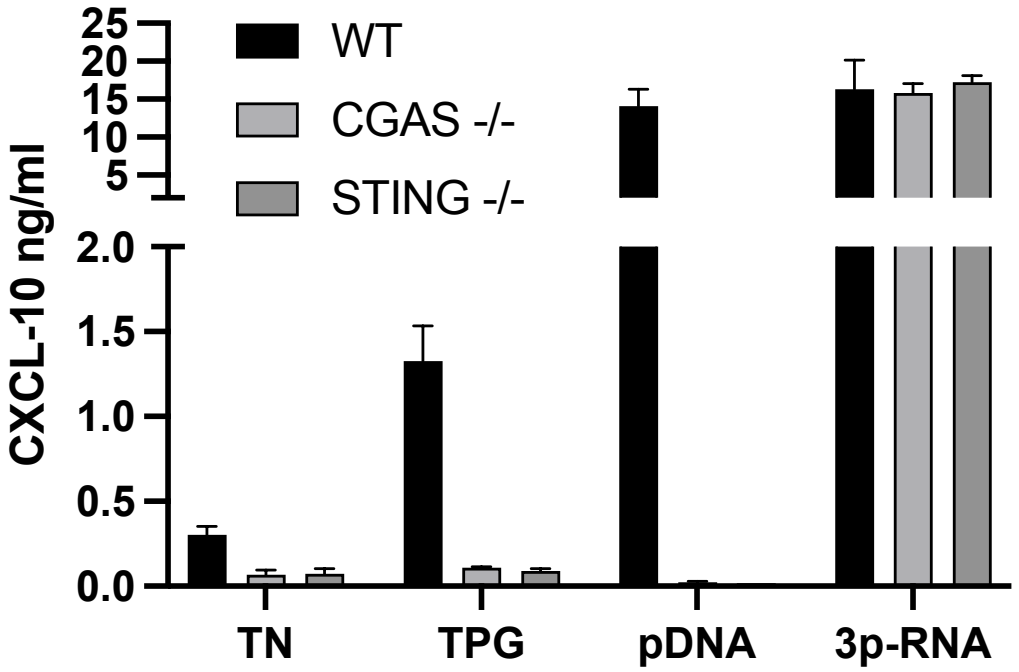

Figure 7: ER stress-induced CXCL-10 secretion is dependent on cGAS and STING in HT29 cells
WT, CGAS -/-, and STING -/- HT 29cells were treated with Tunicamycin (TN, 10 µg/ml) or Thapsigargin (TPG, 1 µM), or transfected with plasmid DNA (pDNA, 400 ng/ml) or 5'-triphosphate dsRNA (3p-RNA, 100 ng/ml). Supernatants were collected after 24 hours and cytokine secretion was assessed via ELISA. Bars are mean + SD of triplicates. Two genotypically distinct CGAS -/- and STING -/- THP-1 cell lines were analyzed, one representative cell line per gene is shown.

3.1.3. The ATF6 branch of the UPR mediates the type-I IFN response to ER stress

ATF6 as well as the IRE1α-XBP1 UPR pathway have been reported to be involved in the regulation of immune responses (Y.-P. Liu et al., 2012; Martinon et al., 2010). However, it is unclear whether a connection between cytosolic DNA sensors and a specific UPR branch exists. Thus, THP-1 cell lines deficient in each master regulator of the UPR, IRE1, PERK, and ATF6, were generated. These cell lines were treated with TPG to determine whether the ER stress-driven innate immune response would be dependent on a specific UPR branch. In IRE1α- ($ERN1^{-/-}$) as well as in PERK-deficient ($EIF2AK3^{-/-}$) cells, the CXCL-10 response to TPG was preserved, whereas it was abrogated in ATF6A- and ATF6B-deficient (ATF6A+B $^{-/-}$) THP-1 cell lines (Figure 8).

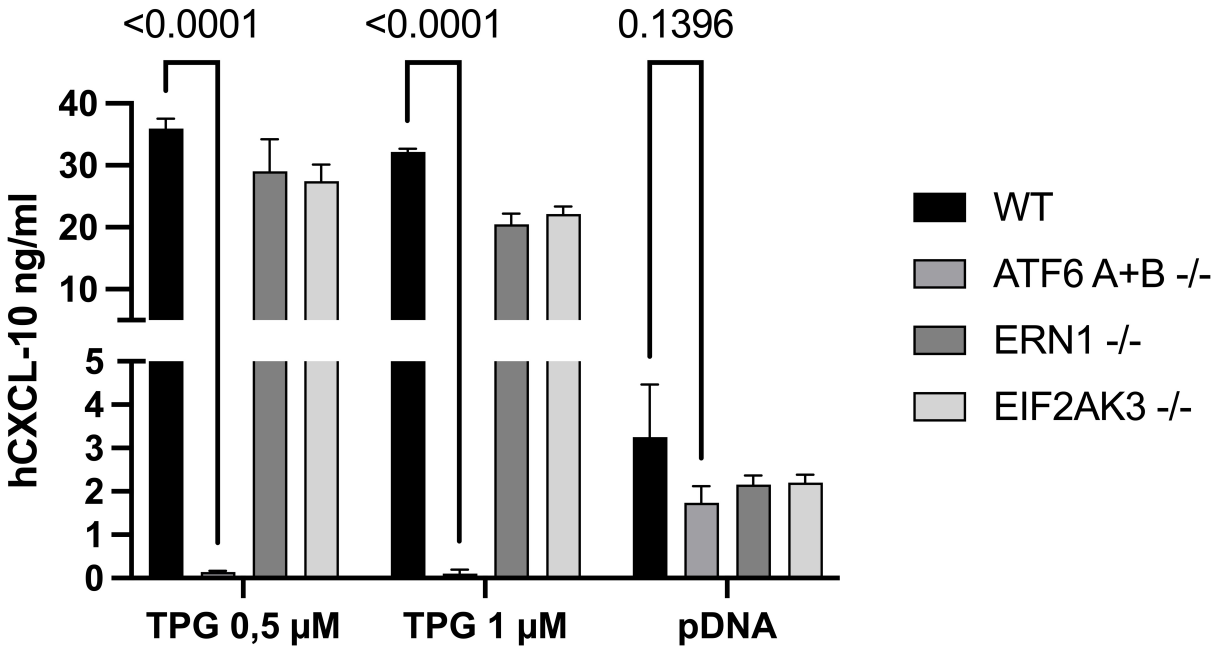

Figure 8: ER stress-induced CXCL-10 secretion requires ATF6
WT, ATF6 -/-, ERN1 -/-, and EIF2AK3 -/- THP-1 cells were treated with two concentrations of Thapsigargin (TPG) or plasmid DNA (pDNA, 100 ng/ml). Supernatants were collected after 24 hours and cytokine secretion was assessed via ELISA. Bars are mean + SD of triplicates, representative of two independent experiments. For each knockout, two genotypically distinct THP-1 cell lines were analyzed, one representative cell line per gene is shown. Significance was determined using two-way ANOVA with Šidák's correction for multiple comparisons.

3.1.4. CXCL-10 secretion following ER stress is driven by mitochondrial DNA

Taken together, a cGAS-dependent type-I IFN response in human immune and non-immune cell lines, driven by the ATF6 branch of the UPR, could be observed. cGAS has been extensively characterized as the innate immune sensor of cytosolic DNA. In the absence of an infectious agent, cytosolic DNA is largely derived from the nuclear or mitochondrial compartments, although cGAS activation following endocytosis of extracellular DNA has been described (de Mingo Pulido et al., 2021). In viral and bacterial infection models, release of mtDNA from damaged mitochondria into the cytosol has been shown to induce a cGAS-dependent type-I IFN response (Aguirre et al., 2017; Huang et al., 2020). In order to characterize the potential role of mtDNA in ER-stress induced cGAS signaling, ρ0 THP-1 cells devoid of mtDNA were generated by prolonged exposure to the DNA-intercalating agent EtBr (Figure 8A) (Widdrington et al., 2017). In order to validate mtDNA depletion, relative copy number abundance of the mitochondrial MT-ND1 gene and the nuclear gene B2M were compared using qPCR (Figure 8B).

Although cGAS/STING-mediated signaling was intact in ρ0 THP-1 cells and could be activated by an exogenous stimulus such as transfected plasmid DNA, ER stress-mediated CXCL-10 secretion was abrogated (Figure 8C). These results raise the possibility that cytosolic mtDNA acts as a DAMP during ER stress by activating cGAS/STING signaling and the type-I IFN response.

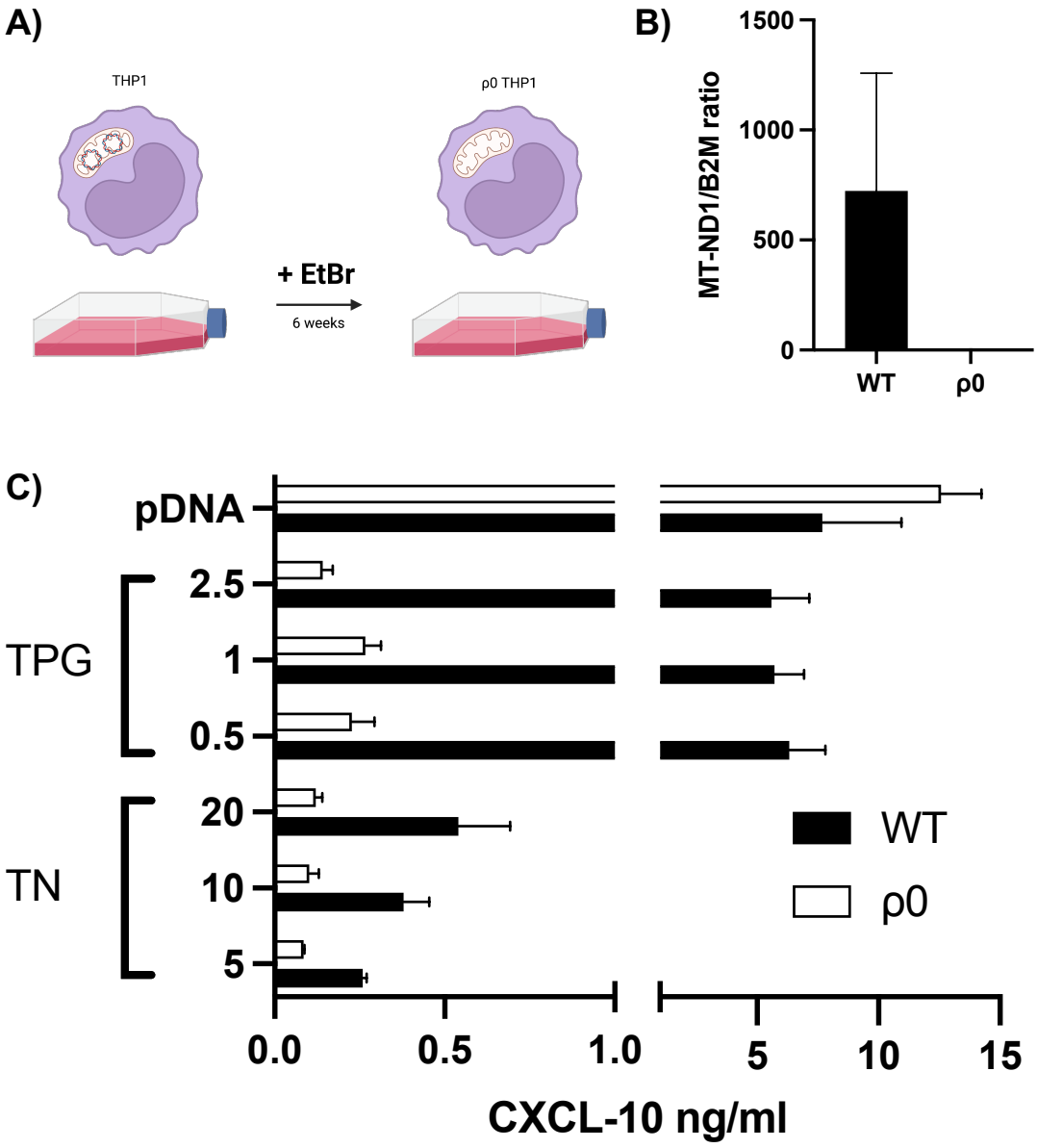

Figure 9: ER stress-induced CXCL-10 secretion is abrogated in mtDNA-deficient ρ0 THP-1 cells

(A) Schematic depiction of mtDNA depletion in THP-1 cells (B) DNA was isolated from WT and ρ0 THP-1 cells and copy numbers of nuclear gene B2M and mitochondrial gene MT-ND1 were assessed via RT-PCR. Bars are mean + SEM from two independent experiments. (C) WT and ρ0 THP-1 cells were treated with the indicated concentrations of Tunicamycin (TN, µg/ml) or Thapsigargin (TPG, µM), or transfected with plasmid DNA (pDNA, 400 ng/ml). Supernatants were collected after 24 hours, and cytokine secretion was assessed via ELISA. Bars are mean + SD of triplicates, representative of three independent experiments.

To confirm that ER stress leads to mtDNA leakage into the cytosol, fluorescence imaging was applied. However, conventional light microscopy provided insufficient resolution to visualize detachment of DNA from mitochondrial structures (data not shown). Thus, I employed super-resolution microscopy in order to achieve an image quality allowing for the distinction of DNA colocalized to mitochondria and DNA in the cytosol (Rust et al., 2006). To investigate whether ER stressor treatment would mediate DNA leakage from mitochondria, primary fibroblasts were treated with TN, and STORM imaging was performed after staining for DNA and the mitochondrial protein TOMM20 using fluorescent probes. After TN treatment, decreased attachment of DNA to mitochondrial structures could be observed, indicating the presence of cytosolic DNA.

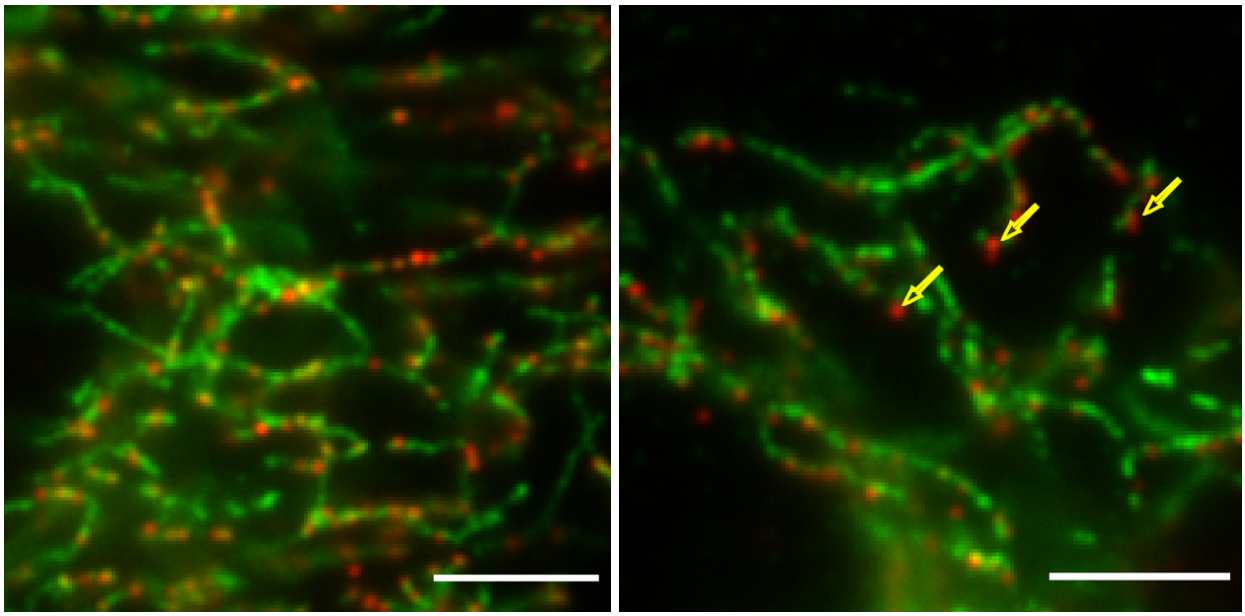

Figure 10: Super-resolution microscopy visualizes DNA release into the cytosol
Human primary fibroblasts treated with DMSO (left) or TN (10 µg/ml, right) for 4 hours. After exposure, cells were fixed and stained for DNA (red) and TOMM20 (mitochondrial membrane marker, green). Yellow arrows indicate examples of DNA stains detached from mitochondrial structures.
Images were obtained using a STORM device in series of 15,000 images and digitally reconstructed. Scale bars = 5 µm.

In summary, these findings support a model of cGAS activation by mtDNA that is released into the cytosol upon treatment with ER stressors, mediating type-I IFN secretion via STING and IRF3. This innate immune response was abrogated in ATF6-

deficient cells, but preserved in cells deficient in IRE1α and PERK, suggesting that ATF6 is the UPR master regulator mediating cytosolic mtDNA release.

3.2 Activation of the inflammasome by proteasome inhibitors

3.2.1. Treatment with proteasome inhibitors induces secretion of IL-1β, but not CXCL-10

ER stress has been described as an activator of the inflammasome in the literature. Both UPR-independent NLRP3 activation as well as IRE1α- and Caspase-2-mediated mitochondrial damage leading to NLRP3 activation have been suggested to play a role (Bronner et al., 2015; Menu et al., 2012). To recapitulate previous data indicating IL-1β release in cells exposed to ER stressors, THP-1 cells previously differentiated with PMA were treated with TN and TPG for 6 and 24 hours (Figure 11A). Surprisingly, no IL-1β could be detected in the cell culture supernatant after 6 or 24 hours of treatment. However, IL-1β was detectable after 24 but not 6 hours of exposure to proteasome inhibitors, thus inducing a delayed response when compared to the prototypical inflammasome activating agent nigericin (Figure 11A). Similar results were observed in the human monocytic cell line BlaER1 (Figure 11C) and in human PBMC (Figure 11D). Conversely, CXCL-10 secretion in THP-1 cells treated with the proteasome inhibitor epoxomicin was undetectable (Figure 11B), contradicting previous studies where proteasome inhibitors have been described as activators of the type-I IFN response and thus have been employed as tools to recapitulate the pathomechanism of CANDLE (Brehm et al., 2015).

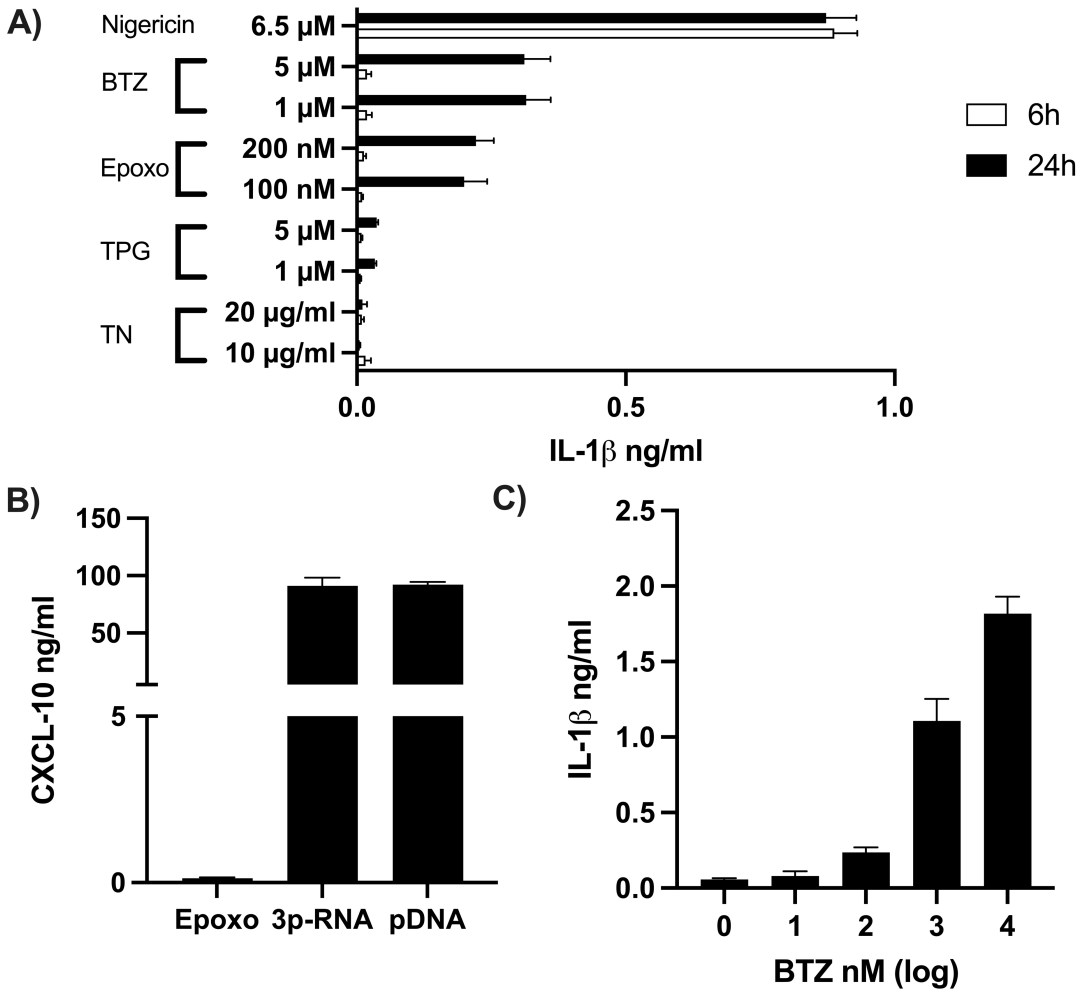
A)
Nigericin
BTZ
Epoxo
TPG
TN
6.5 µM
5 µM
1 µM
200 nM
100 nM
5 µM
1 µM
20 µg/ml
10 µg/ml
6h
24h
0.0
0.5
1.0
IL-1β ng/ml
B)
CXCL-10 ng/ml
150
100
50
5
0
Epoxo
3p-RNA
pDNA
C)
IL-1β ng/ml
2.5
2.0
1.5
1.0
0.5
0.0
0
1
2
3
4
BTZ nM (log)

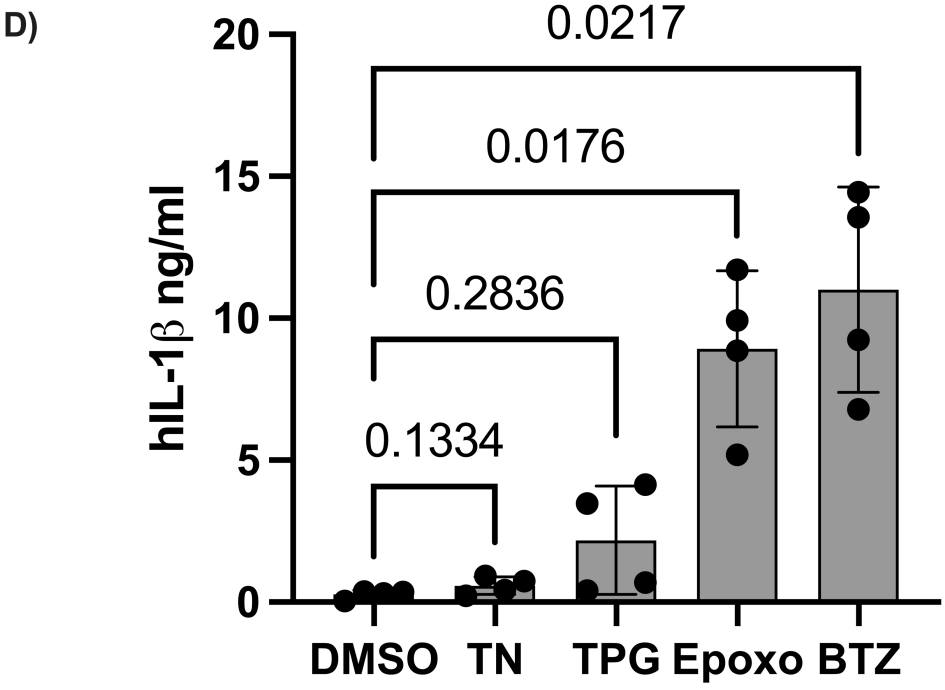
D)
hIL-1β ng/ml
20
15
10
5
0
0.0217
0.0176
0.2836
0.1334
DMSO
TN
TPG
Epoxo
BTZ

Figure 11: Proteasome inhibitors induce IL-1β, but not CXCL-10 secretion
(A) THP-1 cells were primed with PMA and treated with the indicated concentrations of tunicamycin (TN), thapsigargin (TPG), epoxomicin (Epoxo, μM), or bortezomib (BTZ), or with nigericin (6.5 μM) for 6 or 24 hours, as indicated. (B) THP-1 cells were stimulated with Epoxo (100 nM), 5'-triphosphate dsRNA (3p-RNA, 100 ng/ml) or plasmid DNA (pDNA, 400 ng/ml) for 24 hours. (C) Differentiated BlaER1 cells were primed for 4h with Pam3CSK4 (2 μg/ml) and then treated with the indicated concentrations of BTZ for 24 hours. (D) Human PBMC were primed for 4h with Pam3CSK4 (2 μg/ml) and subsequently treated with TN (10 μg/ml), TPG (1 μM), Epoxo (100 nM), or BTZ (1 μM). (A-D) Supernatants were harvested, and concentrations of CXCL10 and IL1β were assessed via ELISA. Bars depict mean + SD of triplicates, representative of at least two independent experiments (A-C) or mean ± SEM of n=4 donors, with each data point representing an individual donor (D). Significance was determined by one-way ANOVA with Dunnett's correction for multiple comparisons (D).

3.2.2. IL-1β secretion occurs at proteasome inhibitor concentrations necessary for cytotoxic activity

To characterize the dose response, PBMC were primed with the TLR2 agonist Pam3CSK4 and then treated with titrated concentrations of BTZ (Figure 12). IL-1β secretion was induced by BTZ treatment in a dose-dependent manner with a half maximal effective concentration (EC_{50}) of 12.34 nM (95% confidence interval 0.3061 to 289.0 nM, Figure 13). Interestingly, higher peak BTZ concentrations than the calculated EC_{50} from this study have been observed in human subjects treated for MM (Reece et al., 2011), raising the possibility of clinically relevant IL-1β induction by BTZ.

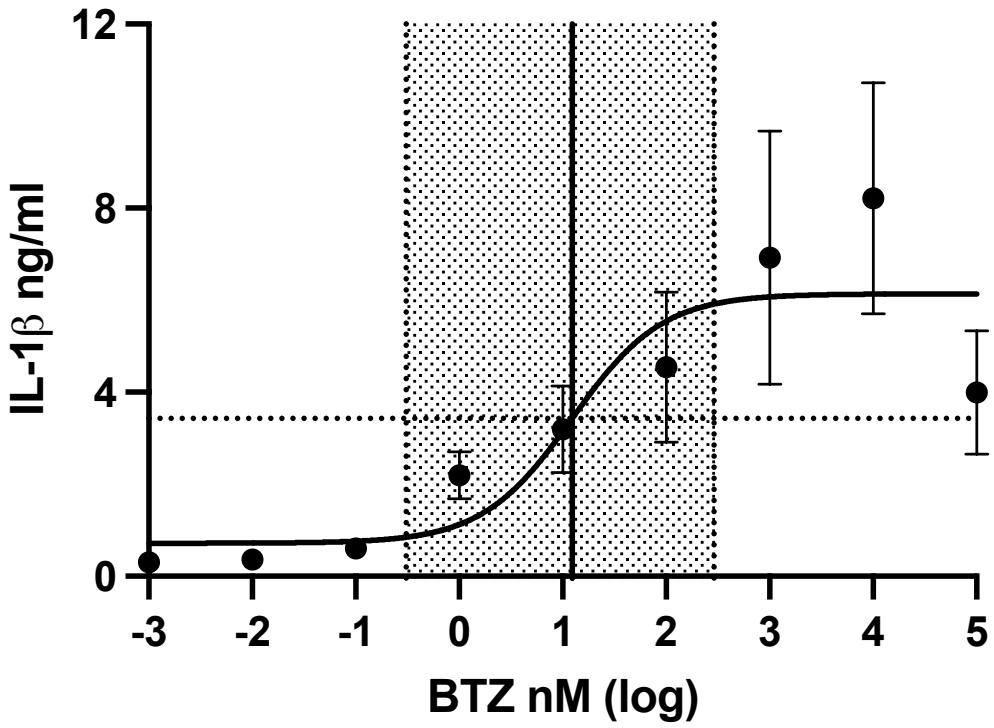

Figure 12: Dose-response curve of Bortezomib-induced IL-1β secretion in PBMC
Human PBMC were primed with Pam3CSK4 (2 µg/ml) and treated with increasing concentrations of Bortezomib (BTZ). Supernatants were collected after 24 hours and cytokine concentrations were assessed via ELISA. Data points are mean ± SEM of n=4 donors. The continuous vertical line represents the EC_{50}, the dotted area represents the 95% confidence interval. The horizontal dotted line represents the calculated half-maximal IL-1β concentration.

The primary clinical application for proteasome inhibitors such as BTZ is in MM treatment. BTZ has been demonstrated to be able to induce remission in a large number of MM patients and is now routinely used in various therapy protocols (Rajkumar, 2020). I aimed to validate cytotoxicity of BTZ in MM cells at concentrations eliciting IL-1β release in PBMC. To this end, the MM cell line KMS-11 and its BTZ-resistant derivate KMS-11/BTZ were treated with increasing concentrations of BTZ, and cytotoxicity was assessed using a fluorometric metabolic assay (Figure 12). KMS-11 cells are widely used for the study of MM as they harbor a translocation between chromosomes 4 and 14, a characteristic feature of high-risk disease in humans (Lauring et al., 2008; Trudel et al., 2004). Half maximal inhibitory concentration (IC_{50}) of BTZ in KMS-11 MM cells was 18.6 nM (95% confidence interval 10.26 to 36.78 nM) and thus similar to the EC_{50} for IL-1β secretion in PBMC. In the BTZ-resistant KMS-11/BTZ cell line, the IC_{50} was

several magnitudes higher (604.9 nM, 95% confidence interval 414.2 to 869.2 nM). Thus, it could be concluded that IL-1β secretion occurs at BTZ concentrations necessary for cytotoxic activity in MM.

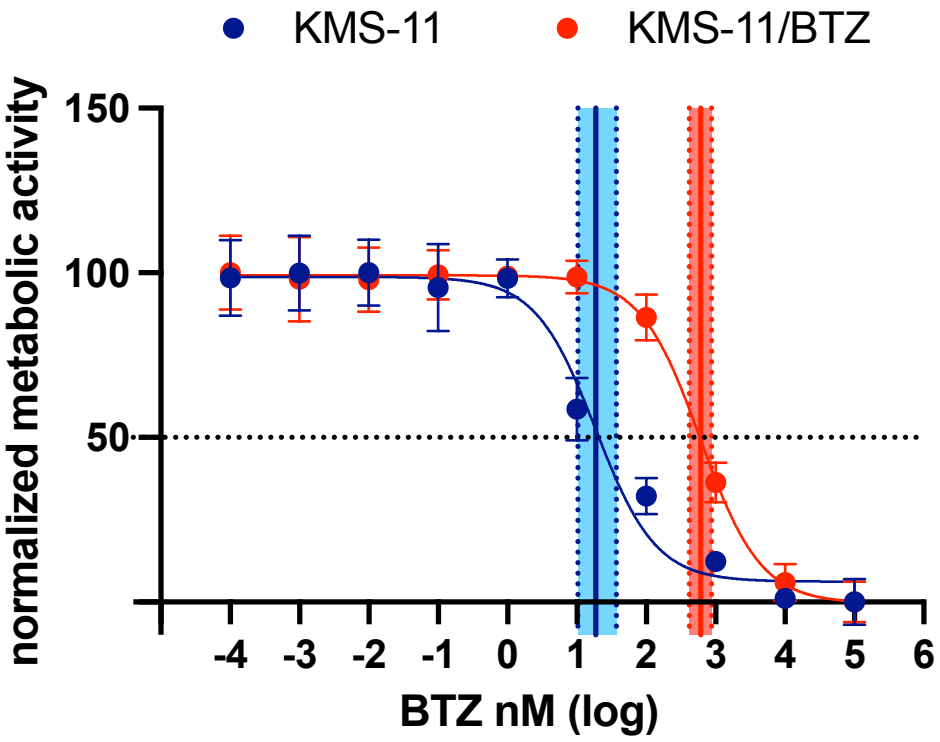

Figure 13: Dose-response curve of Bortezomib-induced cell death in multiple myeloma cell lines
Human multiple myeloma cell lines KMS-11 and KMS-11/BTZ (Bortezomib (BTZ)-resistant) were treated with increasing concentrations of BTZ. After 20 hours, metabolic activity as a surrogate of cell viability was assessed with a fluorescence assay. Data points are mean ± SEM of n=3 independent experiments. Continuous vertical lines indicate IC_{50} concentrations. Colored areas indicate 95% confidence interval.

3.2.3. Hallmarks of inflammasome activation can be detected in cells treated with proteasome inhibitors

ASC is an inflammasome adaptor protein, which is typically required for subsequent caspase 1 activation, although some inflammasome receptors have been demonstrated to initiate complex formation without ASC involvement (Broz & Dixit, 2016). After inflammasome activation, ASC multimerizes and forms a large, prion-like protein

aggregate termed “speck” that can be visualized by light microscopy through staining or the use of fluorescent tags (Cai et al., 2014; Stutz et al., 2013).

In order to quantify ASC aggregation, a THP-1 cell line with stable overexpression of a functional ASC-GFP construct was generated using lentiviral transduction. After treatment of PMA-differentiated ASC-GFP^{+} THP-1 cells with BTZ, fluorescent microscopy was performed to visualize ASC speck formation (Figure 14A). Here, BTZ-treated cells demonstrated an approximately two-fold increase in ASC speck formation compared to the DMSO control (Figure 14B).

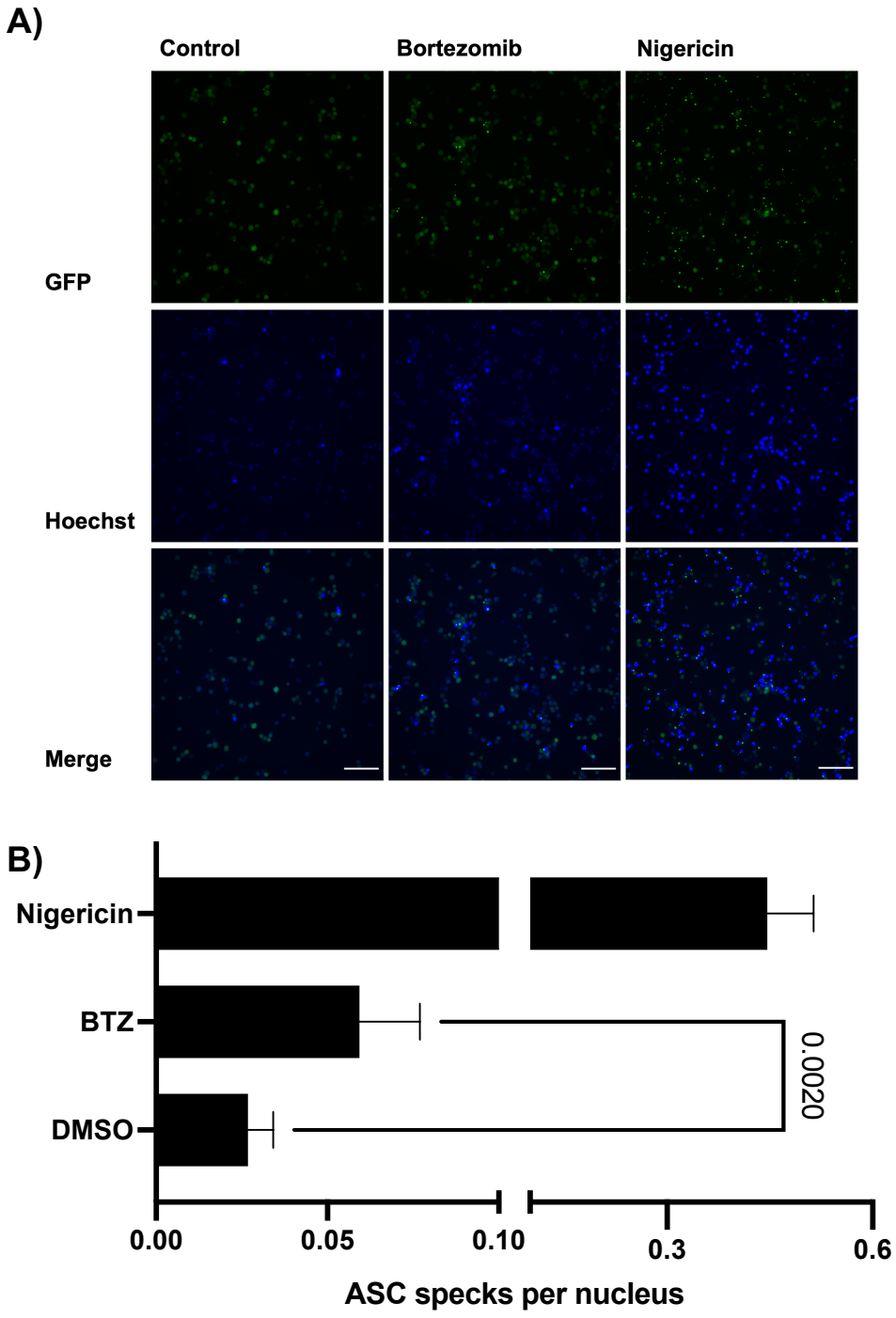

Figure 14: Bortezomib treatment induces formation of ASC specks
THP-1 cells stably overexpressing an ASC-GFP construct were treated with Bortezomib (BTZ, 10 nM) for 90 minutes or with Nigericin (6.5 µM) for 30 minutes. Nuclei were stained with Hoechst 33258 and cells were subsequently imaged on a light microscope to assess ASC speck formation.
(A) One representative region of interest per experimental condition is shown. Scale bar = 50 µm. (B) Quantification of ASC specks. Bars are mean + SD of n=6 regions of

interest, representative of three independent experiments. Significance was determined using Student's two-tailed t test.

The terminal step of canonical inflammasome activation is caspase 1-dependent proteolytic cleavage of inactive pro-IL-1β to bioactive IL-1β. (Broz & Dixit, 2016; Thornberry et al., 1992). However, IL-1β can also be processed by other proinflammatory Caspases such as caspase-4 and -5 or their murine ortholog caspase-11 (Kayagaki et al., 2011). To characterize the putative role of caspase-1 in BTZ-mediated inflammasome activation, WT and caspase-1-deficient (CASP1$^{-/-}$) THP-1 cells were stimulated with titrated concentrations of BTZ. In CASP1 $^{-/-}$ THP-1 cells, the IL-1β response to BTZ stimulation was abrogated at all BTZ concentrations, indicating that the canonical inflammasome mediates IL-1β release after BTZ (Figure 15).

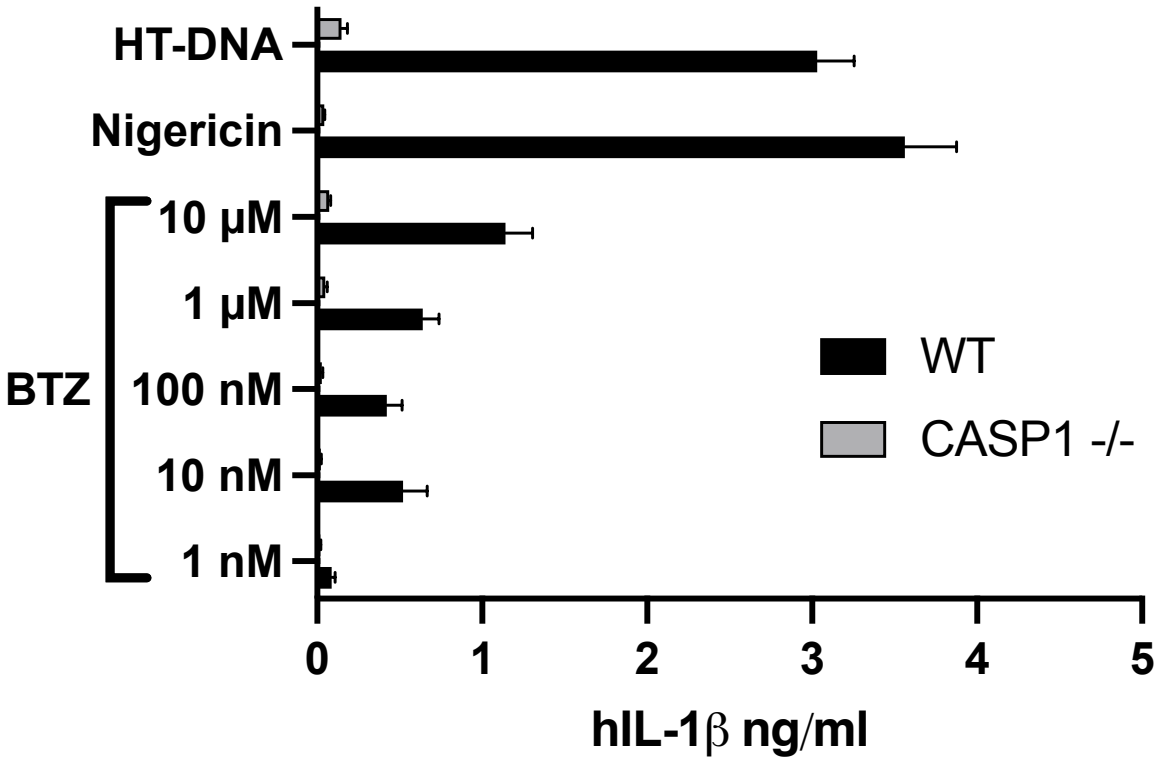

Figure 15: Genetic ablation of Caspase-1 abrogates Bortezomib-induced IL-1β secretion
WT or CASP1 -/- THP-1 cells were primed with PMA and then treated with the indicated concentrations of bortezomib (BTZ), nigericin (6.5 µM), or transfected with herring testes DNA (HT-DNA, 1 µg/ml). Supernatants were collected after 24 hours and cytokine concentration was assessed via ELISA. Bars are mean + SD of triplicates,

representative of three independent experiments. Two genetically distinct CASP1 -/- cell lines were analyzed. One representative cell line is shown.

3.2.4. The BTZ-induced IL-1β response is independent of NLRP3 in PBMC

As mentioned above, several inflammasome receptor proteins have been identified to date. Among the inflammasome proteins currently known, only NLRP3 is currently amenable to pharmacological intervention using a small molecule inhibitor, MCC-950 (Coll et al., 2015). Moreover, NLRP3 is known to trigger inflammasome activation in response to a broad variety of cellular stressors and disturbances of cellular homeostasis, making it *a priori* a plausible candidate in the PI-mediated inflammasome pathway (Lamkanfi & Dixit, 2014). Thus, to investigate the potential role of NLRP3 in PI-mediated inflammasome activation, human PAM3CSK4-primed PBMC were pre-treated with the NLRP3 inhibitor MCC-950 and then stimulated with BTZ and NLRP3-activating controls (Figure 16). As expected, IL-1β secretion following treatment with nigericin and herring testes DNA (htDNA) was abrogated in MCC-950-pre-treated cells. However, MCC-950 treatment did not affect IL-1β levels in cell culture supernatant of BTZ-treated cells, providing evidence that BTZ-mediated inflammasome activation is independent of NLRP3 in human PBMC.

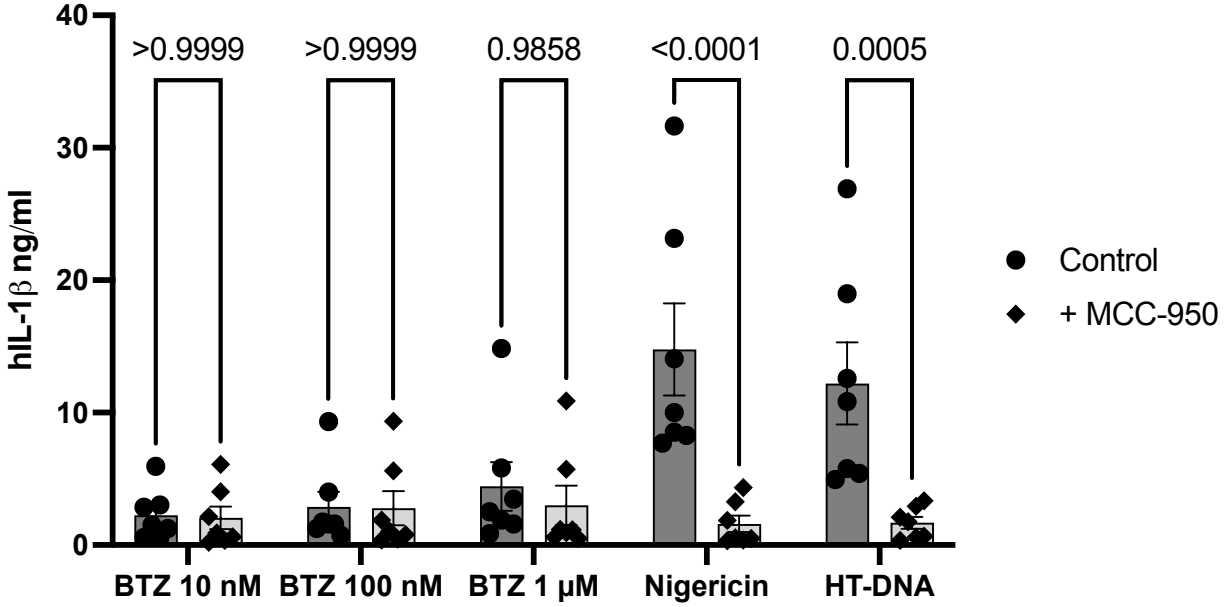

Figure 16: Bortezomib-induced inflammasome activation is independent of NLRP3 in PBMC
PBMC were primed with Pam3CSK4 (2 µg/ml for 4 hours), pre-treated with the NLRP3 inflammasome inhibitor MCC-950 (5 µM) or a DMSO control for 2 hours and then treated with bortezomib (BTZ, indicated concentrations) or nigericin (6.5 µM), or transfected with herring testes DNA (HT-DNA, 1 µg/ml). Supernatants were collected after 24 hours and cytokine concentration was assessed via ELISA. Bars are mean ± SEM of n=7 donors, each data point represents an individual donor. Significance was determined using two-way ANOVA with Šidák's correction for multiple comparisons.

To validate these findings at the genetic level, IL-1β secretion was investigated in NLRP3-deficient THP-1 cells. Here, in contrast to the results obtained in primary human cells using MCC-950, we observed a significant reduction of IL-1β release in response to proteasome inhibitors BTZ (Figure 17A) and epoxomicin (17B) in NLRP3 -/- cells. However, as opposed to other reports, a significant decrease in IL-1β signaling was also present in the DNA-transfected condition (Figure 17A+B), indicating a decreased responsiveness of these NLRP3 -/- THP-1 cell lines to inflammasome activation (Gaidt et al., 2017). Most likely, this is due to clonal effects in cell line generation, which may be caused by wild-type cell heterogeneity or off-target effects of the crRNA (Westermann et al., 2022).
Furthermore, it should be noted that, although THP-1 cells have been widely used as tools to study the inflammasome response to cytosolic DNA, distinct mechanisms of DNA-mediated inflammasome assembly in THP-1 cells and human monocytes have been reported. However, these results indicate a higher grade of NLRP3 dependency in primary monocytes (Gaidt et al., 2017; Hornung et al., 2009).

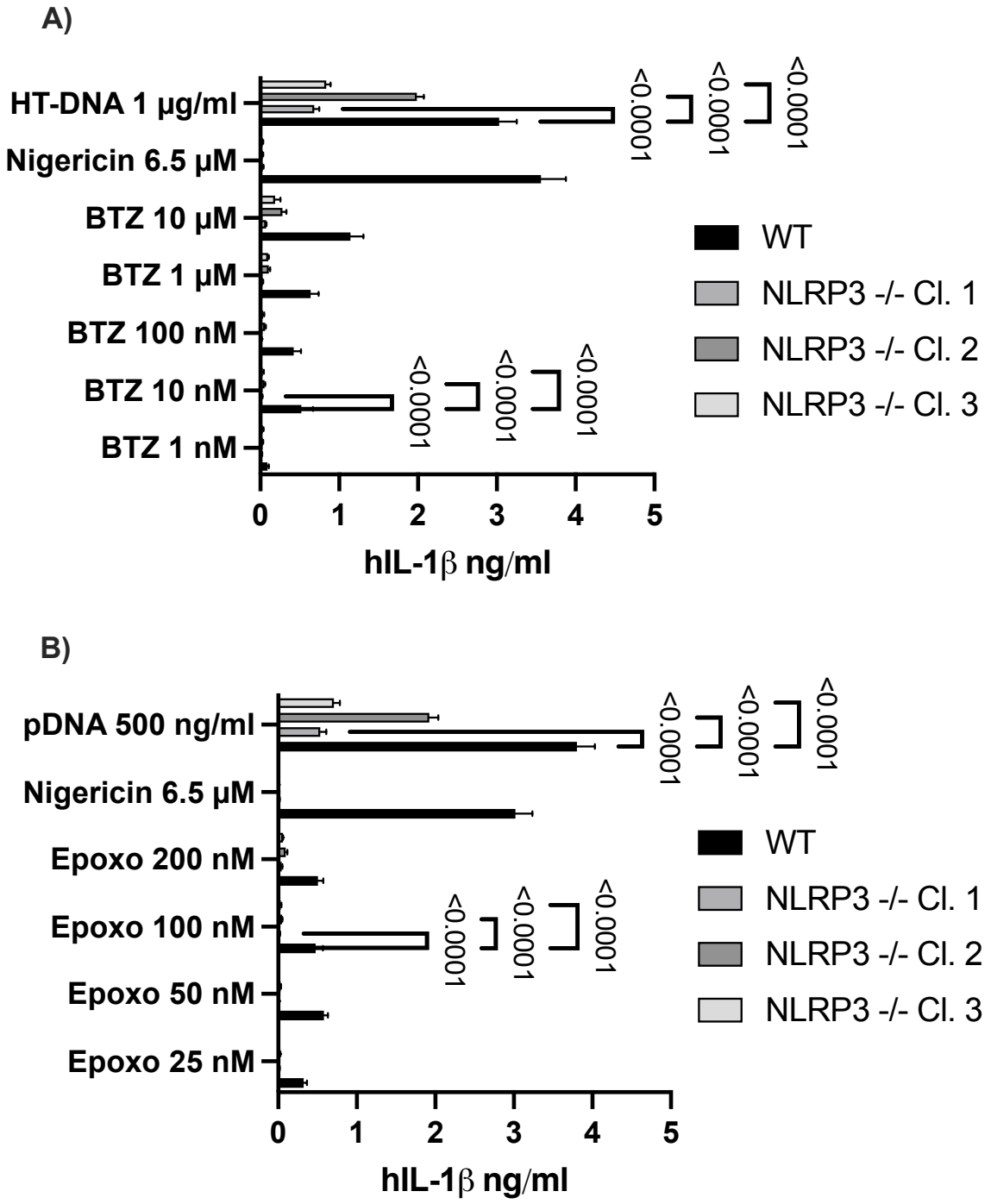

Figure 17: NLRP3 -/- THP-1 cells show diminished IL-1β responses to proteasome inhibitors and transfected DNA

WT and NLRP3$^{-/-}$ THP-1 cells were treated with bortezomib (BTZ, indicated concentrations, panel A), epoxomicin (Epoxo, indicated concentrations, panel B), or nigericin (6.5 µM), or transfected with herring testes DNA (HT-DNA, 1 µg/ml) or plasmid DNA (500 ng/ml). Supernatants were collected after 24 hours, and cytokine concentrations were assessed via ELISA. Bars are mean + SD of triplicates, representative of five (A) and two (B) independent experiments. Significance was

determined using two-way ANOVA with Dunnett's correction for multiple comparisons (A and B)

Altogether, these data confirm canonical inflammasome activation following proteasome inhibitor treatment in human cells. BTZ treatment led to ASC specking and caspase 1-dependent IL-1β secretion in THP-1 cells. In primary human cells, proteasome inhibitors, but not the ER stressors TN and TPG, induced an IL-1β response, and treatment with a small molecule NLRP3 inhibitor did not influence IL-1β levels in BTZ-treated cells as opposed to the response to nigericin treatment or DNA transfection. Taken together with the observation that ER stressors, but not proteasome inhibitors, were shown to induce a type-I IFN response mediated by cGAS-STING, these findings suggest that ER stress and proteasome inhibition are similar, yet distinct perturbations of proteostasis that activate innate immunity through separate pathways.

4. Discussion

4.1. ER stress-mediated activation of innate immunity

4.1.1. ER stressors lead to cGAS/STING-dependent type-I IFN secretion in the presence of mitochondrial DNA

This study describes a novel mechanism by which ER stress induces a type-I IFN-dependent innate immune response. Pharmacologically-induced ER stress, both via inhibition of lysosomal degradation and disruption of cellular calcium homeostasis, induced type-I IFN secretion in human cells. This immune response was dependent on key components of the cytosolic DNA sensing machinery, namely cGAS, STING, and IRF3, and was abrogated in the respective knockout cell lines. Contrastingly, genetic ablation of RIG-I and MAVS showed no effect on ER-stress mediated CXCL-10 secretion as a proxy for the type-I IFN response. Furthermore, experiments with THP-1 cells deficient in each of the three ER stress master regulators ATF6, IRE1, and PERK indicated that only the ATF6 branch of the UPR was required for IFN induction. Moreover, CXCL-10 secretion was no longer observed in $\rho 0$ THP-1 cells devoid of mitochondrial DNA, although recognition of exogenous cGAS and RIG-I ligands was preserved. Super-resolution STORM imaging of primary human fibroblasts confirmed cytosolic presence of mtDNA following treatment with ER stressors. Consequently, it can be postulated that ER stress elicits DNA release from the mitochondria via an ATF6-dependent pathway. The circular mitochondrial genome is largely resistant to TREX1-mediated cytosolic degradation as it lacks free 3’ ends necessary for TREX1 exonuclease activity. It is therefore an optimal ligand for cGAS, which, in turn, induces a type-I IFN response via downstream activation of STING, TBK1, and IRF3 (Figure 18).

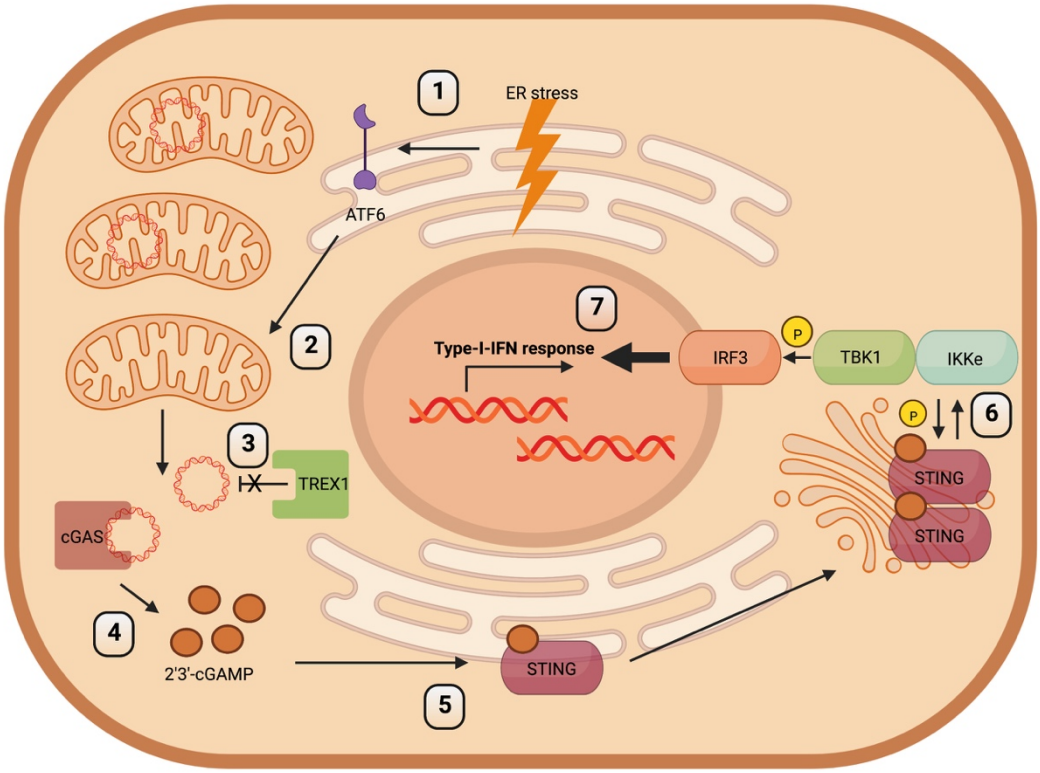

Figure 18: Release of mitochondrial DNA connects the unfolded protein response to nucleic acid sensing
Schematic depiction of the proposed mechanism leading from ER stress to type-I IFN secretion. (1) ER stress activates the UPR, including the ATF6 branch. (2) ATF6 mediates release of mtDNA into the cytosol. (3) mtDNA lacks free 3' and is thus resistant to TREX1 exonuclease-mediated degradation. (4) mtDNA is recognized by cGAS, leading to synthesis of 2'3'-cGAMP. (5) 2'3' cGAMP activates STING. (6) Activated STING multimerizes and binds to TBK1. (7) The TBK1-IRF3 axis initiates a transcriptional response.

4.1.2. cGAS/STING-dependent recognition of mtDNA provides a mechanistic explanation for ER stress-mediated activation of innate immunity

Both the antiviral type-I IFN response and the UPR are initiated by stress signals indicative of threats to cellular integrity. In both pathways, entity, intensity, and duration of input signals determine output quality (Newton & Dixit, 2012). Effector mechanisms range from metabolic alterations aimed at restoring physiological conditions within single cells to programmed cell death in order to preserve tissue integrity by removal of defective cells from tissue (Newton & Dixit, 2012).

Whereas UPR signaling is primarily a cell-intrinsic mechanism to restore cellular homeostasis, effector mechanisms of type-I IFNs and cognate cytokines are largely dependent on paracrine communication. Both pathways act in a coordinated manner in response to danger signals such as viral infection (Smith, 2014).

Enhancement of innate immune signaling through pharmacological ER stress has been extensively characterized (Liu et al., 2012; Smith et al., 2008). A recent study links ER stress and STING-dependent type-I IFN production in mouse neurons. It could be demonstrated that an ER stress-induced IFN response shapes the inflammatory microenvironment after for traumatic brain injury and recruits immune cells such as T helper cells and microglia to the lesion site. Attenuation of ER stress was able to reduce inflammation and improve cognitive function following traumatic brain injury in a mouse model. However, a connecting element between ER stress and antiviral immunity was not determined (Sen et al., 2020).

Furthermore, mitochondrial stress, a condition where the integrity of the mitochondrial membrane is perturbed and contents of the mitochondrial matrix, including cytochrome C and mtDNA, are released into the cytosol, triggers an IFN-driven immune response. Mitochondrial stress and associated inflammatory signaling have been implied in viral infection with both DNA and RNA viruses (Domizio et al., 2022; West et al., 2015). Our results suggest that during ER stress, the ATF6 branch of the UPR initiates a mitochondrial stress response leading to type-I IFN secretion, thus providing a mechanism for viral innate immune recognition that relies on endogenous rather than on viral NA and thus circumvents immune evasion strategies (see section 4.1.3).

Emerging evidence suggests a role for mitochondrial stress-mediated IFN signaling in sterile inflammation (Caielli et al., 2021). The mechanistic findings of this study have been found to play a role in myotonic dystrophy type 2 (DM2), a condition that is caused by expansion of CCTG nucleotide repeats in intron 1 of the zinc finger protein 9 (ZNF9) gene. Interestingly, in contrast to other forms of myotonic dystrophy, DM2 patients exhibit increased prevalence of autoimmune and autoinflammatory phenomena linked to type-I IFN induction (Günther et al., 2022; Tieleman et al., 2009).

Repeat expansion leads to translation of large mRNAs accumulating in the cytoplasm, yet inflammation in DM2 was shown to be independent of cytosolic RNA sensors. Instead, repeat-associated non-AUG translation induced the formation of non-functional

protein aggregates in the cytosol. Consequently, DM2 patient cells display signs of chronic ER stress. Via ATF6, chronic ER stress leads to mitochondrial dysfunction and subsequent mtDNA leakage into the cytosol, inducing a cGAS-dependent type-I IFN response (Günther et al., 2022).
These mechanistic observations explain why DM2 patients display increased levels of ISG transcripts in peripheral blood, and provide a rationale for treatment of autoinflammation with drugs targeting IFN-driven inflammation such as JAK inhibitors in this cohort (Günther et al., 2022).

4.1.3. Type-I IFN secretion following ER stress may counteract viral evasion of immune recognition and enable DNA-dependent immune sensing of RNA viruses

In antiviral defense, type-I IFN signaling requires activation of NA sensors with considerable ligand selectivity in order to avoid inappropriate stimulation, e.g. by self NA. However, the fact that immune recognition critically depends on specific molecular patterns has allowed for pathogens to develop sophisticated escape mechanisms through the course of co-evolution with their hosts, allowing them to escape potential induction of a type-I IFN response (Chan & Gack, 2016). Viral immune escape mechanisms target different levels of NA metabolism and immune sensing.
Viral NA can be concealed from recognition by NA receptors in different ways. Many RNA viruses replicate in specific cellular compartments inaccessible to RLRs. Retroviruses, such as human immunodeficiency virus 1 (HIV-1), use the host exonuclease TREX1 to clear the cytosol of its reverse DNA transcripts and thus avoid DNA sensing by cGAS (Chan & Gack, 2016; Yan et al., 2010). In other instances, interaction of viral proteins with host NA sensor activation enables immune evasion (Gack et al., 2009).
All of the above-described immune evasion mechanisms share the prevention of specific ligand recognition as a common denominator. However, successful viral immune evasion must remain compatible with viral replication. Clearly, protein biosynthesis is an essential part of virus production that cannot be circumvented, and increased cellular protein load is the prototype inductor of ER stress. Thus, ER stress-dependent immune activation by cytosolic recognition of mtDNA is an *ultima ratio* to recognize the presence

of a viral pathogen, largely excluding immune evasion through modification of viral NA or RLR signaling by making use of an endogenous DNA ligand.

“Non-canonical” activation of the cGAS-STING pathway has been proposed as a potential mechanism for the sensing of RNA viruses that evade innate immunity through interaction with RNA sensors (Ni et al., 2018). It has recently been demonstrated that DENV, which contains an RNA genome, induces a type-I IFN response via the cGAS-STING-pathway by curtailing the release of mitochondrial DNA (Sun et al., 2017). In line with the findings presented here, viral replication-induced ER stress provides a possible mechanistic explanation for mtDNA release, illustrating that DNA-dependent recognition of RNA viruses is a product of canonical cGAS activation.

However, type-I IFN signaling following mtDNA recognition depends on the mechanistic integrity of the cGAS-STING pathway (West & Shadel, 2017). Several viruses directly target the cGAS or STING protein for the purpose of immune escape, which would render endogenous mtDNA recognition ineffective for viral clearance. While cGAS-dependent mtDNA recognition induces an immune response to DENV, this virus can induce cleavage of STING to prevent downstream IFN signaling via its NS2B3 protein complex (Aguirre et al., 2017; 2012). In addition to DENV, other RNA viruses have been shown to inhibit DNA sensing mechanisms, indicating that recognition of cytosolic mtDNA might be a common phenomenon in virus infection (Christensen & Paludan, 2017).

In summary, ER stress-induced, mtDNA dependent cGAS-STING activation provides a mechanism of sensing viral infection that is particularly difficult to circumvent during viral replication. The non-specific nature of ER stress as an immune activation signal would be a possible explanation for the relatively modest type-I IFN signaling strength when comparing *in vitro* ER stressor treatment to direct stimulation with NA ligands in primary cells. However, it should be noted that direct transfection of NA to immune cells is supraphysiological, and a comparison of direct and indirect NA receptor stimuli *in vitro* is artificial.

In this study, ER stress-dependent immune activation was investigated in a small molecule model *in vitro*. Further investigation of the interplay of ER stress-dependent immunity and pathogen immune evasion in an infection animal model is warranted to

determine *in vivo* properties and relevance of this newly observed ATF6-dependent mechanism.

4.1.4. Signaling of nucleic acid receptors and the unfolded protein response converges in programmed cell death

If the UPR fails to restore homeostasis during sustained ER stress, it initiates apoptosis in order to eliminate irreversibly damaged cells from the organism (Hetz, 2012). In a similar manner, effector mechanisms of NA sensor activation occur in a sequential manner, starting with cell-intrinsic transcriptional induction of an antiviral state, followed by paracrine signaling to recruit immune cells to the site of inflammation. Analogous to the tiered response to ER stress, cell death serves as the *ultima ratio* of antiviral defense in the case of sustained NA sensor signaling input (Bartok & Hartmann, 2020). Both immunologically silent and immunogenic forms of cell death occur downstream of STING and/or MAVS activation (Bartok & Hartmann, 2020).

During apoptosis, permeabilization of the mitochondrial membrane leads to release of mitochondrial matrix components, including mtDNA, into the cytosol. However, cytosolic mtDNA-induced cGAS activation is prevented by apoptotic caspases (Rongvaux et al., 2014; White et al., 2014). In the present study, immunogenicity of ER stress-induced mtDNA release could be demonstrated, allowing for the hypothesis that mitochondrial membrane permeabilization following ER stress signals can occur independently of cell death.

Previous studies have demonstrated the cooperative contributions of ER stress and innate immune receptor signaling to cell death. As described previously, aberrant activation of NA sensors leads to inappropriate, chronic type-I IFN signaling and autoinflammation. In a mouse model of autoinflammatory disease caused by a heterozygous activating mutation in STING, analogous to human SAVI, T cell apoptosis occurred via activation of UPR genes in a STING-dependent manner. Mechanistically, STING was shown to contain a previously undescribed “UPR” motif that, in STING-mutated cells, reduced both influx and efflux of calcium at the ER, leading to perturbed cellular calcium homeostasis. Inadequate calcium levels sensitized T cells to T cell receptor activation-induced ER stress and subsequent apoptotic cell death. Treatment

with chemical chaperones that alleviate ER stress reduced cell death in this model. At the same time, reconstitution of T cell function via crossing STING-mutated mice with animals harboring a T cell receptor allele that reduced ER stress-induced $CD8^+$ T cell death decreased lung pathology as compared to STING-mutant mice (Wu et al., 2019). The interplay of innate and adaptive immunity and ER stress in this model elegantly demonstrates the complex intersections of NA receptors and the UPR. Interestingly, STING activation was a prerequisite of UPR signaling in the study by Wu et al., whereas the present work demonstrates STING-dependent type-I IFN secretion downstream of ER stress and UPR activation. Although Wu et al. used TN and TPG in their study, they did not assess type-I IFN signaling following treatment of STING-mutated cells or animals. STING signaling upstream and downstream of UPR activation would indicate a forward loop increasing IFN secretion in ER-stress mutated cells. However, the extent of which ER stress-dependent IFN induction contributes to pathology in SAVI and analogous *in vivo* models remains to be determined.

4.2. Inflammasome activation by proteasome inhibitors

4.2.1. Proteasome inhibition induces hallmarks of inflammasome activation

In contrast to pharmacological induction of ER stress, ablation of protein degradation using proteasome inhibitors did not induce a type-I IFN response as measured by CXCL-10 secretion in the present study. These results are surprising, considering that inactivating mutations in proteasome subunits underly type-I IFN-driven autoinflammatory disease and proteasome inhibitors have been used to model proteasome-dependent inflammation (Brehm et al., 2015). It is unlikely that CXCL-10 is an inadequate readout for PRAAS models, as induction of type-I IFN without concomitant CXCL-10 description has not been described. PKR-dependent recognition of cytosolic IL-24 has recently been implicated in the pathomechanism of PRAAS based on investigation of patient cells and in THP-1 knockout cell lines where different proteasome subunits were genetically inactivated. These observations raise the possibility that the absent IFN response to proteasome inhibition in THP-1 cells is due to

differences in the immune response to proteasome inhibition and in genetic modeling of proteasome defects in this cell line (Davidson et al., 2022).
However, immunogenic properties of proteasome inhibition or malfunction are not limited to the type-I IFN response. Other authors have observed IL-1β secretion following exposition to proteasome inhibitors in murine and human cell lines, although these studies did not investigate the underlying molecular mechanisms (Beyar-Katz et al., 2019; Tang et al., 2018). Furthermore, these studies reveal seemingly contradicting effects of IL-1β on MM progression.
This work provides evidence for activation of the inflammasome complex by inhibition of the proteasome. Proteasome inhibitor treatment, in contrast to ER stress, led to secretion of IL-1β that was abrogated in a caspase-1-deficient cell line, and increased ASC specking in BTZ-exposed ASC-GFP$^+$ THP-1 cells could be observed. As ASC specking and caspase-1-dependent IL-1β maturation are hallmarks of inflammasome activation, it can be postulated that proteasome inhibition mediates assembly of this multiprotein complex.

4.2.2. NLRP3-dependent and independent IL-1β release in multiple myeloma and bortezomib treatment occur via different stimuli

Composition of the tumor microenvironment (TME) influences the natural disease course and therapy response in neoplasia (Whiteside, 2008). In particular, inflammatory signaling appears to be of particular importance to tumor progression and efficacy of therapies (Greten & Grivennikov, 2019). Contrasting, seemingly contradictory roles for inflammation in the TME have been described. One the one hand, inflammatory signaling appears to contribute to tumor growth and metastatic spread, while, on the other hand, immunologically “cold” tumors with an immunosuppressive TME seem to respond less well to immunotherapy, indicating that inflammation is required to recruit immune effectors to sites of neoplasia (Greten & Grivennikov, 2019). Different inflammatory signaling pathways appear to have opposing effects in the TME. For example, cyclooxygenase-dependent synthesis of prostaglandins has been described to promote tumor growth and progression, whereas type-I IFNs and other antiviral

cytokines appear to augment sensitivity of tumor cells to immune control mechanisms (Zelenay et al., 2015).

In MM, inflammatory signaling in the TME has been extensively studied. Expanding evidence suggests an important role of non-myeloma immune cells of myeloid progeny, namely macrophages, in MM progression and immune control (García-Ortiz et al., 2021). Macrophages develop from monocytic precursors and can assume different cell identities in a process termed polarization. Classically, M1 polarization is seen as pro-inflammatory and is associated with secretion of inflammatory cytokines such as IL-1β, whereas M2-polarized macrophages have been implicated in the resolution of inflammatory processes through mediators such as IL-10, and in promotion of tumor growth (García-Ortiz et al., 2021).

Active forms of IL-1β and IL-18 are generated through proteolytic cleavage of inactive precursors by Caspase-1 following inflammasome activation. Both cytokines, although pro-inflammatory by classical definition, have been described as acting immunosuppressively in the MM TME. IL-18 impedes effective tumor immune control by induction of myeloid-derived suppressor cells, and increased levels of bone marrow IL-18 is associated with poor prognosis in MM (Nakamura et al., 2018). Similar effects have been observed for IL-1β and have led to the investigation of IL-1 receptor antagonists as drug candidates in MM treatment (Lust et al., 2016).

A recent study has identified a potential mechanism for IL-1β release by macrophages in the TME. After phagocytosis by immune cells, β_2-microglobulin (β2M)-mediated rupture of intracellular lysosomes and subsequent assembly of the NLRP3 inflammasome. NLRP3-mediated IL-1β secretion was observed in an animal model as well as in primary patient cells and was associated with disease progression and therapy resistance. Detrimental effects of β2M phagocytosis could be reversed by treatment with MCC-950. Altogether, these results raise the question whether NLRP3 inhibition may be exploited for therapeutic benefit in MM (Hofbauer et al., 2021).

In this work, IL-1β release following BTZ was investigated in primary human immune cells. In contrast to the inflammasome-mediated immune response to β2M described by Hofbauer et al., BTZ-dependent IL-1β secretion was unaffected by pharmacological inactivation of NLRP3 activity using MCC-950 in my study. However, genetic ablation of

NLRP3 significantly impaired the IL-1β response to both BTZ and epoxomicin in the THP-1 cell line. Unexpectedly, NLRP3 -/- THP-1 cells transfected with DNA also displayed significantly reduced cytokine secretion. These findings might be explained by a redundant NLRP3 dependency of the inflammasome response both to proteasome inhibition as well as to DNA in THP-1 cells, contradicting other studies, supported by the fact that this effect was more or less consistent across three genotypically distinct cell lines, although designed with the same gRNA (Gaidt et al., 2017; Hornung et al., 2009). Alternatively, generally reduced responsiveness to NLRP3-independent inflammasome stimuli due to clonal effects in knockout cell lines may exist (Westermann et al., 2022).
Although IL-1β and cognate cytokines are generally thought to shape the TME in a way that promotes tumor growth and perturbs immune control of neoplastic cells, it is worth noting that another study postulates an inhibitory effect of BTZ-mediated IL-1β on tumor growth *in vivo*, arguing for combination therapy using BTZ and TLR agonists (Tang et al., 2018). However, the authors do not use a MM model but inoculate immune deficient mice, which have a heavily altered TME, with acute myeloid leukemia-derived THP-1 cells, prohibiting any conclusions for MM (Greten & Grivennikov, 2019; Tang et al., 2018).

4.2.3. Potential adverse effects of bortezomib treatment on the multiple myeloma microenvironment

My study makes use of PBMC to investigate the effects of proteasome inhibitor treatment on inflammasome assembly and IL-1β secretion in vitro. PBMC are a heterogeneous composition of innate and adaptive immune cells that can be isolated from peripheral blood using a gradient-based approach. About 50% of cells in PBMC are T lymphocytes. However, innate immune cells such as monocytes and plasmacytoid DCs are also included (Autissier et al. 2010). Inflammasome activity is measurable in T cells and contributes to TH_1 immunity in T lymphocytes. However, it is relatively weak compared to myeloid cells, particularly monocytes, who are accountable for the majority of inflammasome-mediated IL-1β production in PBMC (Arbore et al., 2016).
Although PBMC accurately reflect composition of immune cells of non-granulocytic lineage in peripheral blood, direct *in vitro* stimulation of selected cell types is not

representative of physiological processes. As *in vivo* experiments could not be performed in my study, the cytotoxic effect of BTZ on BTZ-sensitive and resistant MM cell lines was assessed as a surrogate for treatment efficacy. IL-1β secretion from PBMC and cytotoxicity in MM occurred at similar dose levels with a comparable IC_{50}. Both cytotoxicity and inflammasome activation were observed at lower BTZ levels than peak BTZ concentration measured in peripheral blood of MM patients (Reece et al., 2011). These results increase the probability of IL-1β secretion occurring during BTZ treatment in humans. However, the necessity of priming for full assembly of the inflammasome complex under physiological conditions should be taken into account, although the need for an actual priming step in primary human monocytes is debated (Gritsenko et al., 2020). In my experiments, I did not measure IL-18 whose precursor form is constitutively expressed by various immune cell types, or ASC specking in non-primed cells, which is an evident limitation of this study (Gritsenko et al., 2020).

As mentioned in section 4.2.2, IL-1β may promote tumor progression and immunosuppression TME. Due to BTZ efficiently eliciting cytotoxicity on MM cells and demonstrating remarkable success in the clinic, most first-line regimens used for MM treatment in Europe include BTZ administration (Moreau et al., 2019). Other proteasome inhibitors such as carfilzomib, an epoxomicin derivative, are widely used in relapsed or refractory disease (Stewart et al., 2015). The clinical success of proteasome inhibition is undeniable. Nevertheless, the data in the current study demonstrate that BTZ could potentially adversely affect TME composition. Given encouraging results from pre-clinical studies, it is likely that NLRP3 inhibition will be investigated as a therapeutic target in MM in the future (Hofbauer et al., 2021). NLRP3-independent IL-1β release following BTZ treatment in immune cells (see Figure 16) may potentially limit its efficacy and thus deserves further attention.

Proteasome inhibition and glucocorticoids are frequently employed in combination strategies for MM treatment (Moreau et al., 2019; Stewart et al., 2015). Glucocorticoids have been shown to polarize macrophages towards an anti-inflammatory M2 phenotype (Olivares-Morales et al., 2018; Rajkumar, 2020). In malignant disease, anti-inflammatory macrophages have been shown to potentially contribute to disease progression by suppressing tumor immune control, impairing T cell function through anti-inflammatory signaling via IL-10 and other cytokines (Beider et al., 2014; Olivares-Morales et al.,

2018). Thus, BTZ and glucocorticoids may play a dichotomous role in the treatment of MM. While they elicit potent cytotoxicity on malignant cells, their effect on non-malignant cells such as immune cells in the TME may be less favorable.

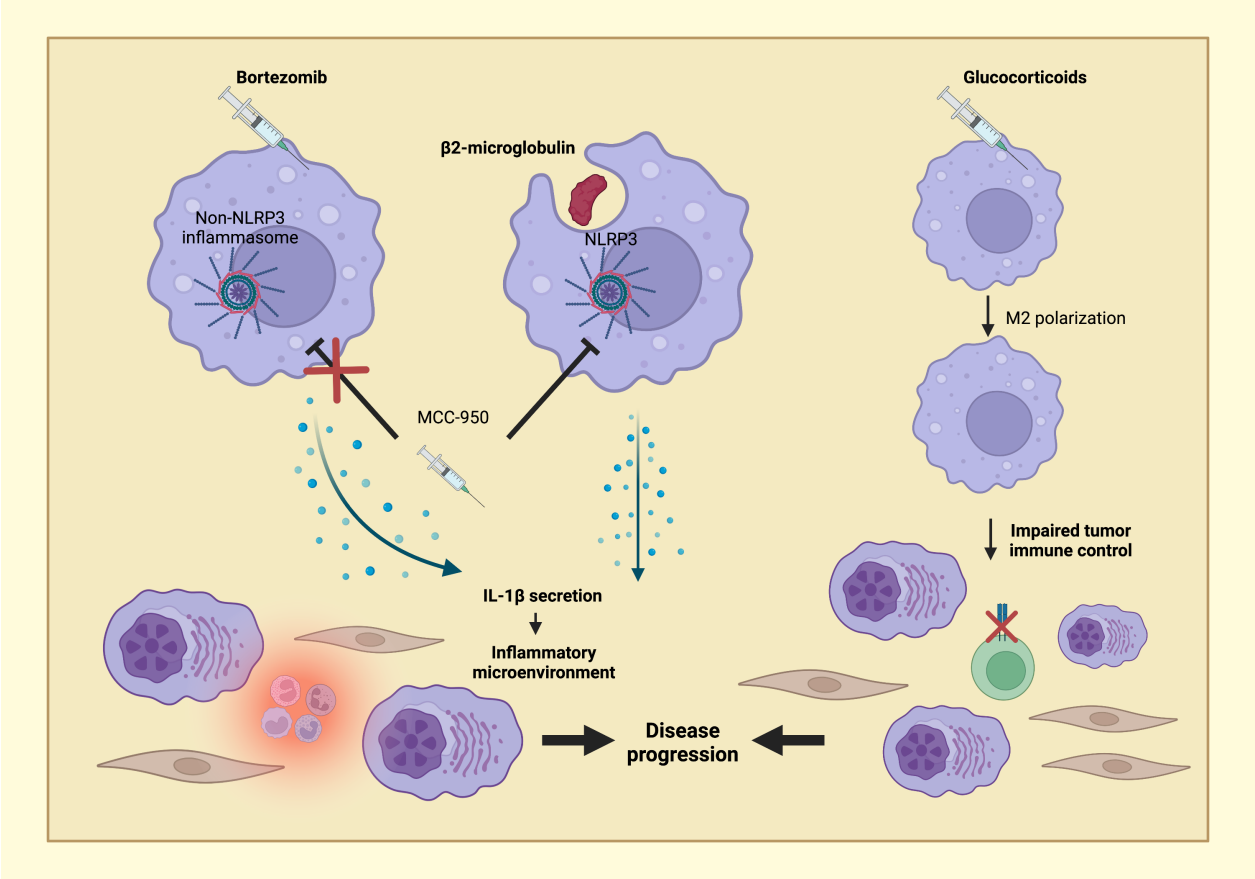

Figure 19: Potential influence of antineoplastic therapy in the multiple myeloma microenvironment
Both recognition of β_2-microglobulin and bortezomib treatment induce release of IL-1β from myeloid cells (Hofbauer et al., 2021). Only the β_2-microglobulin-mediated immune response is amenable to NLRP3 inhibition. Glucocorticoids promote anti-inflammatory macrophage polarization, potentially impairing tumor immune control by innate and adaptive immune cells.

Altogether, my study identifies NRLP3-independent inflammasome activation in primary human immune cells following proteasome inhibition. Possible future research axes include identification of the inflammasome receptor mediating BTZ-induced IL-1β release, and validation of these *in vitro* results in an *in vivo* model.

5. Synopsis

The impact of proteotoxic stress on innate immune activation is currently unclear. Here, I investigated differential effects of ER stress and proteasome inhibition using genetically modified cell lines and primary human cells.

ER stress, both through inhibition of lysosomal degradation using TN and through perturbations of calcium homeostasis using TPG, was found to induce a type-I IFN response in human cells. While ER stress-mediated secretion of CXCL-10, an IFN-inducible protein, was observed in the monocytic leukemia cell line THP-1, it was absent in HEK293T cells that do not express cGAS. In knockout cell lines generated using the CRISPR-Cas9 system, deficient in components of cytosolic DNA and RNA sensing, I observed that CXCL-10 release downstream of ER stress was mediated by cGAS, STING, and IRF3, but not by RIG-I and MAVS, in THP-1 cells. Similar results were obtained in cGAS-/- and STING -/- HT29 cells, a human colon adenocarcinoma cell line. These data indicate that ER stress mediates DNA rather than RNA recognition in the cytosol and led to hypothesize that endogenous DNA would serve as DAMP for cGAS activation in this model. Indeed, ER-stress mediated CXCL-10 secretion was absent in THP-1 cells after depletion of mtDNA (ρ0 THP-1 cells), whereas sensing of exogenously added DNA was intact. Presence of cytosolic DNA in ER stressor-exposed cells could be visualized using super-resolution microscopy. Moreover, mechanistically, the type-I IFN response to ER stress was shown to be dependent on the ATF6 branch of the UPR. Altogether, these findings support a model of ER stress-induced release of DNA from mitochondria mediated by ATF6, which then serves as a ligand for cGAS-STING pathway activation and leads to a type-I IFN response in human cells (see Figure 18). My results elucidate a previously undescribed mechanism for cGAS-dependent sensing of non-DNA innate immune stimuli in infection and in sterile inflammatory conditions, and these data are part of a larger manuscript demonstrating the activation of this pathway during DM2 (Günther et al., 2022).

Contrastingly, no type-I IFN response could be observed in cells treated with proteasome inhibitors such as BTZ. However, exposure to these agents led to IL-1β release in THP-1 cells and in human PBMC. BTZ-dependent IL-1β release in PBMC and BTZ-mediated cytotoxicity occurred at similar concentrations, indicating a potential role

for this phenomenon during MM treatment *in vivo*. The IL-1β response was abrogated in CASP1 -/- THP-1 cells, and ASC specking was observed following proteasome inhibition. Furthermore, IL-1β release was preserved, albeit significantly reduced, in NLRP3 -/- THP-1 cells, and treatment with the NLRP3 small molecule inhibitor MCC-950 did not significantly affect IL-1β levels in BTZ-treated PBMC. These results elucidate a currently undescribed mechanism of NLRP3-independent inflammasome activation through a small molecule.

In summary, the current study adds to the understanding of perturbations in protein turnover by defining two distinct mechanisms of innate immune activation by ER stress and inhibition of the proteasome. Results from this work may have implications for innate immune responses in infection, sterile inflammation, and cancer and warrant further investigation *in vivo*.

6. List of figures

Figure 1: Overview of intracellular nucleic acid recognition
Figure 2: Schematic overview of the unfolded protein response
Figure 3: Assessment of XBP1 splicing after Tunicamycin and Thapsigargin treatment in fibroblasts
Figure 4: IFNB1 and ISG expression following treatment of primary human cells with ER stressors
Figure 5: ER stressors induce CXCL-10 secretion as a surrogate for the type-I IFN response in THP-1 cells, but not in HEK293T cells or primary human cells
Figure 6: ER stress-induced CXCL-10 secretion is abrogated in THP-1 cells deficient in DNA, but not in RNA sensing
Figure 7: ER stress-induced CXCL-10 secretion is dependent on cGAS and STING in HT29 cells
Figure 8: ER stress-induced CXCL-10 secretion requires ATF6
Figure 9: ER stress-induced CXCL-10 secretion is abrogated in mtDNA-deficient ρ0 THP-1 cells
Figure 10: Super-resolution microscopy visualizes DNA release into the cytosol
Figure 11: Proteasome inhibitors induce IL-1β, but not CXCL-10 secretion
Figure 12: Dose-response curve of Bortezomib-induced IL-1β secretion in PBMC
Figure 13: Dose-response curve of Bortezomib-induced cell death in multiple myeloma cell lines
Figure 14: Bortezomib treatment induces formation of ASC specks
Figure 15: Genetic ablation of Caspase-1 abrogates Bortezomib-induced IL-1β secretion
Figure 16: Bortezomib-induced inflammasome activation is independent of NLRP3 in PBMC
Figure 17: NLRP3 -/- THP-1 cells show diminished IL-1β responses to proteasome inhibitors and transfected DNA
Figure 18: Release of mitochondrial DNA connects the unfolded protein response to nucleic acid sensing
Figure 19: Potential influence of antineoplastic therapy in the multiple myeloma microenvironment

7. List of tables

Table 1: Devices
Table 2: Software
Table 3: Consumables
Table 4: Cell Culture Plasticware
Table 5: Cell Culture Reagents
Table 6: Reagents for molecular biology experiments
Table 7: Materials for magnetic cell separation
Table 8: Chemicals
Table 9: Nucleic Acids
Table 10: Commercial Kits
Table 11: Antibodies used for imaging
Table 12: Primer Sequences for RT-PCR
Table 13: guideRNA sequences for CRISPR-mediated generation of knockout cell lines
Table 14: Genomic sequences of target loci in genetically edited cell lines

8. Bibliography

Ablasser, A., Hemmerling, I., Schmid-Burgk, J. L., Behrendt, R., Roers, A., & Hornung, V. TREX1 deficiency triggers cell-autonomous immunity in a cGAS-dependent manner. J Immunol 2014; 192: 5993–5997. http://doi.org/10.4049/jimmunol.1400737

Aguirre, S., Luthra, P., Sanchez-Aparicio, M. T., Maestre, A. M., Patel, J., Lamothe, F., Fredericks, A. C., Tripathi, S., Zhu, T., Pintado-Silva, J., Webb, L. G., Bernal-Rubio, D., Solovyov, A., Greenbaum, B., Simon, V., Basler, C. F., Mulder, L. C., García-Sastre, A., & Fernandez-Sesma, A. Dengue virus NS2B protein targets cGAS for degradation and prevents mitochondrial DNA sensing during infection. Nat Microbiol 2017, 2: 17037–11. http://doi.org/10.1038/nmicrobiol.2017.37

Aguirre, S., Maestre, A. M., Pagni, S., Patel, J. R., Savage, T., Gutman, D., Maringer, K., Bernal-Rubio, D., Shabman, R. S., Simon, V., Rodriguez-Madoz, J. R., Mulder, L. C., Barber, G. N., & Fernandez-Sesma, A. DENV inhibits type I IFN production in infected cells by cleaving human STING. PLoS Pathog 2012; 8: e1002934. http://doi.org/10.1371/journal.ppat.1002934

Aicardi, J., & Goutières, F. A progressive familial encephalopathy in infancy with calcifications of the basal ganglia and chronic cerebrospinal fluid lymphocytosis. Ann Neurol 1984; 15: 49–54. http://doi.org/10.1002/ana.410150109

Andreeva, L., Hiller, B., Kostrewa, D., Lässig, C., de Oliveira Mann, C. C., Jan Drexler, D., Maiser, A., Gaidt, M., Leonhardt, H., Hornung, V., & Hopfner, K. P. cGAS senses long and HMGB/TFAM-bound U-turn DNA by forming protein-DNA ladders. Nature 2017; 549: 394–398. http://doi.org/10.1038/nature23890

Arbore, G., West, E. E., Spolski, R., Robertson, A. A. B., Klos, A., Rheinheimer, C., Dutow, P., Woodruff, T. M., Yu, Z. X., O'Neill, L. A., Coll, R. C., Sher, A., Leonard, W. J., Köhl, J., Monk, P., Cooper, M. A., Arno, M., Afzali, B., Lachmann, H. J., Cope, A .P., Mayer-Barber, K. D. & Kemper, C. T helper 1 immunity requires complement-driven

NLRP3 inflammasome activity in $CD4^+$ T cells. Science 2016; 352: aad1210. http://doi.org/10.1126/science.aad1210

Autissier, P., Soulas, C., Burdo, T. H., & Williams, K. C. Evaluation of a 12-color flow cytometry panel to study lymphocyte, monocyte, and dendritic cell subsets in humans. Cytometry 2010; 77: 410–419. http://doi.org/10.1002/cyto.a.20859

Auwerx, J. The human leukemia cell line, THP-1: a multifacetted model for the study of monocyte-macrophage differentiation. Experientia 1991; 47: 22–31. http://doi.org/10.1007/BF02041244

Balka, K. R., Louis, C., Saunders, T. L., Smith, A. M., Calleja, D. J., D'Silva, D. B., Moghaddas, F., Tailler, M., Lawlor, K. E., Zhan, Y., Burns, C. J., Wicks, I. P., Miner, J. J., Kile, B. T., Masters, S. L., & De Nardo, D. TBK1 and IKKε Act Redundantly to Mediate STING-Induced NF-κB Responses in Myeloid Cells. Cell Rep 2020; 31: 107492. http://doi.org/10.1016/j.celrep.2020.03.056

Bartok, E., & Hartmann, G. Immune Sensing Mechanisms that Discriminate Self from Altered Self and Foreign Nucleic Acids. Immunity 2020; 53: 54–77. http://doi.org/10.1016/j.immuni.2020.06.014

Bauernfried, S., Scherr, M. J., Pichlmair, A., Duderstadt, K. E., & Hornung, V. Human NLRP1 is a sensor for double-stranded RNA. Science 2020; 371: eabd0811. http://doi.org/10.1126/science.abd0811

Beider, K., Bitner, H., Leiba, M., Gutwein, O., Koren-Michowitz, M., Ostrovsky, O., Abraham, M., Wald, H., Galun, E., Peled, A., & Nagler, A. Multiple myeloma cells recruit tumor-supportive macrophages through the CXCR4/CXCL12 axis and promote their polarization toward the M2 phenotype. Oncotarget 2014; 5: 11283–11296. http://doi.org/10.18632/oncotarget.2207

Bettigole, S. E., & Glimcher, L. H. Endoplasmic reticulum stress in immunity. Annu Rev Immuno 2015; 33: 107–138. http://doi.org/10.1146/annurev-immunol-032414-112116

Beyar-Katz, O., Magidey, K., Reiner-Benaim, A., Barak, N., Avivi, I., Cohen, Y., Timaner, M., Avraham, S., Hayun, M., Lavi, N., Bersudsky, M., Voronov, E., Apte, R. N., & Shaked, Y. Bortezomib-induced pro-inflammatory macrophages as a potential factor limiting anti-tumour efficacy. J Pathol 2016; 239: 262–273. http://doi.org/10.1002/path.4723

Beyar-Katz, O., Magidey, K., Reiner-Benaim, A., Barak, N., Avivi, I., Cohen, Y., Timaner, M., Avraham, S., Hayun, M., Lavi, N., Bersudsky, M., Voronov, E., Apte, R. N., & Shaked, Y. Proinflammatory Macrophages Promote Multiple Myeloma Resistance to Bortezomib Therapy. Mol Cancer Res 2019; 17: 2331–2340. http://doi.org/10.1158/1541-7786.MCR-19-0487

Brehm, A., Liu, Y., Sheikh, A., Marrero, B., Omoyinmi, E., Zhou, Q., Montealegre, G., Biancotto, A., Reinhardt, A., Almeida de Jesus, A., Pelletier, M., Tsai, WL., Remmers, E. F., Kardava, L., Hill, S., Kim, H., Lachmann, H. J., Megarbane, A., Chae, J. J., Brady, J., Castillo. R. D., Brown, D., Casano, A. V., Gao, L., Chapelle, D., Huang, Y., Stone, D., Chen, Y., Sotzny, F., Lee, C.C., Kastner, D. L., Torrelo, A., Zlotogorski, A., Moir, S., Gadina, M., McCoy, P., Wesley, R., Rother, K. I., Hildebrand, P. W., Brogan, P., Krüger, E., Aksentijevich, I., & Goldbach-Mansky, R. Additive loss-of-function proteasome subunit mutations in CANDLE/PRAAS patients promote type I IFN production. J Clin Invest 2015; 125: 4196–4211. http://doi.org/10.1172/JCI81260

Bronner, D. N., Abuaita, B. H., Chen, X., Fitzgerald, K. A., Nuñez, G., He, Y., Yin, X. M., & O'Riordan, M. X. Endoplasmic Reticulum Stress Activates the Inflammasome via NLRP3- and Caspase-2-Driven Mitochondrial Damage. Immunity 2015; 43: 451–462. http://doi.org/10.1016/j.immuni.2015.08.008

Brownell, J., Bruckner, J., Wagoner, J., Thomas, E., Loo, Y. M., Gale Jr, M., Liang, T. J., & Polyak, S. J.. Direct, interferon-independent activation of the CXCL10 promoter by NF-

κB and interferon regulatory factor 3 during hepatitis C virus infection. J Virol 2014; 88: 1582–1590. http://doi.org/10.1128/JVI.02007-13

Broz, P., & Dixit, V. M. Inflammasomes: mechanism of assembly, regulation and signalling. Nat Rev Immunol 2016, 16: 407–420. http://doi.org/10.1038/nri.2016.58

Burdette, D. L., Monroe, K. M., Sotelo-Troha, K., Iwig, J. S., Eckert, B., Hyodo, M., Hayakawa, Y., & Vance, R. E. STING is a direct innate immune sensor of cyclic di-GMP. Nature 2011; 478: 515–518. http://doi.org/10.1038/nature10429

Cai, X., Chen, J., Xu, H., Liu, S., Jiang, Q.-X., Halfmann, R., & Chen, Z. J. Prion-like polymerization underlies signal transduction in antiviral immune defense and inflammasome activation. Cell 2014; 156: 1207–1222. http://doi.org/10.1016/j.cell.2014.01.063

Caielli, S., Cardenas, J., de Jesus, A. A., Baisch, J., Walters, L., Blanck, J. P., Balasubramanian, P., Stagnar, C., Ohouo, M., Hong, S., Nassi, L., Stewart, K., Fuller, J., Gu, J., Banchereau, J. F., Wright, T., Goldbach-Mansky, R., & Pascual, V. Erythroid mitochondrial retention triggers myeloid-dependent type I interferon in human SLE. Cell 2021; 184: 4464–4479.e19. http://doi.org/10.1016/j.cell.2021.07.021

Chan, Y. K., & Gack, M. U. Viral evasion of intracellular DNA and RNA sensing. Nat Rev Microbiol 2016; 14: 360–373. http://doi.org/10.1038/nrmicro.2016.45

Christensen, M. H., & Paludan, S. R. Viral evasion of DNA-stimulated innate immune responses. Cell Mol Immunol 2017; 14: 4–13. http://doi.org/10.1038/cmi.2016.06

Civril, F., Deimling, T., de Oliveira Mann, C. C., Ablasser, A., Moldt, M., Witte, G., Hornung, V., & Hopfner, K. P. Structural mechanism of cytosolic DNA sensing by cGAS. Nature 2013; 498: 332–337. http://doi.org/10.1038/nature12305

Coll, R. C., Robertson, A. A., Chae, J. J., Higgins, S. C., Muñoz-Planillo, R., Inserra, M. C., Vetter, I., Dungan, L. S., Monks, B. G., Stutz, A., Croker, D. E., Butler, M. S., Haneklaus, M., Sutton, C. E., Núñez, G., Latz, E., Kastner, D. L., Mills, K. H., Masters, S. L., Schroder, K., Cooper, M.A., & O'Neill, L.A. A small-molecule inhibitor of the NLRP3 inflammasome for the treatment of inflammatory diseases. Nat Med 2015; 21: 248–255. http://doi.org/10.1038/nm.3806

Cooper, G. S., Bynum, M. L. K., & Somers, E. C. Recent insights in the epidemiology of autoimmune diseases: improved prevalence estimates and understanding of clustering of diseases. J Autoimmun 2009; 33: 197–207. http://doi.org/10.1016/j.jaut.2009.09.008

Davidson, S., Yu, C. H., Steiner, A., Ebstein, F., Baker, P. J., Jarur-Chamy, V., Hrovat Schaale, K., Laohamonthonkul, P., Kong, K., Calleja, D. J., Harapas, C. R., Balka, K. R., Mitchell, J., Jackson, J. T., Geoghegan, N. D., Moghaddas, F., Rogers, K. L., Mayer-Barber, K. D., De Jesus, A. A., De Nardo, D., Kile, B.T., Sadler, A.J., Poli, M.C., Krüger, E., Goldbach-Mansky, R., & Masters, S. L. Protein kinase R is an innate immune sensor of proteotoxic stress via accumulation of cytoplasmic IL-24. Sci Immunol 2022; 7: eabi6763. http://doi.org/10.1126/sciimmunol.abi6763

de Almeida, L., Khare, S., Misharin, A. V., Patel, R., Ratsimandresey, R. A., Wallin, M. C., Perlman, H., Greaves, D. R., Hoffman, H. M., Dorfleutner, A., & Stehlik, C. The PYRIN Domain-only Protein POP1 Inhibits Inflammasome Assembly and Ameliorates Inflammatory Disease. Immunity 2015; 43: 264–276. http://doi.org/10.1016/j.immuni.2015.07.018

de Jesus, A. A., Canna, S. W., Liu, Y., & Goldbach-Mansky, R. Molecular mechanisms in genetically defined autoinflammatory diseases: disorders of amplified danger signaling. Annu Rev Immunol 2015; 33: 823–874. http://doi.org/10.1146/annurev-immunol-032414-112227

de Mingo Pulido, Á., Hänggi, K., Celias, D. P., Gardner, A., Li, J., Batista-Bittencourt, B., Mohamed, E., Trillo-Tinoco, J., Osunmakinde, O., Peña, R., Onimus, A., Kaisho, T.,

Kaufmann, J., McEachern, K., Soliman, H., Luca, V. C., Rodriguez, P. C., Yu, X., & Ruffell, B. The inhibitory receptor TIM-3 limits activation of the cGAS-STING pathway in intra-tumoral dendritic cells by suppressing extracellular DNA uptake. Immunity 2021; http://doi.org/10.1016/j.immuni.2021.04.019

Domizio, J. D., Gulen, M. F., Saidoune, F., Thacker, V. V., Yatim, A., Sharma, K., Nass, T., Guenova, E., Schaller, M., Conrad, C., Goepfert, C., de Leval, L., Garnier, C. V., Berezowska, S., Dubois, A., Gilliet, M., & Ablasser, A. The cGAS-STING pathway drives type I IFN immunopathology in COVID-19. Nature 2019; 603: 145–151. http://doi.org/10.1038/s41586-022-04421-w

Dunleavy, K., Pittaluga, S., Czuczman, M. S., Dave, S. S., Wright, G., Grant, N., Shovlin, M., Jaffe, E. S., Janik, J. E., Staudt, L. M., & Wilson, W. H. Differential efficacy of bortezomib plus chemotherapy within molecular subtypes of diffuse large B-cell lymphoma. Blood 2009; 113: 6069–6076. http://doi.org/10.1182/blood-2009-01-199679

Ebstein, F., Poli Harlowe, M. C., Studencka-Turski, M., & Krüger, E. Contribution of the Unfolded Protein Response (UPR) to the Pathogenesis of Proteasome-Associated Autoinflammatory Syndromes (PRAAS). Front Immunol 2019; 10: 2756. http://doi.org/10.3389/fimmu.2019.02756

Gabay, C., & Kushner, I. Acute-phase proteins and other systemic responses to inflammation. N Engl J Med 1999; 340: 448–454. http://doi.org/10.1056/NEJM199902113400607

Gack, M. U., Albrecht, R. A., Urano, T., Inn, K. S., Huang, I. C., Carnero, E., Farzan, M., Inoue, S., Jung, J. U., & García-Sastre, A. Influenza A virus NS1 targets the ubiquitin ligase TRIM25 to evade recognition by the host viral RNA sensor RIG-I. Cell Host Microbe 2009; 5: 439–449. http://doi.org/10.1016/j.chom.2009.04.006

Gack, M. U., Shin, Y. C., Joo, C. H., Urano, T., Liang, C., Sun, L., Takeuchi, O., Akira, S., Chen, Z., Inoue, S., & Jung, J. U. TRIM25 RING-finger E3 ubiquitin ligase is

essential for RIG-I-mediated antiviral activity. Nature 2007; 446: 916–920. http://doi.org/10.1038/nature05732

Gaidt, M. M., Ebert, T. S., Chauhan, D., Ramshorn, K., Pinci, F., Zuber, S., O'Duill, F., Schmid-Burgk, J. L., Hoss, F., Buhmann, R., Wittmann, G., Latz, E., Subklewe, M., & Hornung, V. The DNA Inflammasome in Human Myeloid Cells Is Initiated by a STING-Cell Death Program Upstream of NLRP3. Cell 2017; 171: 1110–1124.e18. http://doi.org/10.1016/j.cell.2017.09.039

Galluzzi, L. et al., for the Nomenclature Committee on Cell Death. Molecular mechanisms of cell death: recommendations of the Nomenclature Committee on Cell Death 2018. Cell Death Differ 2018; 25: 486–541. http://doi.org/10.1038/s41418-017-0012-4

Gao, P., Ascano, M., Wu, Y., Barchet, W., Gaffney, B. L., Zillinger, T., Serganov, A. A., Liu, Y., Jones, R. A., Hartmann, G., Tuschl, T., & Patel, D. J. Cyclic [G(2',5')pA(3“,5”)p] is the metazoan second messenger produced by DNA-activated cyclic GMP-AMP synthase. Cell 2013a; 153: 1094–1107. http://doi.org/10.1016/j.cell.2013.04.046

Gao, P., Ascano, M., Zillinger, T., Wang, W., Dai, P., Serganov, A. A., Gaffney, B. L., Shuman, S., Jones, R. A., Deng, L., Hartmann, G., Barchet, W., Tuschl, T., & Patel, D. J. Structure-function analysis of STING activation by c[G(2',5')pA(3“,5”)p] and targeting by antiviral DMXAA. Cell 2013b; 154: 748–762. http://doi.org/10.1016/j.cell.2013.07.023

García-Ortiz, A., Rodríguez-García, Y., Encinas, J., Maroto-Martín, E., Castellano, E., Teixidó, J., & Martinez-Lopez, J. The Role of Tumor Microenvironment in Multiple Myeloma Development and Progression. Cancers 2021; 13: 217. http://doi.org/10.3390/cancers13020217

Gehrke, N., Mertens, C., Zillinger, T., Wenzel, J., Bald, T., Zahn, S., Tüting, T., Hartmann, G., & Barchet, W. Oxidative damage of DNA confers resistance to cytosolic

nuclease TREX1 degradation and potentiates STING-dependent immune sensing. Immunity 2013; 39: 482–495. http://doi.org/10.1016/j.immuni.2013.08.004

Ghiringhelli, F., Apetoh, L., Tesniere, A., Aymeric, L., Ma, Y., Ortiz, C., Vermaelen, K., Panaretakis, T., Mignot, G., Ullrich, E., Perfettini, J. L., Schlemmer, F., Tasdemir, E., Uhl, M., Génin, P., Civas, A., Ryffel, B., Kanellopoulos, J., Tschopp, J., André, F., Lidereau R., McLaughlin, N. M., Haynes, N. M., Smyth, M. J., Kroemer, G., & Zitvogel, L. Activation of the NLRP3 inflammasome in dendritic cells induces IL-1beta-dependent adaptive immunity against tumors. Nat Med 2009; 15: 1170–1178. http://doi.org/10.1038/nm.2028

Glickman, M. H., & Ciechanover, A. The ubiquitin-proteasome proteolytic pathway: destruction for the sake of construction. Physiol Rev 2002; 82: 373–428. http://doi.org/10.1152/physrev.00027.2001

Goldbach-Mansky, R., Dailey, N. J., Canna, S. W., Gelabert, A., Jones, J., Rubin, B. I., Kim, H. J., Brewer, C., Zalewski, C., Wiggs, E., Hill, S., Turner, M. L., Karp, B. I., Aksentijevich, I., Pucino, F., Penzak, S. R., Haverkamp, M. H., Stein, L., Adams, B. S., Moore, T. L., Fuhlbrigge, R. C., Shaham, B., Jarvis, J. N., O'Neil, K., Vehe, R. K., Beitz, L. O., Gardner, G., Hannan, W. P., Warren, R. W., Horn, W., Cole, J. L., Paul, S. M., Hawkins, P. N., Pham, T. H., Snyder, C., Wesley, R. A., Hoffmann, S. C., Holland, S. M., Butman, J. A., & Kastner, D. L. Neonatal-onset multisystem inflammatory disease responsive to interleukin-1beta inhibition. N Engl J Med 2006; 355: 581–592. http://doi.org/10.1056/NEJMoa055137

Goldberg, A. L., & Rock, K. L. Proteolysis, proteasomes and antigen presentation. Nature 1992; 357:, 375–379. http://doi.org/10.1038/357375a0

Greten, F. R., & Grivennikov, S. I. Inflammation and Cancer: Triggers, Mechanisms, and Consequences. Immunity 2019; 51: 27–41. http://doi.org/10.1016/j.immuni.2019.06.025

Gritsenko, A., Yu, S., Martin-Sanchez, F., Diaz-Del-Olmo, I., Nichols, E. M., Davis, D. M., Brough, D., & Lopez-Castejon, G. Priming Is Dispensable for NLRP3 Inflammasome Activation in Human Monocytes In Vitro. Front Immunol 2020; 11: 565924. http://doi.org/10.3389/fimmu.2020.565924

Gui, X., Yang, H., Li, T., Tan, X., Shi, P., Li, M., Du, F., & Chen, Z. J. Autophagy induction via STING trafficking is a primordial function of the cGAS pathway. Nature 2019; 567: 262–266. http://doi.org/10.1038/s41586-019-1006-9

Günther, C., Rösing, S., Ullrich, F., Meisterfeld, S., Schmidt, S., Eberl, N., Wegner, J., Schlee, M., Wieland, A., Hilbig, D., Reuner, U., Mirtschink, P., Drukewitz, S., Rapp, A., Zillinger, T., Beissert, S., Paeschke, K., Hartmann, G., & Bartok, E. Chronic ER stress promotes cGAS/mtDNA-induced autoimmunity via ATF6 in myotonic dystrophy type 2. Res Sq 2022; http://doi.org/10.21203/rs.3.rs-1784722/v1

Haag, S. M., Gulen, M. F., Reymond, L., Gibelin, A., Abrami, L., Decout, A., Heymann, M., van der Goot, F. G., Turcatti, G., Behrendt, R., & Ablasser, A. Targeting STING with covalent small-molecule inhibitors. Nature 2018; 559: 269–273. http://doi.org/10.1038/s41586-018-0287-8

Hartmann, G. Nucleic Acid Immunity. Adv Immunol 2017; 133: 121–169. http://doi.org/10.1016/bs.ai.2016.11.001

Haze, K., Yoshida, H., Yanagi, H., Yura, T., & Mori, K. Mammalian transcription factor ATF6 is synthesized as a transmembrane protein and activated by proteolysis in response to endoplasmic reticulum stress. Mol Biol Cell 1999; 10: 3787–3799. http://doi.org/10.1091/mbc.10.11.3787

Heinemeyer, W., Ramos, P. C., & Dohmen, R. J. The ultimate nanoscale mincer: assembly, structure and active sites of the 20S proteasome core. Cell Mol Life Sci 2004; 61: 1562–1578. http://doi.org/10.1007/s00018-004-4130-z

Heinz, L. X., Lee, J., Kapoor, U., Kartnig, F., Sedlyarov, V., Papakostas, K., César-Razquin, A., Essletzbichler, P., Goldmann, U., Stefanovic, A., Bigenzahn, J. W., Scorzoni, S., Pizzagalli, M. D., Bensimon, A., Müller, A. C., King, F. J., Li, J., Girardi, E., Mbow, M. L., Whitehurst, C. E., Rebasmen, M., & Superti-Furga, G. TASL is the SLC15A4-associated adaptor for IRF5 activation by TLR7-9. Nature 2020; 581: 316–322. http://doi.org/10.1038/s41586-020-2282-0

Hemmi, H., Takeuchi, O., Kawai, T., Kaisho, T., Sato, S., Sanjo, H., Matsumoto, M., Hoshino, K., Wagner, H., Takeda, K., & Akira, S. A Toll-like receptor recognizes bacterial DNA. Nature 2000; 408: 740–745. http://doi.org/10.1038/35047123

Hetz, C. The unfolded protein response: controlling cell fate decisions under ER stress and beyond. Nat Rev Mol Cell Biol 2012; 13: 89–102. http://doi.org/10.1038/nrm3270

Hideshima, T., Ikeda, H., Chauhan, D., Okawa, Y., Raje, N., Podar, K., Mitsiades, C., Munshi, N. C., Richardson, P. G., Carrasco, R. D., & Anderson, K. C. Bortezomib induces canonical nuclear factor-kappaB activation in multiple myeloma cells. Blood 2009; 114: 1046–1052. http://doi.org/10.1182/blood-2009-01-199604

Hofbauer, D., Mougiakakos, D., Broggini, L., Zaiss, M., Büttner-Herold, M., Bach, C., Spriewald, B., Neumann, F., Bisht, S., Nolting, J., Zeiser, R., Hamarsheh, S., Eberhardt, M., Vera, J., Visentin, C., De Luca, C. M. G., Moda, F., Haskamp, S., Flamann, C., Böttcher, M., Bitterer, K., Völkl, S., Mackensen, A., Ricagno, S., & Bruns, H. β2-microglobulin triggers NLRP3 inflammasome activation in tumor-associated macrophages to promote multiple myeloma progression. Immunity 2021; 54: 1772–1787.e9. http://doi.org/10.1016/j.immuni.2021.07.002

Hornung, V., Ablasser, A., Charrel-Dennis, M., Bauernfeind, F., Horvath, G., Caffrey, D. R., Latz, E., & Fitzgerald, K. A. AIM2 recognizes cytosolic dsDNA and forms a caspase-1-activating inflammasome with ASC. Nature 2009; 458: 514–518. http://doi.org/10.1038/nature07725

Hornung, V., Ellegast, J., Kim, S., Brzózka, K., Jung, A., Kato, H., Poeck, H., Akira, S., Conzelmann, K. K., Schlee, M., Endres, S., & Hartmann, G. 5'-Triphosphate RNA is the ligand for RIG-I. Science 2006; 314: 994–997. http://doi.org/10.1126/science.1132505

Hou, F., Sun, L., Zheng, H., Skaug, B., Jiang, Q.-X., & Chen, Z. J. MAVS forms functional prion-like aggregates to activate and propagate antiviral innate immune response. Cell 2011; 146: 448–461. http://doi.org/10.1016/j.cell.2011.06.041

Huang, L. S., Hong, Z., Wu, W., Xiong, S., Zhong, M., Gao, X., Rehman, J., & Malik, A. B. mtDNA Activates cGAS Signaling and Suppresses the YAP-Mediated Endothelial Cell Proliferation Program to Promote Inflammatory Injury. Immunity 2020; 52: 475–486.e5. http://doi.org/10.1016/j.immuni.2020.02.002

Ivashkiv, L. B., & Donlin, L. T. Regulation of type I interferon responses. Nat Rev Immunol 2014; 14: 36–49. http://doi.org/10.1038/nri3581

Iwasaki, A., & Medzhitov, R. Control of adaptive immunity by the innate immune system. Nat Immunol 2015; 16: 343–353. http://doi.org/10.1038/ni.3123

Janeway, C. A. Approaching the asymptote? Evolution and revolution in immunology. Cold Spring Harb Symp Quant Biol 1989; 54: 1–13. http://doi.org/10.1101/sqb.1989.054.01.003

Kayagaki, N., Warming, S., Lamkanfi, M., Vande Walle, L., Louie, S., Dong, J., Newton, K., Qu, Y., Liu, J., Heldens, S., Zhang, J., Lee, W. P., Roose-Girma, M., & Dixit, V. M. Non-canonical inflammasome activation targets caspase-11. Nature 2011; 479: 117–121. http://doi.org/10.1038/nature10558

Kisselev, A. F., & Goldberg, A. L. Proteasome inhibitors: from research tools to drug candidates. Chem Biol 2001; 8: 739–758. http://doi.org/10.1016/s1074-5521(01)00056-4

Koreth, J., Stevenson, K. E., Kim, H. T., McDonough, S. M., Bindra, B., Armand, P., Ho, V. T., Cutler, C., Blazar, B. R., Antin, J. H., Soiffer, R. J., Ritz, J., & Alyea, E. P., 3rd. Bortezomib-based graft-versus-host disease prophylaxis in HLA-mismatched unrelated donor transplantation. J Clin Oncol 2012; 30: 3202–3208. http://doi.org/10.1200/JCO.2012.42.0984

Kothur, K., Bandodkar, S., Chu, S., Wienholt, L., Johnson, A., Barclay, P., Brogan, P. A., Rice, G. I., Crow, Y. J., & Dale, R. C. An open-label trial of JAK 1/2 blockade in progressive IFIH1-associated neuroinflammation. Neurology 2018; 90: 289–291. http://doi.org/10.1212/WNL.0000000000004921

Kuemmerle-Deschner, J. B. CAPS-pathogenesis, presentation and treatment of an autoinflammatory disease. Sem Immunopathol 2015; 37: 377–385. http://doi.org/10.1007/s00281-015-0491-7

Lama, L., Adura, C., Xie, W., Tomita, D., Kamei, T., Kuryavyi, V., Gogakos, T., Steinberg, J. I., Miller, M., Ramos-Espiritu, L., Asano, Y., Hashizume, S., Aida, J., Imaeda, T., Okamoto, R., Jennings, A. J., Michino, M., Kuroita, T., Stamford, A., Gao, P., Meinke, P., Glickman, J. F., Patel, D. J., & Tuschl, T. Development of human cGAS-specific small-molecule inhibitors for repression of dsDNA-triggered interferon expression. Nat Comm 2019; 10: 2261–14. http://doi.org/10.1038/s41467-019-08620-4

Lamkanfi, M., & Dixit, V. M. Mechanisms and functions of inflammasomes. Cell 2014; 157: 1013–1022. http://doi.org/10.1016/j.cell.2014.04.007

Lauring, J., Abukhdeir, A. M., Konishi, H., Garay, J. P., Gustin, J. P., Wang, Q., Arceci, R. J., Matsui, W., & Park, B. H. The multiple myeloma associated MMSET gene contributes to cellular adhesion, clonogenic growth, and tumorigenicity. Blood 2008; 111: 856–864. http://doi.org/10.1182/blood-2007-05-088674

Lee-Kirsch, M. A. The Type I Interferonopathies. Annu Rev Med 2017; 68: 297–315. http://doi.org/10.1146/annurev-med-050715-104506

Liu, S., Cai, X., Wu, J., Cong, Q., Chen, X., Li, T., Du, F., Ren, J., Wu, Y. T., Grishin, N. V., & Chen, Z. J. Phosphorylation of innate immune adaptor proteins MAVS, STING, and TRIF induces IRF3 activation. Science 2015; 347: aaa2630–aaa2630. http://doi.org/10.1126/science.aaa2630

Liu, Y., de Jesus, A.A., Marrero, B., Yang, D., Ramsey, S.E., Sanchez, G.A.M., Tenbrock, K., Wittkowski, H., Jones, O.Y., Kuehn, H.S., Lee, C.R., DiMattia, M.A., Cowen, E.W., Gonzalez, B., Palmer, I., DiGiovanna, J. J., Biancotto, A., Kim, H., Tsai, W. L., Trier, A. M., Huang, Y., Stone, D. L., Hill, S., Kim, H. J., St Hilaire, C., Gurprasad, S., Plass, N., Chapelle, D., Horkayne-Szakaly, I., Foell, D., Barysenka, A., Candotti, F., Holland, S. M., Hughes, J. D., Mehmet, H., Issekutz, A. C., Raffeld, M., McElwee, J., Fontana, J. R., Minniti, C. P., Moir, S., Kastner, D. L., Gadina, M., Steven, A. C., Wingfield, P. T., Brooks, S. R., Rosenzweig, S. D., Fleisher, T. A., Deng, Z., Boehm, M., Paller, A. S., & Goldbach-Mansky, R. Activated STING in a vascular and pulmonary syndrome. N Engl J Med 2014; 371: 507–518. http://doi.org/10.1056/NEJMoa1312625

Liu, Y. P., Zeng, L., Tian, A., Bomkamp, A., Rivera, D., Gutman, D., Barber, G. N., Olson, J. K., & Smith, J. A. Endoplasmic reticulum stress regulates the innate immunity critical transcription factor IRF3. J Immunol 2012; 189: 4630–4639. http://doi.org/10.4049/jimmunol.1102737

Luckheeram, R. V., Zhou, R., Verma, A. D., & Xia, B. $CD4^+$T cells: differentiation and functions. Clin Dev Immunol 2012; 925135. http://doi.org/10.1155/2012/925135

Lust, J. A., Lacy, M. Q., Zeldenrust, S. R., Witzig, T. E., Moon-Tasson, L. L., Dinarello, C. A., & Donovan, K. A. Reduction in C-reactive protein indicates successful targeting of the IL-1/IL-6 axis resulting in improved survival in early stage multiple myeloma. Am J Hematol 2016; 91: 571–574. http://doi.org/10.1002/ajh.24352

Margolis, S. R., Wilson, S. C., & Vance, R. E. Evolutionary Origins of cGAS-STING Signaling. Trends Immunol 2017; 38: 733–743. http://doi.org/10.1016/j.it.2017.03.004

Martinon, F., Chen, X., Lee, A.-H., & Glimcher, L. H. TLR activation of the transcription factor XBP1 regulates innate immune responses in macrophages. Nat Immunol 2010; 11: 411–418. http://doi.org/10.1038/ni.1857

McDermott, M. F., Aksentijevich, I., Galon, J., McDermott, E. M., Ogunkolade, B. W., Centola, M., Mansfield, E., Gadina, M., Karenko, L., Pettersson, T., McCarthy, J., Frucht, D. M., Aringer, M., Torosyan, Y., Teppo, A. M., Wilson, M., Karaarslan, H. M., Wan, Y., Todd, I., Wood, G., Schlimgen, R., Kumarajeewa, T. R., Cooper, S. M., Vella, J. P., Amos, C. I., Mulley, J., Quane, K. A., Molloy, M. G., Ranki, A., Powell, R. J., Hitman, G. A., O'Shea, J. J., & Kastner, D. L. Germline mutations in the extracellular domains of the 55 kDa TNF receptor, TNFR1, define a family of dominantly inherited autoinflammatory syndromes. Cell 1999; 97: 133–144. http://doi.org/10.1016/s0092-8674(00)80721-7

Medzhitov, R. Origin and physiological roles of inflammation. Nature 2008; 454: 428–435. http://doi.org/10.1038/nature07201

Medzhitov, R., & Janeway, C. Innate immunity. N Engl J Med 2020; 343: 338–344. http://doi.org/10.1056/NEJM200008033430506

Menu, P., Mayor, A., Zhou, R., Tardivel, A., Ichijo, H., Mori, K., & Tschopp, J. ER stress activates the NLRP3 inflammasome via an UPR-independent pathway. Cell Death Dis 2012; 3: e261–e261. http://doi.org/10.1038/cddis.2011.132

Michalski, S., de Oliveira Mann, C. C., Stafford, C. A., Witte, G., Bartho, J., Lammens, K., Hornung, V., & Hopfner, K. P. Structural basis for sequestration and autoinhibition of cGAS by chromatin. Nature 2020; 587: 678–682. http://doi.org/10.1038/s41586-020-2748-0

Miltenyi, S., Müller, W., Weichel, W., & Radbruch, A. High gradient magnetic cell separation with MACS. Cytometry 1990; 11: 231–238. http://doi.org/10.1002/cyto.990110203

Moreau, P., for the CASSIOPEIA investigators. Bortezomib, thalidomide, and dexamethasone with or without daratumumab before and after autologous stem-cell transplantation for newly diagnosed multiple myeloma (CASSIOPEIA): a randomised, open-label, phase 3 study. Lancet 2019; 394: 29–38. http://doi.org/10.1016/S0140-6736(19)31240-1

Mouchess, M. L., Arpaia, N., Souza, G., Barbalat, R., Ewald, S. E., Lau, L., & Barton, G. M. Transmembrane mutations in Toll-like receptor 9 bypass the requirement for ectodomain proteolysis and induce fatal inflammation. Immunity 2011; 35: 721–732. http://doi.org/10.1016/j.immuni.2011.10.009

Muñoz-Planillo, R., Kuffa, P., Martínez-Colón, G., Smith, B. L., Rajendiran, T. M., & Núñez, G. K^+ efflux is the common trigger of NLRP3 inflammasome activation by bacterial toxins and particulate matter. Immunity 2013; 38: 1142–1153. http://doi.org/10.1016/j.immuni.2013.05.016

Murata, S., Yashiroda, H., & Tanaka, K. Molecular mechanisms of proteasome assembly. Nat Rev Mol Cell Biology 2009; 10: 104–115. http://doi.org/10.1038/nrm2630

Murphy, K., & Weaver, C. (eds.). Janeway Immunologie (9. Auflage 2018), 1–1227.

Nakamura, K., Kassem, S., Cleynen, A., Chrétien, M. L., Guillerey, C., Putz, E. M., Bald, T., Förster, I., Vuckovic, S., Hill, G. R., Masters, S. L., Chesi, M., Bergsagel, P. L., Avet-Loiseau, H., Martinet, L., & Smyth, M. J. Dysregulated IL-18 Is a Key Driver of Immunosuppression and a Possible Therapeutic Target in the Multiple Myeloma Microenvironment. Cancer Cell 2018; 33: 634–648.e5. http://doi.org/10.1016/j.ccell.2018.02.007

Netea, M. G., Joosten, L. A., Latz, E., Mills, K. H., Natoli, G., Stunnenberg, H. G., O'Neill, L. A., & Xavier, R. J. Trained immunity: A program of innate immune memory in

health and disease. Science 2016; 352: aaf1098–aaf1098. http://doi.org/10.1126/science.aaf1098

Newton, K., & Dixit, V. M. Signaling in innate immunity and inflammation. Cold Spring Harb Perspect Biol 2012; 4: a006049–a006049. http://doi.org/10.1101/cshperspect.a006049

Ni, G., Ma, Z., & Damania, B. cGAS and STING: At the intersection of DNA and RNA virus-sensing networks. PLoS Pathog 2018; 14: e1007148. http://doi.org/10.1371/journal.ppat.1007148

Olivares-Morales, M. J., De La Fuente, M. K., Dubois-Camacho, K., Parada, D., Diaz-Jiménez, D., Torres-Riquelme, A., Xu, X., Chamorro-Veloso, N., Naves, R., Gonzalez, M. J., Quera, R., Figueroa, C., Cidlowski, J. A., Vidal, R. M., & Hermoso, M. A. Glucocorticoids Impair Phagocytosis and Inflammatory Response Against Crohn's Disease-Associated Adherent-Invasive Escherichia coli. Front Immunol 2018; 9: 1026. http://doi.org/10.3389/fimmu.2018.01026

Ostendorf, T., Zillinger, T., Andryka, K., Schlee-Guimaraes, T. M., Schmitz, S., Marx, S., Bayrak, K., Linke, R., Salgert, S., Wegner, J., Grasser, T., Bauersachs, S., Soltesz, L., Hübner, M. P., Nastaly, M., Coch, C., Kettwig, M., Roehl, I., Henneke, M., Hoerauf, A., Barchet, W., Gärtner, J., Schlee, M., Hartmann, G., & Bartok, E. Immune Sensing of Synthetic, Bacterial, and Protozoan RNA by Toll-like Receptor 8 Requires Coordinated Processing by RNase T2 and RNase 2. Immunity 2020; 52: 591–605.e6. http://doi.org/10.1016/j.immuni.2020.03.009

Pathare, G. R., Decout, A., Glück, S., Cavadini, S., Makasheva, K., Hovius, R., Kempf, G., Weiss, J., Kozicka, Z., Guey, B., Melenec, P., Fierz, B., Thomä, N. H., & Ablasser, A. Structural mechanism of cGAS inhibition by the nucleosome. Nature 2020; 587: 668–672. http://doi.org/10.1038/s41586-020-2750-6

Pellom, S. T., Dudimah, D. F., Thounaojam, M. C., Sayers, T. J., & Shanker, A. Modulatory effects of bortezomib on host immune cell functions. Immunotherapy 2015; 7: 1011–1022. http://doi.org/10.2217/imt.15.66

Rajkumar, S. V. Multiple myeloma: 2020 update on diagnosis, risk-stratification and management. Am J Hematol 2020; 95: 548–567. http://doi.org/10.1002/ajh.25791

Rapino, F., Robles, E. F., Richter-Larrea, J. A., Kallin, E. M., Martinez-Climent, J. A., & Graf, T. C/EBPα induces highly efficient macrophage transdifferentiation of B lymphoma and leukemia cell lines and impairs their tumorigenicity. Cell Rep 2013; 3: 1153–1163. http://doi.org/10.1016/j.celrep.2013.03.003

Reece, D. E., Sullivan, D., Lonial, S., Mohrbacher, A. F., Chatta, G., Shustik, C., Burris, H., 3rd, Venkatakrishnan, K., Neuwirth, R., Riordan, W. J., Karol, M., von Moltke, L. L., Acharya, M., Zannikos, P., & Keith Stewart, A. Pharmacokinetic and pharmacodynamic study of two doses of bortezomib in patients with relapsed multiple myeloma. Cancer Chemother Pharmacol 2011; 67: 57–67. http://doi.org/10.1007/s00280-010-1283-3

Reich, S., Nguyen, C. D. L., Has, C., Steltgens, S., Soni, H., Coman, C., Freyberg, M., Bichler, A., Seifert, N., Conrad, D., Knobbe-Thomsen, C. B., Tews, B., Toedt, G., Ahrends, R., & Medenbach, J. A multi-omics analysis reveals the unfolded protein response regulon and stress-induced resistance to folate-based antimetabolites. Nat Comm 2020; 11: 2936–15. http://doi.org/10.1038/s41467-020-16747-y

Reimold, A. M., Iwakoshi, N. N., Manis, J., Vallabhajosyula, P., Szomolanyi-Tsuda, E., Gravallese, E. M., Friend, D., Grusby, M. J., Alt, F., & Glimcher, L. H. Plasma cell differentiation requires the transcription factor XBP-1. Nature 2001; 412: 300–307. http://doi.org/10.1038/35085509

Rice, G. I., Meyzer, C., Bouazza, N., Hully, M., Boddaert, N., Semeraro, M., Zeef, L. A. H., Rozenberg, F., Bondet, V., Duffy, D., Llibre, A., Baek, J., Sambe, M. N., Henry, E., Jolaine, V., Barnerias, C., Barth, M., Belot, A., Cances, C., Debray, F. G., Doummar, D.,

Frémond, M. L., Kitabayashi, N., Lepelley, A., Levrat, V. , Melki, I., Meyer, P., Nougues, M. C., Renaldo, F., Rodero, M. P., Rodriguez, D., Roubertie, A., Seabra, L., Uggenti, C., Abdoul, H., Treluyer, J. M., Desguerre, I., Blanche, S., & Crow, Y. J. Reverse-Transcriptase Inhibitors in the Aicardi–Goutières Syndrome. N Engl J Med 2018; 379: 2275–2277. http://doi.org/10.1056/NEJMc1810983

Richardson, P. G., Barlogie, B., Berenson, J., Singhal, S., Jagannath, S., Irwin, D., Rajkumar, S. V., Srkalovic, G., Alsina, M., Alexanian, R., Siegel, D., Orlowski, R. Z., Kuter, D., Limentani, S. A., Lee, S., Hideshima, T., Esseltine, D. L., Kauffman, M., Adams, J., Schenkein, D. P., & Anderson, K. C. A phase 2 study of bortezomib in relapsed, refractory myeloma. N Engl J Med 2003, 348: 2609–2617. http://doi.org/10.1056/NEJMoa030288

Rock, K. L., Gramm, C., Rothstein, L., Clark, K., Stein, R., Dick, L., Hwang, D., & Goldberg, A. L. Inhibitors of the proteasome block the degradation of most cell proteins and the generation of peptides presented on MHC class I molecules. Cell 1994; 78: 761–771. http://doi.org/10.1016/s0092-8674(94)90462-6

Rodero, M. P., Tesser, A., Bartok, E., Rice, G. I., Della Mina, E., Depp, M., Beitz, B., Bondet, V., Cagnard, N., Duffy, D., Dussiot, M., Frémond, M. L., Gattorno, M., Guillem, F., Kitabayashi, N., Porcheray, F., Rieux-Laucat, F., Seabra, L., Uggenti, C., Volpi, S., Zeef, L. A. H., Alyanakian, M. A., Beltrand, J., Bianco, A. M. , Boddaert, N., Brouzes, C., Candon, S., Caorsi, R., Charbit, M., Fabre, M., Faletra, F., Girard, M., Harroche, A., Hartmann, E., Lasne, D., Marcuzzi, A., Neven, B., Nitschke, P., Pascreau, T., Pastore, S., Picard, C., Picco, P., Piscianz, E., Polak, M., Quartier, P., Rabant, M., Stocco, G., Taddio, A., Uettwiller, F., Valencic, E., Vozzi, D., Hartmann, G., Barchet, W., Hermine, O., Bader-Meunier, B., Tommasini, A., & Crow Y. J. Type I interferon-mediated autoinflammation due to DNase II deficiency. Nature Communications 2017; 8: 2176–15. http://doi.org/10.1038/s41467-017-01932-3

Rongvaux, A., Jackson, R., Harman, C. C., Li, T., West, A. P., de Zoete, M. R., Wu, Y., Yordy, B., Lakhani, S. A., Kuan, C. Y., Taniguchi, T., Shadel, G. S., Chen, Z. J., Iwasaki,

A., & Flavell, R. A. Apoptotic caspases prevent the induction of type I interferons by mitochondrial DNA. Cell 2014; 159: 1563–1577. http://doi.org/10.1016/j.cell.2014.11.037

Rosenblum, M. D., Remedios, K. A., & Abbas, A. K. Mechanisms of human autoimmunity. J Clin Invest 2015; 125: 2228–2233. http://doi.org/10.1172/JCI78088

Rust, M. J., Bates, M., & Zhuang, X. Sub-diffraction-limit imaging by stochastic optical reconstruction microscopy (STORM). Nat Methods 2006; 3: 793–795. http://doi.org/10.1038/nmeth929

San Miguel, J. F. for the VISTA investigators. Bortezomib plus melphalan and prednisone for initial treatment of multiple myeloma. N Engl J Med 2008; 359: 906–917. http://doi.org/10.1056/NEJMoa0801479

Sandstrom, A., Mitchell, P. S., Goers, L., Mu, E. W., Lesser, C. F., & Vance, R. E. Functional degradation: A mechanism of NLRP1 inflammasome activation by diverse pathogen enzymes. Science 2019; 364: eaau1330. http://doi.org/10.1126/science.aau1330

Schlee, M., Roth, A., Hornung, V., Hagmann, C. A., Wimmenauer, V., Barchet, W., Coch, C., Janke, M., Mihailovic, A., Wardle, G., Juranek, S., Kato, H., Kawai, T., Poeck, H., Fitzgerald, K. A., Takeuchi, O., Akira, S., Tuschl, T., Latz, E., Ludwig, J., & Hartmann, G. Recognition of 5' triphosphate by RIG-I helicase requires short blunt double-stranded RNA as contained in panhandle of negative-strand virus. Immunity 2009; 31: 25–34. http://doi.org/10.1016/j.immuni.2009.05.008

Schneider, W. M., Chevillotte, M. D., & Rice, C. M. Interferon-stimulated genes: a complex web of host defenses. Annu Rev Immunol 2014; 32: 513–545. http://doi.org/10.1146/annurev-immunol-032713-120231

Schoggins, J. W., Wilson, S. J., Panis, M., Murphy, M. Y., Jones, C. T., Bieniasz, P., & Rice, C. M. A diverse range of gene products are effectors of the type I interferon antiviral response. Nature 2011; 472: 481–485. http://doi.org/10.1038/nature09907

Schuberth-Wagner, C., Ludwig, J., Bruder, A. K., Herzner, A. M., Zillinger, T., Goldeck, M., Schmidt, T., Schmid-Burgk, J. L., Kerber, R., Wolter, S., Stümpel, J. P., Roth, A., Bartok, E., Drosten, C., Coch, C., Hornung, V., Barchet, W., Kümmerer, B. M., Hartmann, G., & Schlee, M. A Conserved Histidine in the RNA Sensor RIG-I Controls Immune Tolerance to N1-2'O-Methylated Self RNA. Immunity 2015; 43: 41–51. http://doi.org/10.1016/j.immuni.2015.06.015

Sen, T., Saha, P., Gupta, R., Foley, L. M., Jiang, T., Abakumova, O. S., Hitchens, T. K., & Sen, N. Aberrant ER Stress Induced Neuronal-IFNβ Elicits White Matter Injury Due to Microglial Activation and T-Cell Infiltration after TBI. J Neurosci 2020; 40: 424–446. http://doi.org/10.1523/JNEUROSCI.0718-19.2019

Shi, J., Zhao, Y., Wang, K., Shi, X., Wang, Y., Huang, H., Zhuang, Y., Cai, T., Wang, F., & Shao, F. Cleavage of GSDMD by inflammatory caspases determines pyroptotic cell death. Nature 2015; 526: 660–665. http://doi.org/10.1038/nature15514

Siomi, H., & Siomi, M. C. On the road to reading the RNA-interference code. Nature 2009; 457: 396–404. http://doi.org/10.1038/nature07754

Smith, J. A. A new paradigm: innate immune sensing of viruses via the unfolded protein response. Front Microbiol 2014; 5: 222. http://doi.org/10.3389/fmicb.2014.00222

Smith, J. A., Turner, M. J., DeLay, M. L., Klenk, E. I., Sowders, D. P., & Colbert, R. A. Endoplasmic reticulum stress and the unfolded protein response are linked to synergistic IFN-beta induction via X-box binding protein 1. Eur J Immunol 2008; 38: 1194–1203. http://doi.org/10.1002/eji.200737882

Stetson, D. B., & Medzhitov, R. Recognition of cytosolic DNA activates an IRF3-dependent innate immune response. Immunity 2006a, 24: 93–103. http://doi.org/10.1016/j.immuni.2005.12.003

Stetson, D. B., & Medzhitov, R. Type I interferons in host defense. Immunity 2006b; 25: 373–381. http://doi.org/10.1016/j.immuni.2006.08.007

Stewart, A. K., for the ASPIRE investigators. Carfilzomib, lenalidomide, and dexamethasone for relapsed multiple myeloma. N Engl J Med 2015; 372: 142–152. http://doi.org/10.1056/NEJMoa1411321

Stutz, A., Horvath, G. L., Monks, B. G., & Latz, E. ASC speck formation as a readout for inflammasome activation. Methods Mol Biol 2013; 1040: 91–101. http://doi.org/10.1007/978-1-62703-523-1_8

Sun, B., Sundström, K. B., Chew, J. J., Bist, P., Gan, E. S., Tan, H. C., Goh, K. C., Chawla, T., Tang, C. K., & Ooi, E. E. Dengue virus activates cGAS through the release of mitochondrial DNA. Sci Rep 2017; 7: 3594–8. http://doi.org/10.1038/s41598-017-03932-1

Sun, L., Wu, J., Du, F., Chen, X., & Chen, Z. J. Cyclic GMP-AMP synthase is a cytosolic DNA sensor that activates the type I interferon pathway. Science 2013; 339: 786–791. http://doi.org/10.1126/science.1232458

Tang, A. C., Rahavi, S. M., Fung, S. Y., Lu, H. Y., Yang, H., Lim, C. J., Reid, G. S., & Turvey, S. E. Combination therapy with proteasome inhibitors and TLR agonists enhances tumour cell death and IL-1β production. Cell Death Dis 2018; 9: 162–13. http://doi.org/10.1038/s41419-017-0194-1

Teicher, B. A., & Tomaszewski, J. E. Proteasome inhibitors. Biochem Pharmacol 2015; 96: 1–9. http://doi.org/10.1016/j.bcp.2015.04.008

Terns, M. P., & Terns, R. M. CRISPR-based adaptive immune systems. Curr Opin Microbiol 2011; 14: 321–327. http://doi.org/10.1016/j.mib.2011.03.005

Thornberry, N. A., Bull, H. G., Calaycay, J. R., Chapman, K. T., Howard, A. D., Kostura, M. J., Miller, D. K., Molineaux, S. M., Weidner, J. R., & Aunins, J. A novel heterodimeric cysteine protease is required for interleukin-1 beta processing in monocytes. Nature 1992; 356: 768–774. http://doi.org/10.1038/356768a0

Thuerauf, D. J., Marcinko, M., Belmont, P. J., & Glembotski, C. C. Effects of the isoform-specific characteristics of ATF6 alpha and ATF6 beta on endoplasmic reticulum stress response gene expression and cell viability. J Biol Chem 2007; 282: 22865–22878. http://doi.org/10.1074/jbc.M701213200

Tieleman, A. A., Broeder, den, A. A., van de Logt, A.-E., & van Engelen, B. G. M. Strong association between myotonic dystrophy type 2 and autoimmune diseases. J Neurol Neurosurg Psychiatry 2009; 80: 1293–1295. http://doi.org/10.1136/jnnp.2008.156562

Trudel, S., Ely, S., Farooqi, Y., Affer, M., Robbiani, D. F., Chesi, M., & Bergsagel, P. L. Inhibition of fibroblast growth factor receptor 3 induces differentiation and apoptosis in t(4;14) myeloma. Blood 2004; 103: 3521–3528. http://doi.org/10.1182/blood-2003-10-3650

Tsaytler, P., Harding, H. P., Ron, D., & Bertolotti, A. Selective inhibition of a regulatory subunit of protein phosphatase 1 restores proteostasis. Science 2011; 332: 91–94. http://doi.org/10.1126/science.1201396

van Galen, P., Kreso, A., Mbong, N., Kent, D. G., Fitzmaurice, T., Chambers, J. E., Xie, S., Laurenti, E., Hermans, K., Eppert, K., Marciniak, S. J., Goodall, J. C., Green, A. R., Wouters, B. G., Wienholds, E., & Dick, J. E. The unfolded protein response governs integrity of the haematopoietic stem-cell pool during stress. Nature 2014; 510: 268–272. http://doi.org/10.1038/nature13228

van Schadewijk, A., van't Wout, E. F. A., Stolk, J., & Hiemstra, P. S. A quantitative method for detection of spliced X-box binding protein-1 (XBP1) mRNA as a measure of endoplasmic reticulum (ER) stress. Cell Stress Chaperones 2012; 17: 275–279. http://doi.org/10.1007/s12192-011-0306-2

Walter, P., & Ron, D. The unfolded protein response: from stress pathway to homeostatic regulation. Science 2011; 334: 1081–1086. http://doi.org/10.1126/science.1209038

West, A. P. Mitochondrial dysfunction as a trigger of innate immune responses and inflammation. Toxicology 2017; 391: 54–63. http://doi.org/10.1016/j.tox.2017.07.016

West, A. P., & Shadel, G. S. Mitochondrial DNA in innate immune responses and inflammatory pathology. Nat Rev Immunol 2017; 17: 363–375. http://doi.org/10.1038/nri.2017.21

West, A. P., Khoury-Hanold, W., Staron, M., Tal, M. C., Pineda, C. M., Lang, S. M., Bestwick, M., Duguay, B. A., Raimundo, N., MacDuff, D. A., Kaech, S. M., Smiley, J. R., Means, R. E., Iwasaki, A., & Shadel, G. S. Mitochondrial DNA stress primes the antiviral innate immune response. Nature 2015; 520: 553–557. http://doi.org/10.1038/nature14156

Westermann, L., Li, Y., Göcmen, B., Niedermoser, M., Rhein, K., Jahn, J., Cascante, I., Schöler, F., Moser, N., Neubauer, B., Hofherr, A., Behrens, Y. L., Göhring, G., Köttgen, A., Köttgen, M., & Busch, T. Wildtype heterogeneity contributes to clonal variability in genome edited cells. Sci Rep 2022; 12: 18211–13. http://doi.org/10.1038/s41598-022-22885-8

White, M. J., McArthur, K., Metcalf, D., Lane, R. M., Cambier, J. C., Herold, M. J., van Delft, M. F., Bedoui, S., Lessene, G., Ritchie, M. E., Huang, D. C., & Kile, B. T. Apoptotic caspases suppress mtDNA-induced STING-mediated type I IFN production. Cell 2014; 159: 1549–1562. http://doi.org/10.1016/j.cell.2014.11.036

Whiteside, T. L. The tumor microenvironment and its role in promoting tumor growth. Oncogene 2008; 27: 5904–5912. http://doi.org/10.1038/onc.2008.271

Widdrington, J. D., Gomez-Duran, A., Steyn, J. S., Pyle, A., Ruchaud-Sparagano, M. H., Scott, J., Baudouin, S. V., Rostron, A. J., Simpson, J., & Chinnery, P. F. Mitochondrial DNA depletion induces innate immune dysfunction rescued by IFN-γ. J Allergy Clin Immunol 2017; 140: 1461–1464.e8. http://doi.org/10.1016/j.jaci.2017.04.048

Wu, Jianjun, Chen, Y.-J., Dobbs, N., Sakai, T., Liou, J., Miner, J. J., & Yan, N. STING-mediated disruption of calcium homeostasis chronically activates ER stress and primes T cell death. J Exp Med 2019; 216: 867–883. http://doi.org/10.1084/jem.20182192

Wu, Jiaxi, Sun, L., Chen, X., Du, F., Shi, H., Chen, C., & Chen, Z. J. Cyclic GMP-AMP is an endogenous second messenger in innate immune signaling by cytosolic DNA. Science 2013; 339: 826–830. http://doi.org/10.1126/science.1229963

Wu, J., Rutkowski, D. T., Dubois, M., Swathirajan, J., Saunders, T., Wang, J., Song, B., Yau, G. D., & Kaufman, R. J. ATF6alpha optimizes long-term endoplasmic reticulum function to protect cells from chronic stress. Dev Cell 2007; 13: 351–364. http://doi.org/10.1016/j.devcel.2007.07.005

Xu, Z., Chen, Z.-M., Wu, X., Zhang, L., Cao, Y., & Zhou, P. Distinct Molecular Mechanisms Underlying Potassium Efflux for NLRP3 Inflammasome Activation. Front Immunol 2020; 11: 609441. http://doi.org/10.3389/fimmu.2020.609441

Yamamoto, K., Sato, T., Matsui, T., Sato, M., Okada, T., Yoshida, H., Harada, A., & Mori, K. Transcriptional induction of mammalian ER quality control proteins is mediated by single or combined action of ATF6alpha and XBP1. Dev Cell 2007; 13: 365–376. http://doi.org/10.1016/j.devcel.2007.07.018

Yan, N., & Chen, Z. J. Intrinsic antiviral immunity. Nat Immunol 2012; 13: 214–222. http://doi.org/10.1038/ni.2229

Yan, N., Regalado-Magdos, A. D., Stiggelbout, B., Lee-Kirsch, M. A., & Lieberman, J. The cytosolic exonuclease TREX1 inhibits the innate immune response to human immunodeficiency virus type 1. Nat Immunol 2010; 11: 1005–1013. http://doi.org/10.1038/ni.1941

Yoshida, H., Matsui, T., Yamamoto, A., Okada, T., & Mori, K. XBP1 mRNA is induced by ATF6 and spliced by IRE1 in response to ER stress to produce a highly active transcription factor. Cell 2001; 107: 881–891. http://doi.org/10.1016/s0092-8674(01)00611-0

Zelenay, S., van der Veen, A. G., Böttcher, J. P., Snelgrove, K. J., Rogers, N., Acton, S. E., Chakravarty, P., Girotti, M. R., Marais, R., Quezada, S. A., Sahai, E., & Reis e Sousa, C. Cyclooxygenase-Dependent Tumor Growth through Evasion of Immunity. Cell 2015; 162: 1257–1270. http://doi.org/10.1016/j.cell.2015.08.015

Zeng, L., Liu, Y.-P., Sha, H., Chen, H., Qi, L., & Smith, J. A. XBP-1 couples endoplasmic reticulum stress to augmented IFN-beta induction via a cis-acting enhancer in macrophages. J Immunol 2010, 185: 2324–2330. http://doi.org/ 10.4049/jimmunol.0903052

9. Acknowledgements

First and foremost, I would like to thank Prof. Dr. Eva Bartok. This project would not have been possible without your almost encyclopedic knowledge, your constant support concerning this and other projects, and your round-the-clock availability. Thank you for your valuable advice on writing this thesis and other works. Secondly, I thank Dr. Thomas Zillinger for his patient approach to introducing me into the world of experimental research and for his hands-on support in the lab throughout this project. Furthermore, my thanks go to Prof. Dr. Gunther Hartmann for valuable advice on my doctoral project as well as more general advice on life as a scientist, and to Dr. Winfried Barchet, the “original” supervisor of this thesis.

My lab colleagues at the ICCCP have been indispensable for the completion of this work, not only by supporting me in the lab, but also by creating an environment that made even the most annoying experiments enjoyable. In particular, my gratitude goes to Saskia Schmitz and Hildegard Schilling for technical assistance and troubleshooting, and to Katarzyna Andryka-Cegielski and Maximilian Nastaly for providing cells, showing me how to take pictures of them, and critically discussing experimental results.

Moreover, I would like to thank the Imaging Core Facility, particularly Dr. Hannes Beckert, for the opportunity to use super-resolution microscopy for my project, Prof. Dr. Susanne Schoch McGovern for providing mouse neurons, Dr. Stefanie Held for providing myeloma cell lines, and the Flow Cytometry Core Facility.

I am grateful to the BonnNI program of the Else Kroener Fresenius foundation and the ImmunoSensation Cluster of Excellence not only for financial support, but also for great educational opportunities.

Above all, I would like to thank my family for their unconditional support and for making not only this thesis, but all of my education possible, my friends for making it memorable, and Klara, for everything.